ISSN 8755-6839

SCIENCE OF **TSUNAMI HAZARDS**

Journal of Tsunami Society International

Volume 32 Number 2 2013

WWW.TSUNAMISOCIETY.ORG

TSUNAMI SOCIETY INTERNATIONAL, 1741 Ala Moana Blvd. #70, Honolulu, HI 96815, USA.

SCIENCE OF TSUNAMI HAZARDS is a CERTIFIED OPEN ACCESS Journal included in the prestigious international academic journal database DOAJ, maintained by the University of Lund in Sweden with the support of the European Union. SCIENCE OF TSUNAMI HAZARDS is also preserved, archived and disseminated by the National Library, The Hague, NETHERLANDS, the Library of Congress, Washington D.C., USA, the Electronic Library of Los Alamos, National Laboratory, New Mexico, USA, the EBSCO Publishing databases and ELSEVIER Publishing in Amsterdam. The vast dissemination gives the journal additional global exposure and readership in 90% of the academic institutions worldwide, including nation-wide access to databases in more than 70 countries.

OBJECTIVE: Tsunami Society International publishes this interdisciplinary journal to increase and disseminate knowledge about tsunamis and their hazards.

Submit manuscripts of research papers, notes or letters to the Editor. If a research paper is accepted for publication the author(s) must submit a scan-ready manuscript, a Doc, TeX or a PDF file in the journal format. Issues of the journal are published electronically in PDF format. There is a minimal publication fee for authors who are members of Tsunami Society International for three years and slightly higher for non-members. Tsunami Society International members are notified by e-mail when a new issue is available. Permission to use figures, tables and brief excerpts from this journal in scientific and educational works is granted provided that the source is acknowledged.

Recent and all past journal issues are available at: http://www.TsunamiSociety.org CD-ROMs of past volumes may be purchased by contacting Tsunami Society International at postmaster@tsunamisociety.org Issues of the journal from 1982 thru 2005 are also available in PDF format at the Los Alamos National Laboratory Library http://epubs.lanl.gov/tsunami/

ISSN 8755-6839

SCIENCE OF **TSUNAMI HAZARDS**

Journal of Tsunami Society International

Volume 32 **Number 3** **2013**

NUMERICAL MODEL STUDY OF TSUNAMI GENERATED BY POTENTIAL EARTHQUAKE WITHIN THE KOMANDORSKY SEISMIC GAP IN THE WESTERN ALEUTIAN ISLAND ARC

R. Kh. Mazova[1], B. V. Baranov[2], L. I. Lobkovsky[2] N. A. Baranova[1], K. A. Dozorova[2], O. N. Chaykina[2]

[1]*Nizhny Novgorod State Technical Institute, Nizhny Novgorod, raissamazova@yandex.ru*
[2]*P.P. Shirshov Institute of Oceanology RAS, Moscow, bbaranov@rambler.ru*

ABSTRACT

The Komandorsky seismic gap has distinctive boundaries and a length of 650 km. Its period of "seismic silence" comes close to the maximum recurrence interval for great earthquakes in the Aleutian Island Arc - the stress concentration here probably having reached the critical value. So, estimation of possible earthquake and tsunami characteristics within this gap becomes a significant problem. The closest analog of a similar gap is the area where the 2004 Sumatra-Andaman catastrophic event occurred. Thus, for the present study we used the same modeling scheme as we used for that event. It was assumed that a source length of 650 km, consisting of 9 blocks, and an earthquake with a moment magnitude M_W=8.5. Several block motion scenarios were considered. The tsunami generation and propagation in the Pacific Ocean and the possible wave characteristics on near and far-field coasts were estimated. Modeling of such an event showed that the wave heights on different Pacific coasts will vary from 3 to 9 meters. A tsunami wave with a 9-meter height is capable in causing significant loss of human life and economic damage.

Keywords: *Komandorsky seismic gap, seismic forecast, earthquake source, tsunami source, tsunami modeling*

Vol. 32, No. 3, page 131 (2013)

1. INTRODUCTION

The last decade of the 20th Century was characterized by a gradual growth in the number of great earthquakes. In the subsequent decade the growth increased by 2.5 times (AMMON, 2010) - thus the problem of forecasting great earthquakes and modeling their associated tsunamis became of vital importance. As a rule, it is well known that great earthquakes with magnitude $M_w \geq 7.8$ along subduction zones generate tsunamis. Recent great events indicated that tsunamis caused by far greater losses of human life and destruction of property than the seismic ground surface oscillations (AMMON ET AL., 2005; LAY, KANAMORI, 2011). The threat of the tsunami hazard extends not only to coasts near the generating source but also to far-field locations.

Many aspects of earthquake and tsunami investigations are interlinked. Different approaches are being used by investigations, but common objective of all is to forecast such disasters and their potential impact. Research investigations include: a) identification of potential hazardous sources (seismic gaps); b) study of their structure and seismic regime; c) numerical simulation of the propagation of the generated tsunami, and d) estimates of tsunami run up heights at near and at distant coastal areas.

The present study uses the location, time and source structure of a potential great earthquake capable of generating a tsunami, based on a block model ("keyboard model") of earthquake generation along a zone of subduction (LOBKOVSKY ET AL., 1991). The methodology being used is as follows: The island arc wedge is cut into separate major segments by transverse faults penetrating down to the top of the under-thrusting plate. These fault blocks of the island-arc wedge (keyboards) represent minor elements of interaction between the under-thrusting and overhanging plates. A typical block size is about 100 km. However, in some cases the energy is released simultaneously along several neighboring blocks and thus, the length of resulting great earthquake's source area corresponds to the total length of all these blocks.

Earlier in 2006, on the basis of this model, a seismic forecast was proposed for the Central Kurile seismic gap and a simulation was undertaken of the generated tsunami by the predicted earthquake (LOBKOVSKY AT AL, 2006). On November 15, 2006 a great earthquake (M_w=8.3) occurred in the predicted area, which generated a significant tsunami (LAVEROV AT AL, 2007). Data obtained after this event demonstrated reasonably good correlation with the calculated values and thus confirmed the validity of the forecast and of the tsunami simulation (LOBKOVSKY ET AL, 2010).

In the present work, the same approach was applied to estimate the seismic potential of the Komandorsky seismic gap located in the Western Aleutian Island Arc, as well as for the numerical simulation of propagation and run-up of the tsunami that can be generated by such potential earthquake source.

2. THE KOMANDORSKY SEISMIC GAP

2.1. General Characteristics

Investigation of Aleutian Island Arc seismic activity has shown that great earthquakes within the arc occurred during separate time intervals. One seismic gap period in part of the arc lasted from 1938 to

1965 (SYKES, 1971; MCCANN ET AL., 1979; SYKES ET AL., 1981). Sources of these great earthquakes filled the frontal part of the Aleutian Arc, with the exclusion of three areas (Fig.1). Specific seismic gaps were identified and named as the Komandorsky, Unalaska and Shumagin regions (SYKES, 1971; HOUSE ET AL., 1981; DAVIES ET AL., 1981). The term "seismic gap" is used for areas of seismic belts in island arcs and active continental margins, where great earthquakes did not occur during the last 50-100 years. Such gaps are regarded as the most possible earthquake sites for future events (FEDOTOV, 1965; MCCANN ET AL., 1979; MOGI, 1968A; NISHENKO, 1991). After 1965, three great earthquakes with moment magnitude Mw ≥ 7.8 occurred within the Aleutian Arc. However, their sources did not "fill" the seismic gaps listed above, thus these regions are still considered as the most hazardous parts of the arc (RUPPERT ET AL., 2007; WESSON ET AL., 2008; BARANOV, DOZOROVA, 2010).

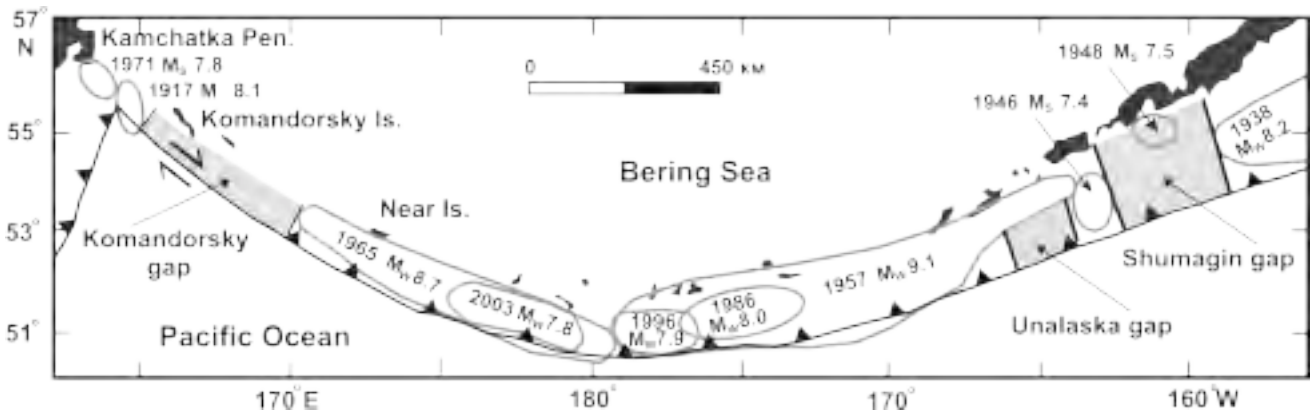

Figure 1. *Location of earthquakes sources (M≥7.4) and seismic gaps in the Aleutian Island Arc after (Sykes et al., 1971), with addition of earthquake sources in 1986, 1996 and 2003. The Line with the triangles marks the subduction zone; the line with arrows marks a transform fault.*

The Komandorsky gap is located in the frontal part of the Komandorsky group of the Western Aleutian Islands. According to the historic record, two earthquakes with magnitudes M=7.5±0.7 occurred in the western part of the Aleutian Arc in 1849 and 1858, but there is no information on their source location (SYKES ET AL., 1981). During the entire period of instrumental observations, only one earthquake with magnitude of M_w=8.1 was recorded on 30 January1917. Macroseismic data of the 1917 earthquake (VIKULIN, 1986) indicates the source to have been located in the Komandorsky segment of the Aleutian Arc. This quake's source had dimensions of 180x90 km, was oriented obliquely to the arc's strike (see Fig.1) and occupied only the northwestern part of the Komandorsky seismic gap. The remaining gap lies between the areas impacted by the 1917 and 1965 earthquakes, and has a length of about 550 km (see Fig.1). The total length of the Komandorsky gap - together with sources of events in 1917 and 1971 - is about 650 km.

The long-term absence of great earthquakes within the western part of the arc, indicates absence of crustal displacements along the boundary between the Pacific Plate and the frontal part of the

Komandorsky segment - suggesting consequently, accumulation of stress and of elastic deformation approaching a critical level. This supposition is supported by specific distribution of strong earthquakes with magnitudes of $M \geq 6$ (BARANOV, DOZOROVA, 2010) and data from GPS observations (AVE'LALLEMENT, OLDOW, 2000; LEVIN ET AL., 2006).

2.2. Earthquakes Distribution and Crustal Displacements

The distribution of strong earthquakes having magnitudes $M \geq 6$ is shown in Fig. 2. Most of their epicenters are located mainly in the rear parts of the Komandorsky block. In the frontal part, strong earthquakes were recorded only near the junction of the Aleutian and Kurile-Kamchatka trenches. The frontal region between the sources of the 1917 and 1965 earthquakes has been seismically inactive in 40 year period for the earthquakes with $M \geq 6$. This fact may justify that displacements between the North American and the Pacific plates to the west of 170° E occur mainly along the rear boundary of the Komandorsky segment. A section of the arc located between the source areas of the 1917 and the 1965 earthquakes, moves together with the Pacific plate. It has long been known that the western segment of the Aleutian Arc is not a subduction zone, but a transform fault (CORMIER, 1975). Analysis of all available earthquake mechanism solutions (RUPPERT ET AL., 2008) has shown that shear displacements prevail to the west of 170°E.

Also, GPS data confirms that blocks of the Aleutian Island Arc move in a western direction with an increasing shear component the displacement rates range accordingly from 3.1, to 9.6 and 31.4 mm/year, for the eastern, the central and the western parts of the arc, respectively (AVE'LALLEMENT, OLDOW, 2000). The displacement rate becomes even greater in the westernmost termination of the Aleutian Arc (the Komandorsky block) where oblique subduction transforms into strike-slip. The GPS measurements have shown such a trend during several years, with Bering Island approaching Kamchatka at a rate of about 50 mm/year (LEVIN ET.AL, 2006). This value constitutes about 2/3 of the convergence rate (79 mm/year) between the Pacific and Eurasian (Okhotsk) plates near the junction of the Aleutian and Kurile-Kamchatka trenches, (DEMETS ET AL., 1994). In this connection it is supposed (SELIVERSTOV, 2009) that presently right-lateral displacement of the Pacific plate relatively Komandorsky Basin structures mainly occurs not along the faults located in the frontal part of Komandorsky Block, but along the fault in its rear part. So, both GPS data and earthquake distribution point on coupling of Komandorsky segment and Pacific Plate and, consequently, there is concentration of stress and deformations on this boundary. This conclusion agrees with belief that Komandorsky Block is a seismic gap. Long-time "silence" of this seismic gap may be possibly explained by the specific structure of this part of the island arc.

2.3. Block Structure of Aleutian Arc and Komandorsky Seismic Gap

The Aleutian Arc consists of adjacent blocks of Earth crust with length from tens to hundreds of kilometers (GEIST ET AL., 1988). The blocks are bordered by canyons and they are also governed by faults, and cut the frontal (southern) part of the arc, transversally to its general strike. The canyons also border sources of great earthquakes, as for example those in 1965 and 1957. The sources of these events border along the transversal fault confined to Amlya canyon. The source area of the 1965 earthquake, stretches in a western direction for a distance 650 km and is limited from the west by the canyon system of the Near Islands. The source consists of three blocks with lengths ranging from 100 to 180 km. To the east from Amlya the canyon source of the 1957 earthquake stretches for a distance 1200 km. Also, this source consists of three large blocks with lengths ranging from 100 to 450 km. The source of the 1957 earthquake is more homogeneous than that of the 1965 event. This may imply that segments in the first case move as a single body and thus the length of earthquake faults reaches 1200 km (NISHENKO, MCCANN, 1979).

For the main Aleutian subduction zone, estimates of changes in stress orientation were obtained by the method of earthquake source mechanism inversion for main subduction zone (LU, WYSS, 1996). As a result, boundaries, along which the change of stress orientation occurs, were distinguished. The boundaries coincide with terminations of great earthquakes sources and fault zones. Marine expeditions to the Western Aleutians (SELIVERSTOV, 1998; BARANOV ET AL., 1991; GAEDICKE ET AL., 2000) provided evidence of the existence of several active faults, parallel to this section of the island arc (Fig. 2). Right-lateral dislocations along the fault system lead to forming pul-apart basins, which are located both in the rear and the frontal parts of the arc. The biggest among them is the Steller Basin (Fig. 3), which is formed immediately on the Aleutian Trench axis where the biggest displacement rates between Pacific and North American plates are supposed. The Steller Basin has

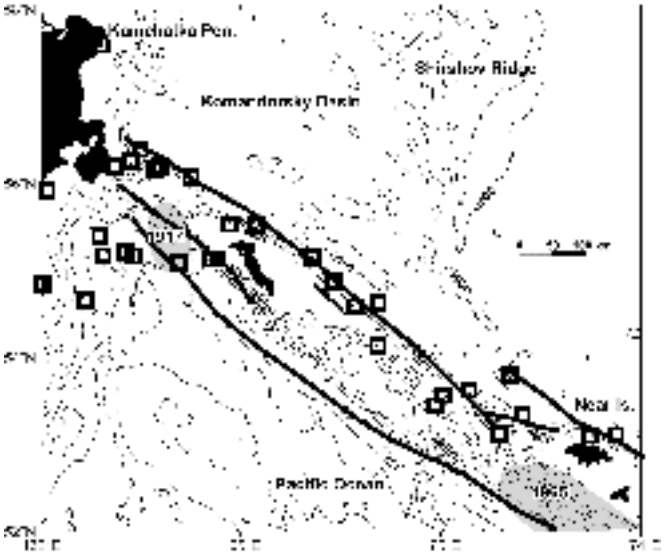

Figure 2. *Distribution of shallow earthquakes in the Komandorsky segment from 1973 till 21.02.2013, M≥6, PDE Catalog. Thick lines mark dextral strike-slips, grey ovals indicate rupture zone of the great earthquakes. Contour interval is 1000 m, after (Smith, Sandwell, 1977).*

typical rhomboid contours, which are governed by dextral shears of nearly NW strike and by normal faults of nearly NS orientation. To the southeast of the Steller Basin, numerous canyons cut the oceanic slope of the Komandorsky Islands to the point of Near Islands. The canyons correspond to the faults – they supposedly represent feathering structures of Komandorsky Shear Zone. Transversal faults cut the Komandorsky seismic gap into nine blocks with lengths ranging from 50 to 60 km (Fig.3).

Existing mathematical concepts at the present time provide the opportunity to create models of tsunami generation and propagation for different cases, including the simulation of tsunami from a source, consisting of several crustal blocks (LOBKOVSKY ET AL, 2006A; LOVKOVSKY ET AL., 2006B).

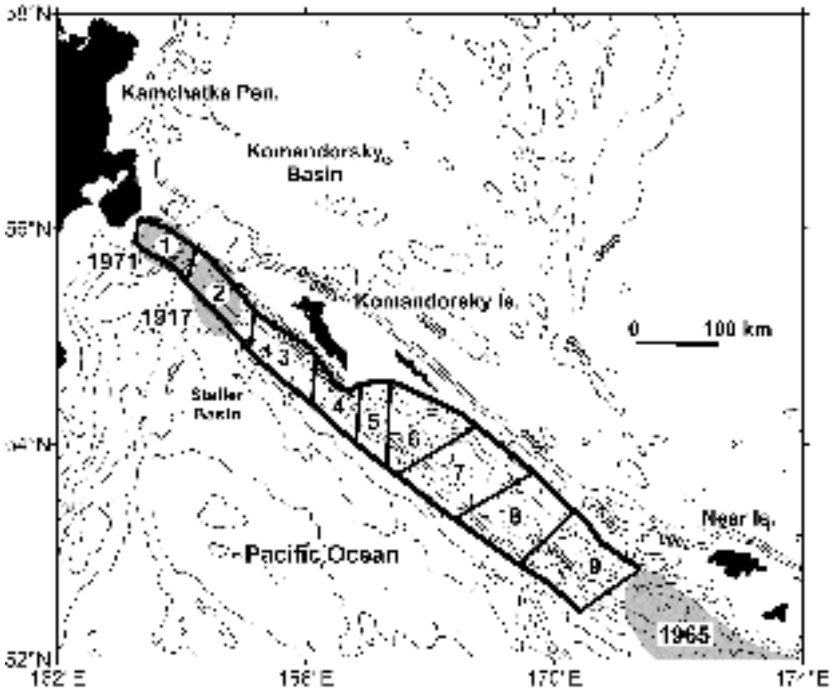

Figure 3. *Block structure of the Komandorsky seismic gap. Thick lines show dextral strike-slips, thin lines – scarps and canyons cutting the gap into 9 blocks. Grey ovals mark great earthquakes sources. Contour interval is 1000 m, after (SMITH, SANDWELL, 1977).*

2.4. The Problem Setting Boundary Conditions

The December 29, 2004, Sumatra-Andaman earthquake was used as an analog for the present simulation since it occurred under similar geodynamic conditions. Both, the Northern Sunda Arc and the Western Aleutian Arc are associated with zones of subduction, which subduction gradually change to dextral shear. Therefore, the scenario of a potential great earthquake along the Komandorsky gap area may be the same as that for the 2004 Sumatra-Andaman earthquake. The

latter event had a source area that was 1300 km in length and consisted of 9 to 12 sub-sources or blocks (AMMON ET AL., 2005; LAY ET AL., 2005). Fault rupturing occurred in a SE-NW direction during 10 minutes at the rate 2 km/sec (STEIN, OKAL, 2005). Peak displacements along the southern part reached 20 m (JI, 2005) and the tsunami source had a length 1000 km and a width of 250 km (FINE ET AL., 2005). In terms of the "keyboard model", this event is interpreted as having nearly simultaneous dislocation of a large number of blocks-keys, triggering a giant earthquake source region that generated a mega-tsunami. As previously stated, a similar scenario is most probable for an earthquake along the Komandorsky seismic gap. Assuming that a future earthquake source will occupy the whole Komandorsky seismic gap, its source is estimated to be about 650 km its length, which would be half the size of the 2004 Sumatra-Andaman seismic source of the tsunami. Time parameters used for the simulation were based on this analogy. In the postulated model described by the present study, the fault rupture propagates in E-W direction and lasts 5 minutes (300 sec). The earthquake's source region is cut into 9 blocks by transverse faults (Fig. 3). The displacements in the eastern segment of the fault are of the thrust type, while in the western segment are of strike-slip type. The magnitude of the potential earthquake is M_W= 9.0. The maximum height of block uplift in the eastern part is postulated to be 18m.

3. NUMERICAL SIMULATION OF TSUNAMI GENERATION AND PROPAGATION

3.1. Numerical model study

The following nonlinear shallow-water equations were used (Lobkovsky at al. 2006a) for the numerical simulation of the tsunami generated by a potential earthquake in the Komandorsky seismic gap.

$$\begin{cases} \dfrac{\partial u}{\partial t} + u\dfrac{\partial u}{\partial x} + v\dfrac{\partial u}{\partial y} + g\dfrac{\partial \eta}{\partial x} = f_1 \\ \dfrac{\partial v}{\partial t} + u\dfrac{\partial v}{\partial x} + v\dfrac{\partial v}{\partial y} + g\dfrac{\partial \eta}{\partial y} = f_2 \\ \dfrac{\partial \eta}{\partial t} + \dfrac{\partial}{\partial x}[(\eta + H - B)u] + \dfrac{\partial}{\partial y}[(\eta + H - B)v] = \dfrac{\partial B}{\partial t} \end{cases} \qquad (3.1)$$

where $f_1 = \dfrac{-C_h}{H+\eta} u\sqrt{u^2+v^2}$, $f_2 = \dfrac{-C_h}{H+\eta} v\sqrt{u^2+v^2}$ corresponds to the bottom friction;

x,y are the space coordinates along the axes *Ox* and *Oy,* respectively; *t* is the time;

$u(x, y, t)$, $v(x, y, t)$ are the average over depth horizontal components of fluid flow rate;

$\eta(x,y, t)$ is the displacement of free surface relatively its undisturbed level;

H is the maximum depth of the basin at undisturbed water, function $B(x, y, t)$ describes displacement of bottom surface relatively to initial position (accounting dynamic characteristics of seismic motion);

g is the gravity factor, $Ch = \frac{(H + \eta - B)^{0.4}}{sh}$ is the bottom friction coefficient (Shezi coefficient), sh is the roughness coefficient.

A bathymetry map of the Pacific Ocean with resolution 1000m was used for modeling. A time step of 1 sec was chosen for the simulation and for each step, the wave failure conditions were checked. Specifically the modeling calculation area included a quadrant bordering from 125°E to 100°W and from 30°N to 60°N and the total network included 4042×1808=7,307,936 nodes. The total reflection condition (corresponding to a vertical wall boundary) was postulated in the last offshore point at a water depth of 10 m, which permitted fixing of maximum and minimum values of wave level displacement at this depth. There are many difference's schemes approximating Eqn. 3.1, but chosen for the present study was that of Marchuk et al. (1983), because it demonstrates high algorithmic flexibility. This scheme was used to take into account the kinematics and dynamics of motions in the earthquake source.

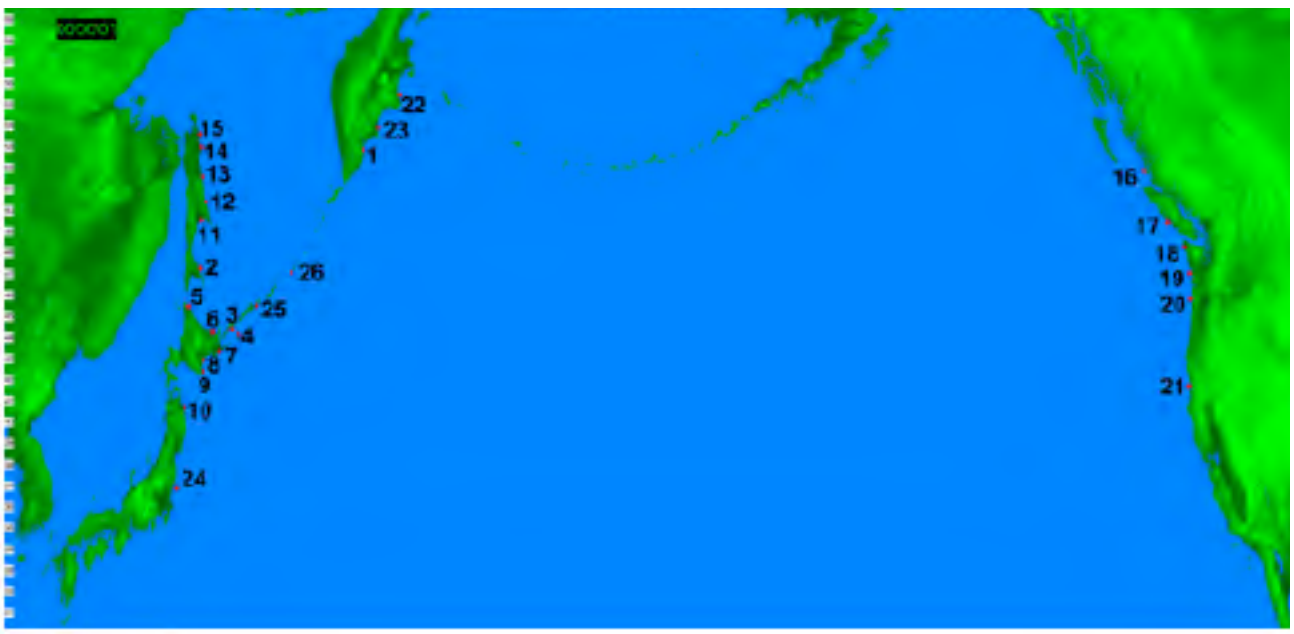

Figure 4. Segment of the Pacific Basin used for the numerical simulation. The locations of virtual tide gauges are marked by red dots and identified by numbers.

The calculations were carried out for the designated northern Pacific Basin segment and values were determined for the virtual tide gauges shown in Fig. 4. Data obtained from these tide gauges was used for the analysis of wave field characteristics in calculated water area.

Basing on the postulated type of realization of the potential earthquake process, computation of

tsunami source, generated by seismic source, was performed with the hypothesis that there is only vertical component in the displacement of the source blocks (see Fig. 4). Table 1 gives the top-plane coordinates of blocks, the beginning time of their uplift and the heights and time periods of such uplift. The tsunami source is formed during 300 seconds after the beginning of the earthquake and its source area develops from SE to NW direction. The tsunami source shape is directly affected by the given kinematics of the blocks in the earthquake source region (see Fig. 5 and Table 1). Finally, in using parameters of vertical displacement in the earthquake source for the simulation, it is also necessary to take into account the hydrodynamic character of the problem. In a case where the time of block uplifting is relatively small (see Table 1), instantaneous piston-type movement is realized. In such a case, due to water incompressibility and and the hydrostatic character of pressure, the ocean

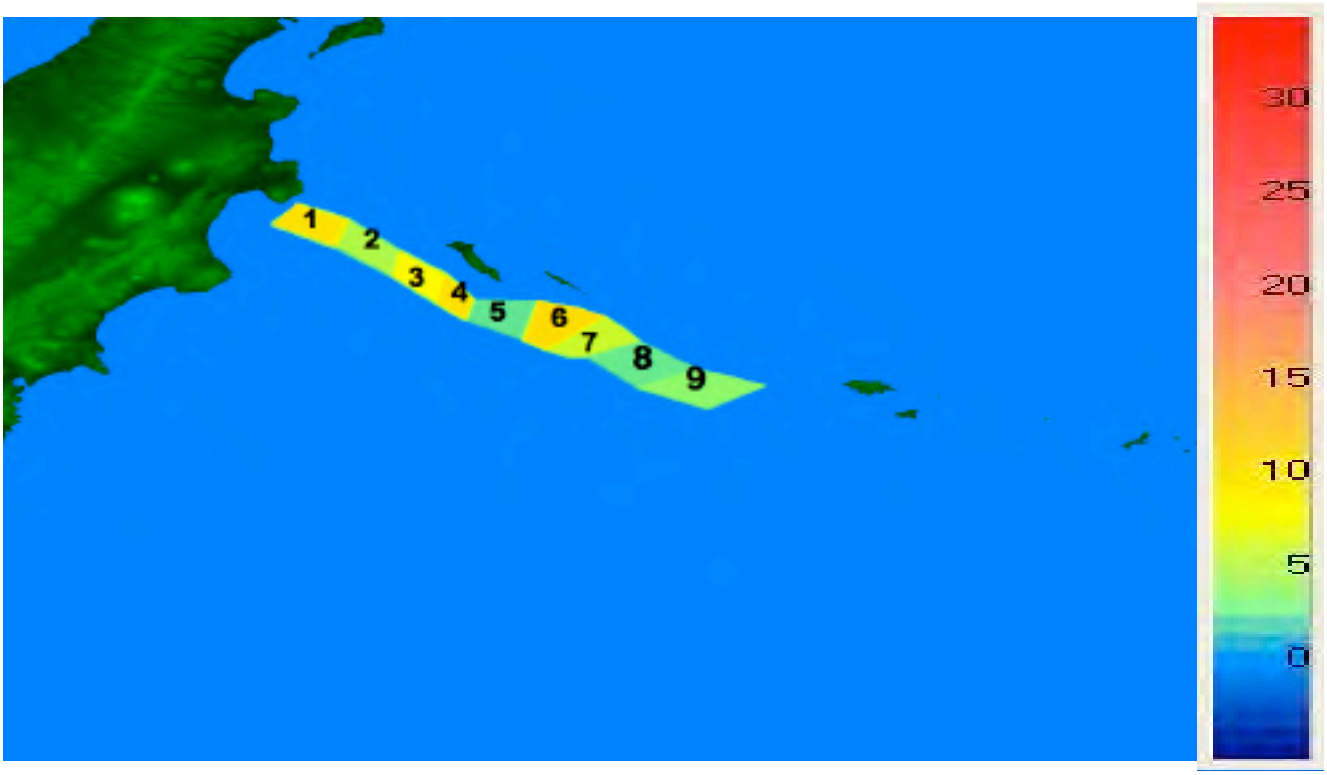

Figure 5. *Location of seismic source. The color of each block corresponds to its maximum vertical lift (the data are presented in Table 1), as well as to color scale presented on the right.*

water surface uplifts as much as the bottom block's surface (see Table 1). But in a case of slower uplifting of blocks 1-6, the wave height will decrease proportionally to $1/r^2$. So it becomes necessary to increase the initial displacement of the seismic source block in order to simulate correctly the water surface heights in the tsunami source (estimated by formulas which relate earthquake magnitude to resulting wave height). Thus vertical displacements in blocks 1-6 are assumed to be somewhat bigger than values calculated by these formulas. Forming such a source generates a tsunami and two processes occur simultaneously: wave generation by uplifting of next block in the seismic source and

the propagation of the wave from this block and wave generation from subsequent blocks. After the 6th minute, the generation process is terminated and only the process of wave propagation in the ocean is considered. Thus, chosen block kinematics in the seismic source region, lead to a complicated dynamic process affecting the whole ocean surface. In the present simulation the wave propagation was conducted for only a part of the Pacific Ocean, in directions, which included the Kurile Islands, the Okhotsk Sea and the central part of the western coasts of the North America.

Figure 6 represents characteristic time moments demonstrating the process of tsunami source generation. From this, and in accordance with chosen scenario (Table 1), it becomes obvious that the tsunami source region develops in SE-NW direction and that the source sharp depends directly on the postulated kinematics of the seismic source blocks.

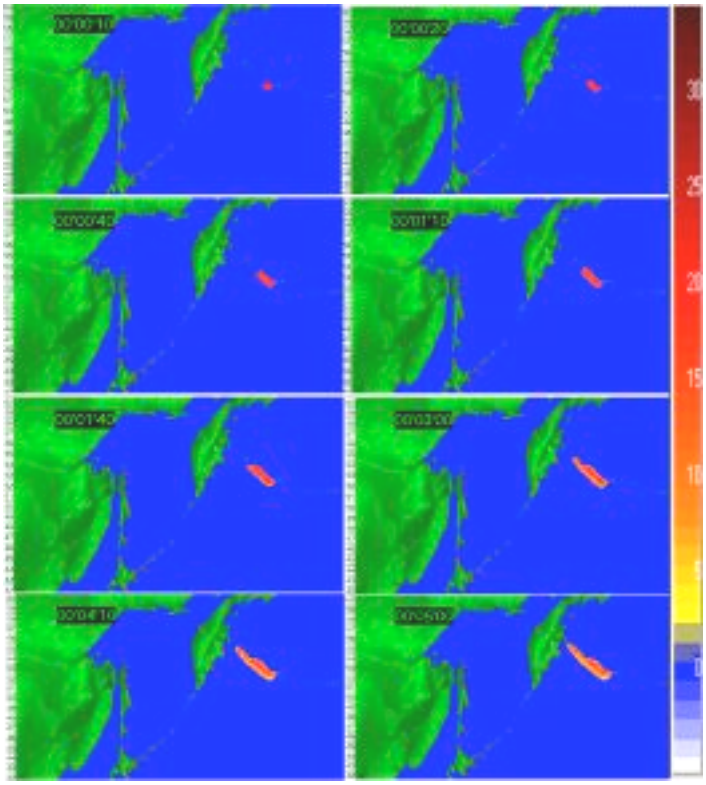

Figure 6. *Tsunami source generation by model seismic source.*

Table 1. Parameters of blocks (keys) movements for simulation

Block number	1	2	3	4	5	6	7	8	9
Block coordinates X1 (E)	164,37	164,37	165,37	166,17	166,67	167,67	168,07	168,77	169,67
Y1 (N)	54,53	54,53	54	53,53	53,235	52,883	52,706	52,588	52,034
X2 (E)	164,79	164,79	165,52	166,32	166,82	167,92	169,12	169,72	170,72
Y2 (N)	54,895	54,895	54,449	54,037	53,596	53,567	53,302	52,861	52,39
X3 (E)	163,4	165,37	166,17	166,67	167,67	168,07	168,77	169,67	170,89
Y3 (N)	54,845	54	53,53	53,235	52,883	52,706	52,588	52,034	51,671
X4 (E)	163,83	165,52	166,32	166,82	167,92	169,12	169,72	170,72	171,92
Y4 (N)	55,162	54,449	54,037	53,596	53,567	53,302	52,861	52,39	52,096
Start time, T_o, sec	250	180	130	100	70	40	20	10	0
Stop time, T, sec	300	250	180	130	100	70	40	20	10
Shift value, B, m	12	13	13	13	14	16	18	18	18

Data of 28 virtual tide gauges located along Pacific Ocean coasts (Fig. 1) were used for the analysis of wave field characteristics which were obtained as a result of the given scenario. The results of the calculation are presented in Table 2. Also indicated in this Table are the coordinates, the maximum and minimum wave heights at 10-meter isobath, the arrival phase of the first wave and the travel time for each point.

Figure 7 presents characteristic stages of tsunami wave propagation in the ocean for six characteristic moments: a) 2 h 13 min travel along Kurile islands; b) 2 h 45 min wave reaching Hokkaido Island; c) 3 h 53 min wave reaching the middle of Honshu Island; d) 4 h 43 min continuous tsunami propagation along Honshu Island and in the direction of western coast of North America; e) 6 h 23 min wave arriving at the coast of North America; f)7 h 30 min wave continues propagation along the coast of North America.

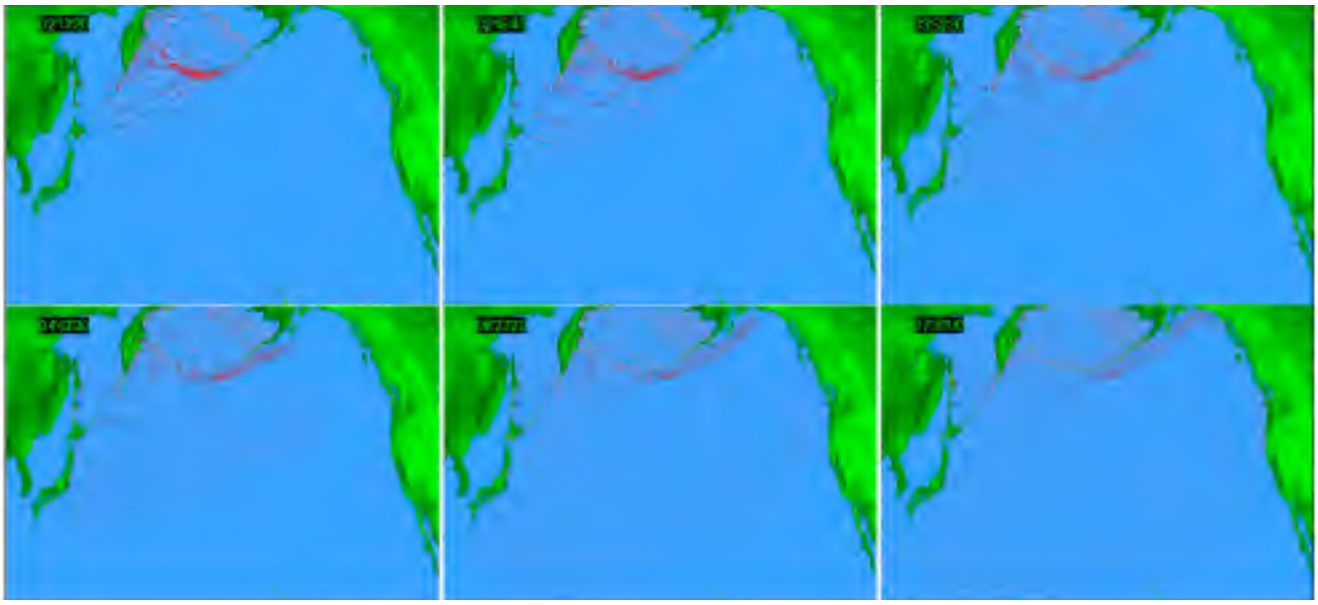

Figure 7. *Tsunami wave propagation in calculated basin at realization of given scenario for 6 time moments*

Analysis of the results obtained shows that the highest waves are observed along the east and southeast of Kamchatka (points 22 and 23) and on Simushir Island (point 26). Similarly, the results show that smaller amplitude waves penetrated through the Bussol and Krusenstern straits, further into the Okhotsk Sea and towards the eastern coasts of Sakhalin Island. The biggest among these waves are observed in points 2, 14 and 13. In points 2 and 14, the lowest run-down is recorded as well as the highest run-up (over 4.4 meters in point 14). Relative growth in tsunami wave height is observed near the Japanese Islands. Near Hokkaido Island (point 7) the tsunami is over 3 m high at the 10-meter isobath and near Honshu Island (point 10) the wave reaches a height over 2.5 m. It should be noted that at points 10 and 24 the intensive run-down is observed after first wave crest. Along the central parts of the western coast of North America, the highest tsunami wave heights are observed at points 19, 20 and 21, but also significant run-downs is observed as well.

Table 2. Results of the numerical simulation

Number of virtual tide gauge	Maximum wave height in point, m	Minimum wave height in point, m	Approaching phase of first wave	Approaching time of first wave
Sakhalin island				
2	3,06	-3,84	+	2 h 28 min
11	2,23	-2,70	+	2 h 31 min
12	2,98	-2,15	-	2 h 15

Number of virtual tide gauge	Maximum wave height in point, m	Minimum wave height in point, m	Approaching phase of first wave	Approaching time of first wave
Sakhalin island				
				min
13	2,52	-2,17	-	2 h 14 min
14	4,41	-3,85	-	2 h 23 min
15	1,49	-1,92	+	2 h 33 min
Kamchatka peninsula				
22	13,95	-10,94	+	18 min
23	10,27	-14,20	+	25 min
Kurile island arc				
3	2,34	-1,94	+	2 h 28 min
4	2,76	-2,65	+	2 h 21 min
25	3,31	-2,10	+	2 h 05 min
26	4,10	-1,12	+	1 h 27 min
Japan Honshu, Hokkaido				
6	4,13	-4,34	+	2 h 55 min
7	3,05	-2,24	+	2 h 45 min
9	1,43	-1,26	+	3 h 05 min

Number of virtual tide gauge	Maximum wave height in point, m	Minimum wave height in point, m	Approaching phase of first wave	Approaching time of first wave
Sakhalin island				
10	2,55	-1,78	-	3 h 31 min
24	3,95	-2,90	+	4 h 30 min
28	3,99	-3,69		4 h 13 min
Central part of western coast of the North America				
16	0,89	-1,26	-	5 h 45 min
18	3,22	-2,89	+	6 h 37 min
19	4,53	-3,64	-	6 h 48 min
20	3,79	-4,67	+	6 h 58 min
21	3,02	-2,96	+	7 h 50 min

Figure 8 demonstrates the distribution of maximum tsunami wave heights throughout the whole area of the investigation. The highest waves, designated by the yellow-colored areas, occur along the eastern

coasts of Kamchatka, the western and partly central Aleutian Islands, on the northeast coasts of the Kurile Islands and near small islands within the Bering Sea. Relatively high waves, designated by the red-colored areas are seen near Japan (Honsu and Hokkaido Islands), Eastern Sakhalin Island and the central part of North America's western coasts.

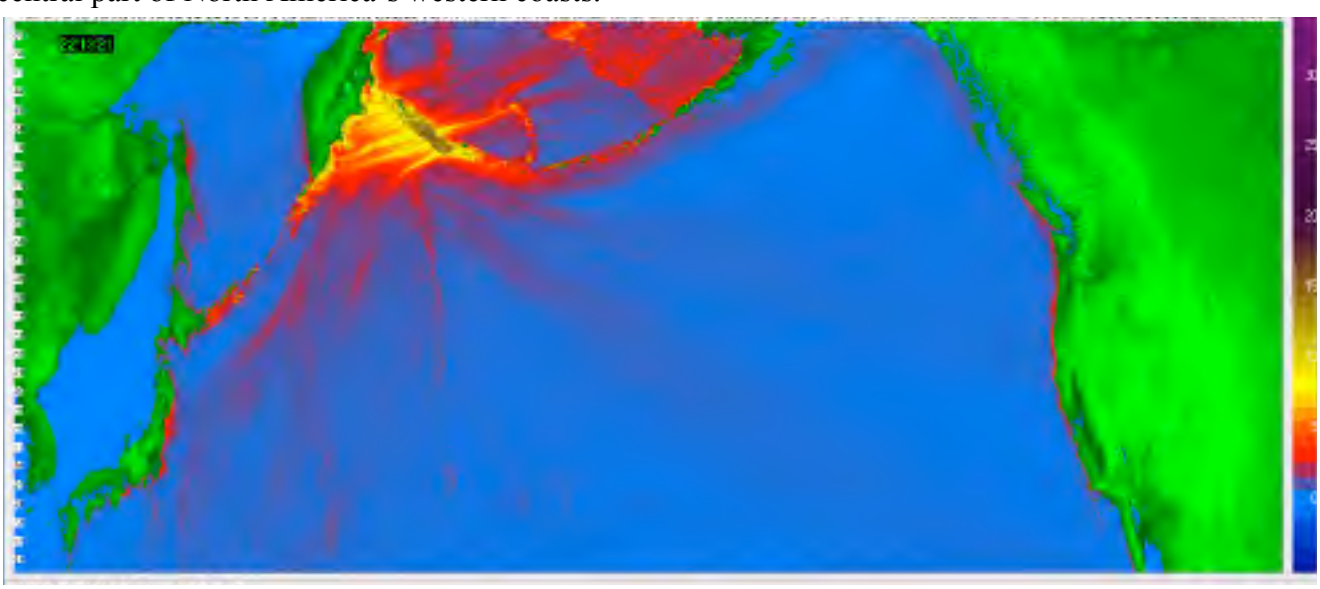

Figure 8. *Maximum tsunami wave distribution in given basin as a result of numerical simulation*

3.2. Spectral analysis of wave characteristics

Based on the computation results obtained, a wavelet analysis was performed for points located near the Russian coast, the Japanese islands of Hokkaido and Honshu, as well as for points along the middle segment of the western coast of North America. Spectrograms constructed for points 12 and 14, located near Sakhalin Island, are practically close to those obtained by computations of wave fields from sources located in the seismic gap of the Middle Kuriles [Lobkovsky et al. 2010]. At the same time, spectral characteristics obtained by computation of wave fields from a seismic source located in the Aleutian seismic gap and for the region of Japan islands, have essential differences. Resonance effects arising between south Kamchatka and the western Aleutians where the seismic source is located can explain them. Long-term transitional processes (multiple re-reflections of waves) lead to the formation of numerous waves coming to Kurile Islands, as well as to the eastern coasts of Japan and to the central part of the western coast of North America. So, for point 26 located near Simushir Island (Fig. 9), there are well observed low-frequency intervals from 200 to 300 min and from 350 to 400 min. There are regions with frequencies equal to 1.5-2 cycles per hour (cph) that corresponds to a wave period 30-40 min, with intensity near 20 dB. In these time intervals all of the wave energy is concentrated in low-frequency interval. After 400 min all energy transfers to more high-frequency region excluding regions from 550 to 650 min.

For the same reason the part of high-frequency components is noticeably higher in tide gauge record for point 7. It should be noted that at such location of the seismic source, and hence, of the tsunami source, at all points where tide gauges are located, high-frequency components arise together with low-frequent or somewhat later. It depends on the character of wave interaction coming from the open sea and propagating along coasts and island chains. The latter give multiple high-frequency re-reflections.

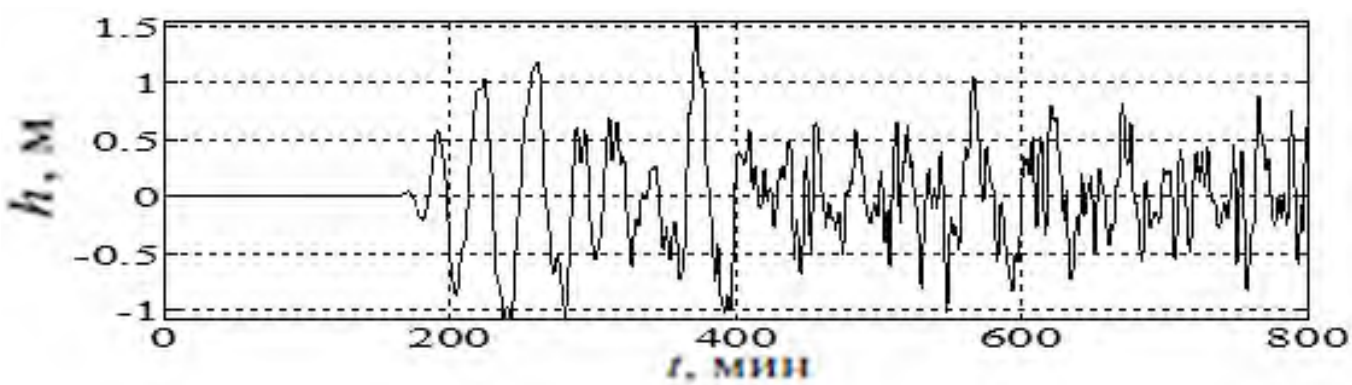

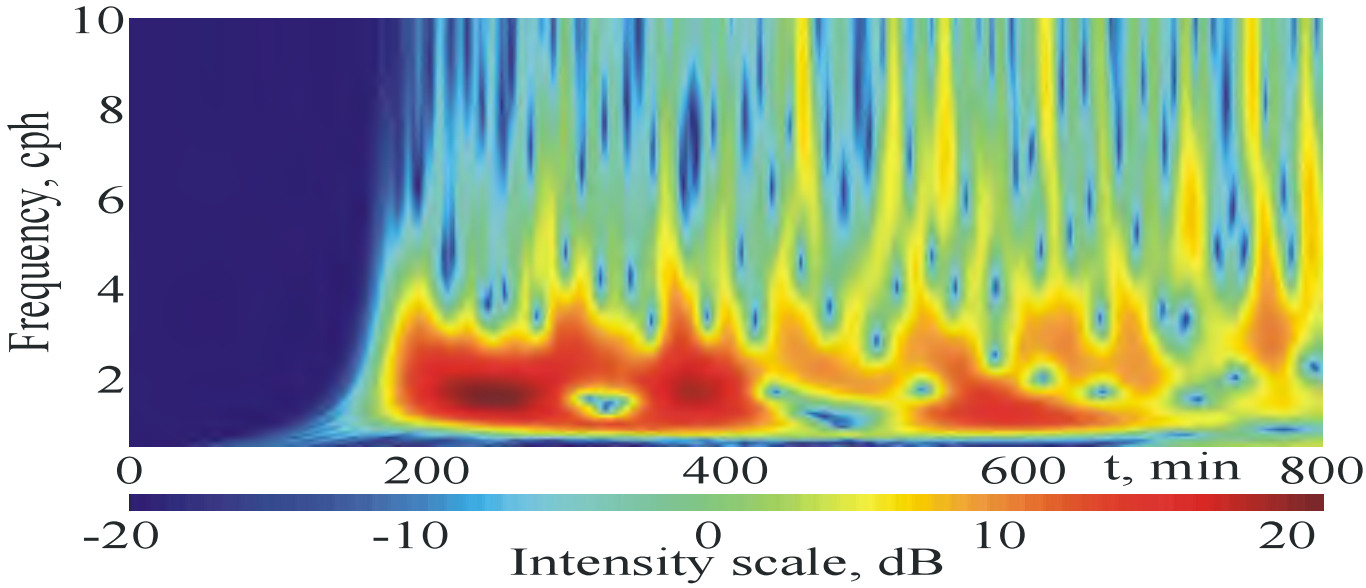

Figure 9. *The computed tide gauge records and spectrogram for point 26*

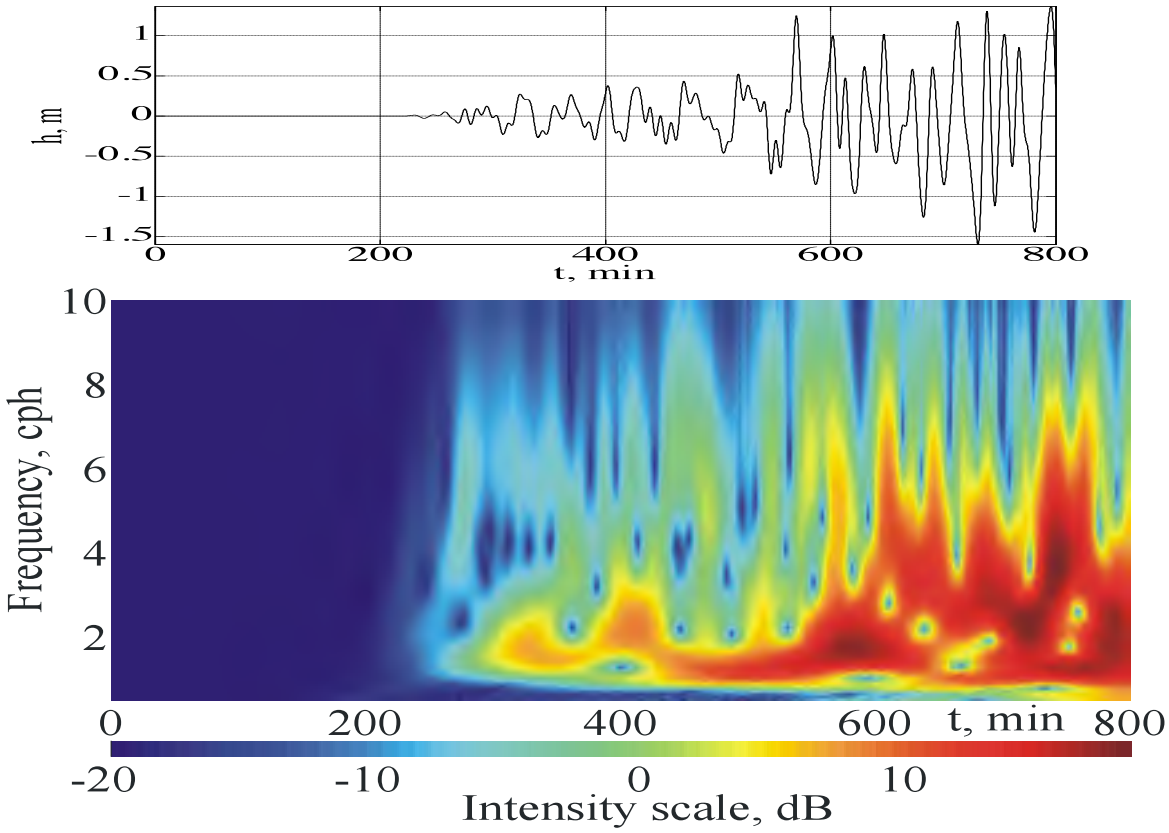

Figure 10. *The computed tide gauge records and spectrogram for point 7.*

At point 7, the low-frequency component is weak enough within the time interval ranging from 250 to 450 min. However, beginning from 450 min, the intensity of the low-frequency component increases and at 550-600 min range it reaches a maximum near frequency 2 cph, which corresponds to 30-min waves, with intensity near 15 dB. Approximately from 600 min to 750 min, most of the energy is concentrated in the range from 2 to 6 cph. One can distinctly see a low-frequency component in intervals 300-400 min, 500 min and further in the region of 700 and 750 min (with little gaps in intensity, but it is not essential against a background of intensive low-frequency regions). The low-frequency component is characterized by frequencies ranging from 1.5 to 2 cph and from 1.5 to 1 cph, which corresponds to 30-40 min and 40-60 min wave periods. The high-frequency components begin to manifest themselves at 450 min and are repeated regularly further after 30-40 min. One can see that the character of the spectrogram in the low-frequency region from approximately 250 to 400 min corresponds to the character of the spectrogram for point 26 in the range of 170-300 min. It is clearly seen that, in spite of the fact that point 7 is closer to point 26 as compared with point 9 (see Fig. 3), judging by the spectrogram character of the wave, the processes are more similar in points 9 and 26 than those in points 7 and 26.

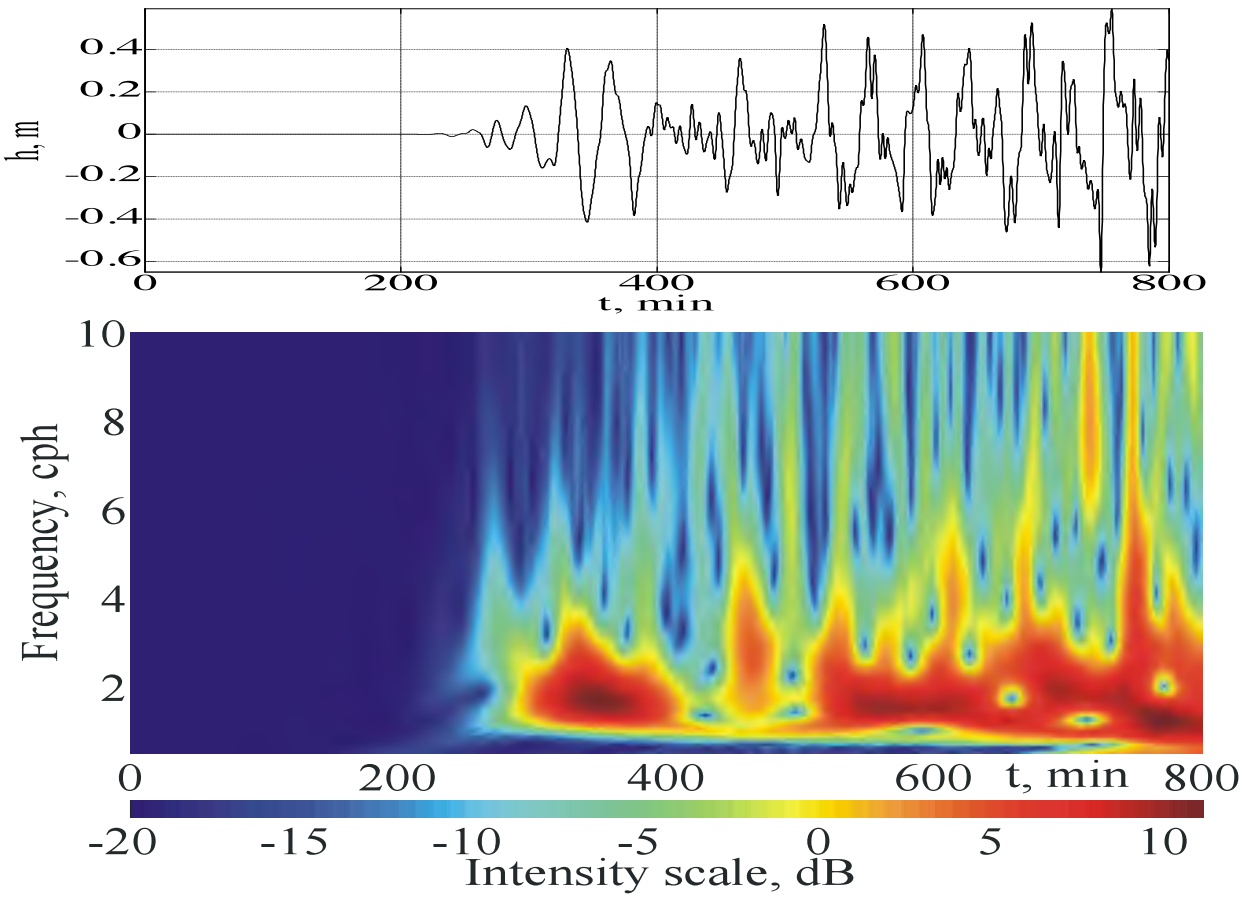

Figure 11. *The computed tide gauge records and spectrogram for points 9.*

Waves arrive at points 10 and 24 (Figs.12, 13) mainly from the open-sea direction, thus respectively, the portion of their high-frequency components in tide gauge records decreases. The component with frequency 2 cph (from 330 to 500 min, from 600 to 700 min) dominating at point 24 is significantly weaker as compared with that of point 10. At point 10, a low-frequency component prevails up to 450 min but its intensity is weak enough (about 7-10 dB). Regular, high frequency sparks of energy from 3 to 10 cph with intensity to 17 dB, appear after 450 min. At point 24, the low-frequency component occurs between the time-interval 330-500 min with little decay of intensity, which is again repeated during the time interval ranging from 600-800 min, for frequencies about 2 cph, i.e. 30 min waves. High-frequency components begin from 300 min and repeat up to 470 min. Afterwards, their intensity becomes weaker, though the regularity may still be traced. It should be noted that the initial frequency segment in many aspects repeats the character of spectrogram for point 26.

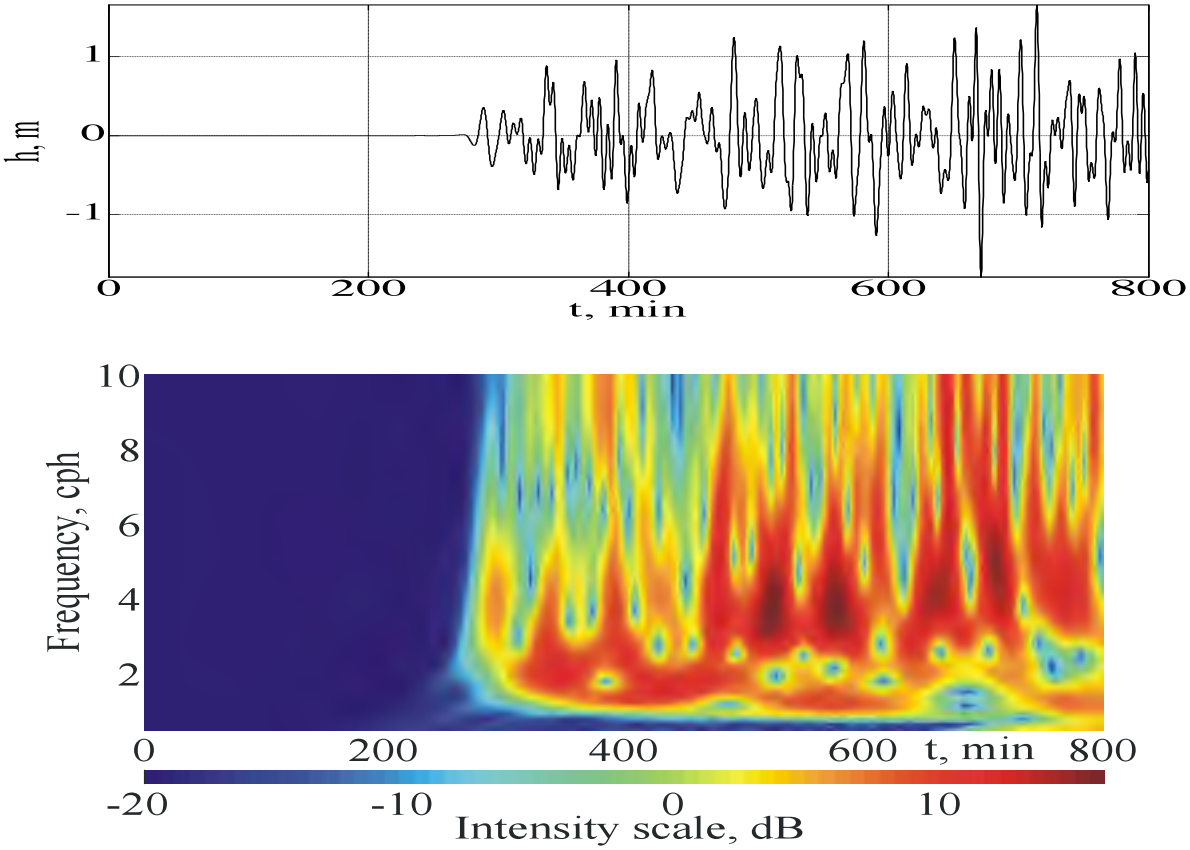

Figure 12. *The computed tide gauge records and spectrogram for points 10*

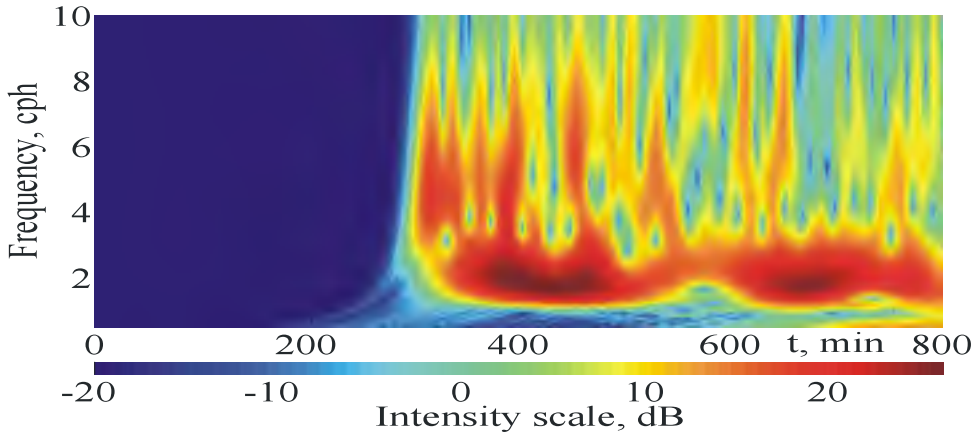

Figure 13. *The computed tide gauge records and spectrogram for points 24*

The waves come to points 19 and 17 (Figs. 14, 15) from an open-sea direction. The energy and wave frequency composition in points 17 and 19 are in many details similar. There is an increase of the wave's energy, with simultaneous broadening of the bandwidth occurs for these points beginning from 350 min. At point 17, beginning from 550 min, the energy increases. From 600 to 650 min a sharp spark appears and a local maximum is observed, approximately from 3 to 7 cph. The next local maximum is formed in the region of 750 min, from 1.5 to 5 cph (10-40-min waves). At point 19 in the range of 350-550 min, the intensity is low. From 550 to 750 min there is a sharp increase of intensity in interval from 1 to 6 cph (10-60 min waves). From 750 to 800 min, there is energy spark from 0.5 to 6.5 cph that corresponds to 2-hour waves with intensity 25 dB.

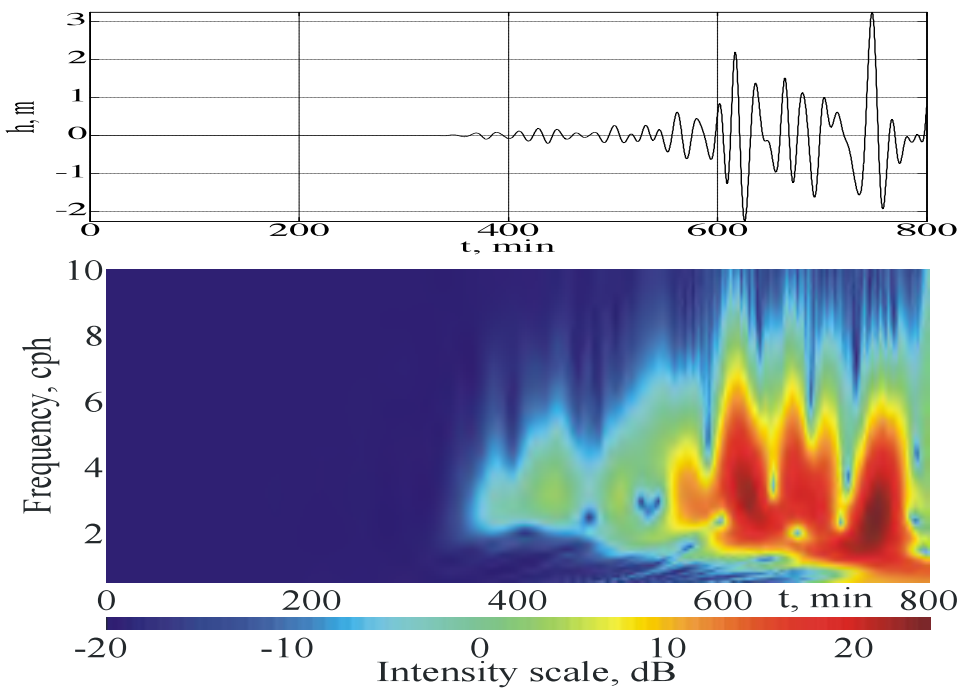

Figure 14. *The computed tide gauge records and spectrogram for points 17.*

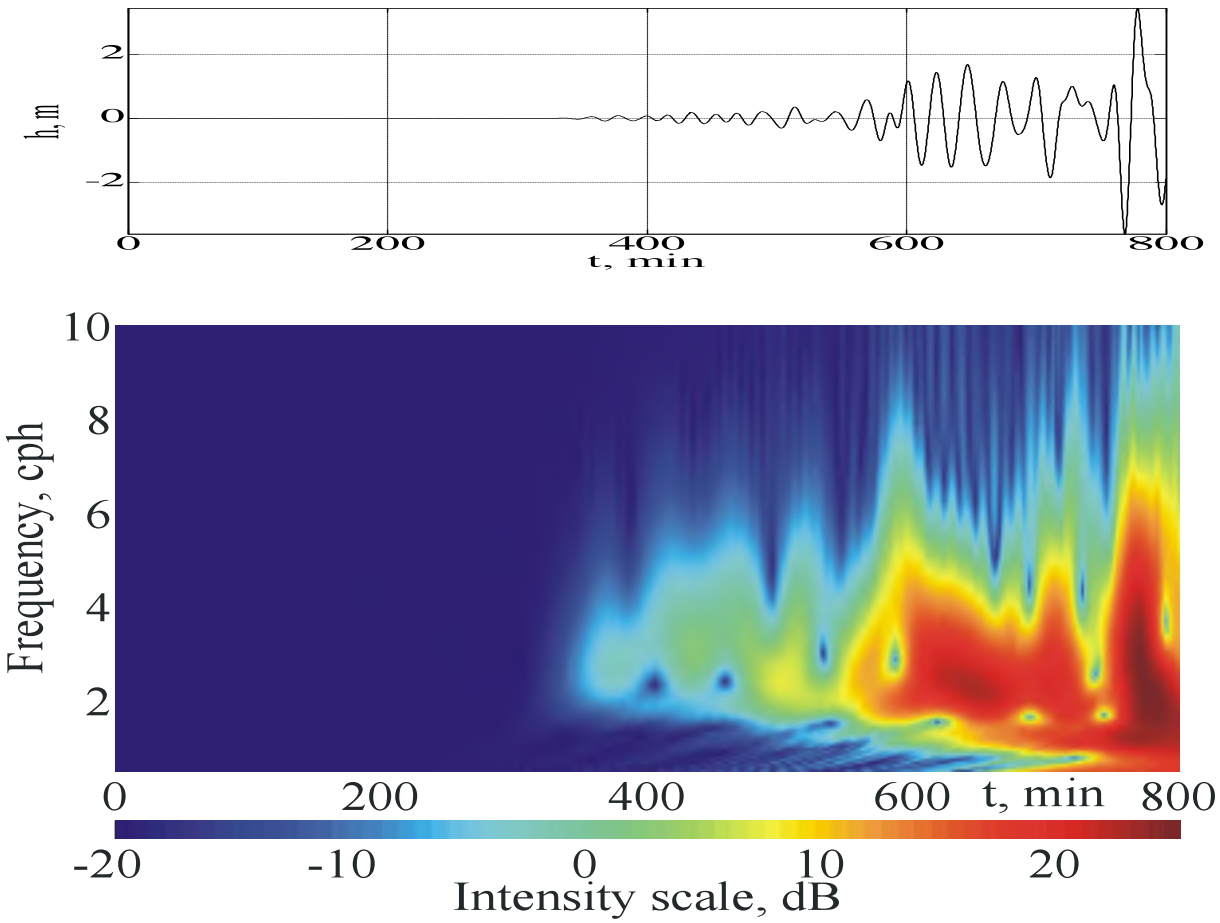

Figure 15. *The computed tide gauge records and spectrogram for points 19.*

4. DISCUSSION

As mentioned earlier, the main objectives of earthquake and tsunami source investigations are to forecast their occurrence and their environmental impact. Presently, there are three categories of seismic forecast: long-term, medium-term and short-term. The first two categories are considered below for the Komandorsky seismic gap.

A long-term forecast covering about 100 year time interval is based on investigations of seismic activity of most active subduction zones. The essence of the long-term forecast lies in distinguishing seismic gaps which are areas in regions of subduction zones in which areas great earthquakes did not occur for a long period of time (FEDOTOV, 1965; MCCANN ET AL., 1979; MOGI, 1968A; NISHENKO, 1991). The Komandorsky seismic gap was distinguished in the western part of Aleutian Island Arc in the framework of a long-term seismic forecast (SYKES, 1971). The recurrence interval for great earthquakes is unknown for this region - the last instrumentally recorded event with a reconstructed

magnitude of Mw=8.1 having occurred about 100 years ago in 1917. However, the source of this event included only the western part of the above-distinguished seismic gap. Analysis of historical documents shows that two earthquakes with magnitudes M=7.5±0.7 occurred in the western part of the Aleutian arc in 1849 and in 1858, but it is impossible to determine the location of their sources (SYKES ET AL., 1981). Estimates of recurrence intervals for great earthquakes in the whole Aleutian Island Arc vary from 50 to 103 years (DAVIES ET AL., 1981). So up to now, a period of calmness has lasted for about 100 years - at least for the western part of the Komandorsky seismic gap - which corresponds to the maximum estimate of the recurrence interval for great earthquakes along the Aleutian Island Arc.

Instrumental observations and recordings of all great earthquakes on the Globe begun about 100 years ago. On the other hand, there are subduction zones areas - such as the Komandorsky seismic gap - where no great earthquake has registered during this period. Thus, an important question arises as to how the seismic potential of such an area may be estimated. This issue became extremely important after the December 26, 2004 Sumatra and the March 11, 2011 Japan disasters. Such catastrophic earthquakes and tsunamis forced many researchers to rethink that the seismic forecasts have been rather conservative. The forecasts were based only on data for the instrumental period of observations and did not take into account previous historical periods, when such catastrophes did occur but were not adequately documented.

Similarly, it was believed earlier that the Komandorsky seismic gap is unable to generate great earthquakes because of its specific structure (CORMIER, 1975). However, after the 2004 Sumatra-Andaman earthquake which occurred in a similar geodynamic situation, this belief has been revised and presently the seismic potential of the Komandorsky seismic gap is considered to be very high and may even generate an earthquake with a maximum magnitude of Mmax=9.2 (Wesson et al., 2008).

The second category is the medium-term forecast. Its time interval covers from several days to several years. It is based on studies of ongoing processes immediately connected with preparation process of the fault, namely the transformation of stresses, the final stage of energy accumulation in seismogenic block and foreshocks (precursory shocks).

In many cases great earthquakes do not occur unexpectedly. As a rule, increases or decreases of seismic activity are observed shortly before a main quake strikes (WYSS, 1997). Foreshock activity appears several days, months or years before the main event for 10-30% of the total number of great earthquakes (SHIBAZAKI, MATSUURA, 1995; CONSOLE, MURRU, 1996; MAEDA, 1996). Such foreshock regularity has been observed for Aleutian Arc earthquakes. For instance, during the foreshock stage of the 1957 earthquake, seismic swarms occurred at both terminations of the source. At the western termination (180ºW) a seismic swarm appeared for three years before the main shock and in January 1957 a swarm was registered during one week at the eastern termination (168ºW) (HOUSE ET AL., 1981). Earlier, it was presumed that foreshock swarm in 1957 was caused by partial rupture which preceding the main faulting of this great earthquake. If a seismic gap had been previously didtinguished for this area the appearance of these two distinct seismic swarms, could have served as a medium-term seismic forecast of the great earthquake of 1957 (HOUSE ET AL., 1981).

Seismic swarms, which may be interpreted as foreshock activity, had been also registered before the 2004 Sumatra-Andaman earthquake. On the southeastern boundary of its source, a series of a 17

earthquakes with one having a maximum magnitude 7.4 (PDE Catalogue) were recorded on November 2, 2002 - two years before the main 2004 event. The Sumatra-Andaman earthquake is considered here as being analogous of a possible, future, great earthquake in Komandorsky seismic gap. Thus, an increase of seismic activity around the gap and especially along its boundaries should be considered as a medium-term forecasting indicator – these facts have been pointed to preparation process of great earthquake in this area.

The numerical model study of tsunami generation and propagation from such a great earthquake in the Komandorsky seismic gap was performed on the basis of a numerical simulation, for the purpose of estimating the maximum wave heights that may be expected at a number of Pacific Ocean coasts. On Kamchatka, the tsunami waves can be expected to reach great heights throughout the whole coastline. Also, the Kurile Islands will undergo an intensive impact of tsunami waves propagating along their Pacific coasts, although the results of the present study indicate a decrease of energy in some parts of the island arc. In Sakhalin, the study indicates that the highest waves are observed in the northeast of the island. This can be easily explained by the influence of the most intensive wave front passing through the Krusenstern Strait and rotating obliquely to Sakhalin Island. On the Japanese Islands, significant wave heights can be expected - especially on the eastern coast of Hokkaido Island. The whole central part of the western coast of North America is expected to be impacted by tsunami waves originating from a great earthquake along the Komandorsky Islands region. Tsunami waves with heights ranging from 1.5 to 3 m at the 4 m isobate can demonstrate amplification in 1.5-3 times in the coastal zone (Pelinovsky, Mazova, 1992). Thus, the simulation shows that a potential great earthquake in the Komandorsky Islands can generate a tsunami that may cause real damage in many coastal areas of the Pacific Ocean and of the Okhotsk Sea.

The analysis performed by this investigation demonstrates that an extensive seismic source in the Komandorsky gap can generate a destructive tsunami, but that the character of the waves propagating in the Pacific Ocean essentially differs from those generated from a seismic source in the Central Kuriles. One of the principal aspects of this difference is in formation of kind of resonator under location of extended seismic source in the region of western Aleutes. The keyboard source, located in such manner, forms wave trains directed both along Kurile Islands chain and towards the open ocean. The effects of wave front interference are most distinctly manifested when the waves approach the Japan islands of Hokkaido and Honshu. This can be clearly seen in the constructed spectrograms of the data obtained from the selected virtual tide gauges along Japan's coasts. An analogous but less defined picture is observed for the spectrograms constructed with the data obtained from the selected virtual tide gauges along the central part of the western coast of North America.

5. CONCLUSIONS

Estimates of the recurrence interval for great earthquakes within the Aleutian Island Arc ($M_w \geq 7.8$) vary from 50 to 103 years, with the average recurrence being 80 years (Davies et al., 1981). The recurrence for great earthquakes in the Komandorsky seismic gap is estimated at 95 years - this being close to the maximum. This leads to the conclusion that seismic stress concentration has reached a critical value. The existence of such a gap in the western Aleutian Arc should be viewed as a long-

term forecast indicator, pointing to the high seismic potential of this area to generate a significant tsunamigenic earthquake.

As previously stated, the Komandorsky seismic gap has distinctive boundaries – in the east it was the source of the 1965 earthquake and in the west it was the source of the 1971 earthquake. Registration of strong earthquakes with magnitudes of M≈7 along the boundaries of the gap will be considered as medium-term forecast indicators pointing on to the potential, perhaps near-future occurrence of a great earthquake in this area.

Numerical simulation of a tsunami generated by the postulated source of this earthquake has shown that the wave heights on a number of Pacific coasts will vary from 3 to 9 meters. Tsunami waves with a 9-meter height are capable of far-field, inland inundation and destruction, which can cause significant human loss and economic damage.

ACKNOWLEDGEMENT

This work was supported by the Russian Foundation for Basic Research, project no. 12-05-00808.

REFERENCES

BARANOV, B.V., DOZOROVA, K.A. (2010). Extension zones in Kurile-Kamchatka and Aleutian island arcs and long-term seismic forecast. *Physical, geological and biological investigations of seas and oceans*. Ed. R.I. Nigmatulin. Nauchnyi mir, Moscow, Russia. 280-300. (In Russian).

VIKULIN A.V. (1986). Variant of long-term seismic forecast for Kamchatsky Bay and Kronotskiyi Penincula. *Vulkanologiya i seismologiya* **3**,72-83. (In Russian).

LAVEROV N.P., LOBKOVSKY L.I., BARANOV B.V., MAZOVA R.KH, KARP B.YA. (2007). Catastrophe on Sumatra: lessons and forecasts. *Nauka v Rossii* **1**, 4–11. (In Russian).

LEVIN V.YE., MAGUS'KIN M.A., BAKHTIAROV V.F. AT AL. (2006). Multi-system geodesic monitoring of recent Earth cruast motions on Kamchatka and Komandorskyskiye Islands. *Vulkanologiya i seismologiya* **3**,54-67.

LOBKOVSKY L.I., MAZOVA R.KH., KATAEVA L.YU., BARANOV B.V. (2006). Generation and propagation of catastrophic tsunamis in the Okhotsk Sea water area. Possible scenarios. *Doklady Academii Nauk* **410**,528-531. (In Russian).

LOBKOVSKY L.I., MAZOVA R.KH., KISEL'MAN B.A., MOROZOVA A.O. (2010). Numerical modeling and spectral analysis of tsunami on November, 15, 2006 in Kurile-Kamchatka region. *Okeanologiya* **50:4**,1-10. (In Russian).

SELIVERSTOV N.I. (1998). Structure of near-Kamchatka water areas and geodynamics of Kurile-Kamchatka and Aleutian island arcs junction area. Nauchnyi mir, Moscow, Russia. (In Russian).

SELIVERSTOV N.I. (2009). Geodynamics of Kurile-Kamchatka and Aleutian island arcs junction area. KamGRU im. Vitusa Beringa. Petropavlovsk-Kamchatsky. Russia. (In Russian).

FEDOTOV S.A. (1965). Regularities of distribution of strong earthquakes on Kamchatka, Kurile Islands and North-Eastern Japan. *Trudy IFZ* **36**, 66-93. (In Russian).

AMMON C.J., C.JI, H.-K. THIO, ET AL. (2005). Rupture Process of the Great Sumatra-Andaman Earthquake. *Science* **308**,1133-1139.

AVÉ LALLEMANT H.G., OLDOW J.S. (2000). Active displacement partitioning and arc-parallel extension of the Aleutian volcanic arc based on Global Positioning System geodesy and kinematic analysis. *Geology* **28:8**, 739-742.

BARANOV, B.V., SELIVERSTOV, N.I., MURAVEV, A.V., ET. AL. (1991). The Komandorskysky Basin as a product of spreading behind a transform plate boundary. *Tectonophysics* **199**,237-269.

CONSOLE R., MURRU M. (1996). Probability gain due to foreshocks following quiescence tested by synthetic catalogs. *Seismological Society of America Bulletin* **86**,911-913.

CORMIER, V.F. (1975). Tectonics near the junction of the Aleutian and Kuril-Kamchatka Arcs and a mechanism for Middle Tertiary magmatism in the Kamchatka Basin. *Geological Society of America Bulletin* **86**,443-453.

DAVIES J.N., SYKES L., HOUSE L., JACOB K. (1981). Shumagin seismic gap, Alaska: History of great earthquakes, tectonic setting and evidence for high seismic potential. *Journal of Geophysical Research* **86**,3821-3855.

DEMETS, C., GORDON, R.G., ARGUS, D.F., ET AL. (1994). Effect of recent revisions to the geomagnetic reversal time scale on estimates of current plate motion. *Geophysical Research Letters* **21**,2191-2194.

FINE I.V., RABINOVICH A.B., THOMSON R.E. (2005). The dual source region for the 2004 Sumatra tsunami. *Geophysical Research Letters* **32**, L16602, doi:10.1029/2005GL023521.

GAEDICKE, CH. BARANOV B., SELIVERSTOV N., ET AL. (2000). Structure of an active arc-continent collision area: the Aleutian–Kamchatka junction. *Tectonophysics* **325,**63–85.

GEIST E.L., CHILDS J.R., SCHOLL D.W. (1988). The origin of summit basins of the Aleutian Ridge: implications for block rotation of an arc massif. *Tectonics* **7:2**,327-341.

HOUSE L.S., SYKES L.R., DAVIES J.N., JACOB K.H. (1981). Identification of a possible seismic gap near Unalaska Island, Eastern Aleutians, Alaska. *Earthquake Prediction – An International Review Maurice Ewing Series* **4**, 81- 92.

JI C. (2005). Magnitude 9.0 earthquake off the west coast of northern Sumatra: Preliminary rupture model, report. U.S.Geol.Surv.,Denver,Colo. http://neic.usgs.gov/neis/eq_depot/2004/eq_041226/neic_slav_ff.html)

MAEDA, K. (1996). The use of foreshocks in probabilistic prediction along the Japan and Kuril Trenches. *Seismological Society of America Bulletin* **86**,242-254.

MCCANN, W., NISHENKO, S.P., SYKES, L.R., KRAUSE, J., (1979). Seismic gaps and plate boundaries: seismic potential for major boundaries. *Pure Applied Geophysics* **117**,1082–1147.

MOGI, K. (1968A). Some features of recent seismic activity in and near Japan (1). *Bull. Earthq. Res. Inst. Tokyo University*. **46**,1225-1235.

MOGI, K. (1968A). Development of aftershock areas of great earthquakes. *Bull. Earthq. Res. Inst. Tokyo University* **46**,175-203.

LAY T., H.KANAMORI, C.J.AMMON, ET AL. (2005). The Great Sumatra-Andaman Earthquake of 26 December 2004. *Science* 30,1127-1133.

LAY T., KANAMORI H. (2011). Insight from the great 2011 Japan earthquake. *Physics Today* December,33–39.

LOBKOVSKY L. I., KERCHMAN V. I., BARANOV B. V., PRISTAVAKINA E. I. (1991). Analysis of seismotectonic processes in subduction zones from the standpoint of a keyboard model of great earthquakes. *Tectonophysics* **199**, 211-236.

LOBKOVSKY L. I., BARANOV B.V., DOZOROVA K.A**.,** MAZOVA R. KH., BARANOVA N.A. The Komandorsky Seismic Gap: Earthquake Prediction and Tsunami Modeling // Proceedings of the Fifth International Tsunami Symposium (ISPRA-2012), Tsunami Society International, 3-5 Sept. 2012, Joint Research Centre, Ispra, Italy, 11page

NISHENKO S.P. (1991). Circum-Pacific seismic potential, 1989-1999. *Pure and Applied Geophysics* 135:2/3, 169-260.

PELINOVSKY, E.N., & MAZOVA R. KH., (1992), Exact analytical solution of nonlinear problem of tsunami wave runup on slops with different profiles, *Natural Hazards*, **6**(3), 227-249.

RUPPERT N. A., LEES J. M., KOZYREVA N. P. (2007). Seismicity, Earthquakes and Structure Along the Alaska-Aleutian and Kamchatka-Kurile Subduction Zones: A Review. In: Volcanism and Subduction: The Kamchatka Region Geophysical Monograph Series 172. American Geophysical Union. 10.1029/172GM12, 129-144.

SHIBAZAKI, B. & MATSU'URA, M. (1995). Foreshocks and pre-events associated with the nucleation of large earthquakes. *Geophysical Research Letters* **22**, 1305-1308.

SMITH W. H. F., SANDWELL D. T. (1977). Global sea floor topography from satellite altimetry and ship depth sounding. *Science* **277**,1956-1962.

STEIN S., OKAL E. (2005). Speed and size of the Sumatra earthquake. *Nature* **434:7053**,581-582.

SYKES, L.R. (1971). Aftershock zones of great earthquakes, seismicity gaps, and earthquake prediction for Alaska and Aleutians. *Journal of Geophysical Research* **76**,8021-8041.

SYKES, L.R., KISSLINGER, J.B., HOUSE, L., DAVIS, J.N., JACOB, K.H., (1981). Rupture Zones and Repeat Times of Great Earthquakes Along the Alaska–Aleutian Arc, 1784–1980. In: Simpson, D.W., Richards, P.G. (Eds.), Earthquake Prediction, an International Review, Maurice Ewing Series, *AGU, Washington, D.C.* **Vol. 4**, 73–80.

VOLTSINGER, N.E., KLEVANNY, K.A., PELINOVSKY, E.N. 1989. Long-wave dynamics of coastal zone (Gidrometeoizdat, Leningrad, USSR, 1989).

WESSON R. L., BOYD O. S., MUELLER C. S., AND FRANKEL A. D. (2008). Challenges in Making a Seismic Hazard Map for Alaska and the Aleutians. In: Active Tectonics and Seismic Potential of Alaska Geophysical Monograph Series 179. American Geophysical Union. P..10.1029/179GM22, 385-397

WYSS M. (1997). Can earthquakes be predicted? *Science* **278; 5337**, 487-490.

ISSN 8755-6839

SCIENCE OF **TSUNAMI HAZARDS**

Journal of Tsunami Society International

Volume 32 **Number 3** **2013**

GEOLOGICAL INVESTIGATION OF PALAEOTSUNAMIS IN THE SAMOAN ISLANDS: INTERIM REPORT AND RESEARCH DIRECTIONS

Shaun Williams[1] , James Goff[2] , Johnny Ah Kau, Faigame Sale[3] , Catherine Chagué-Goff[2,4] and Tim Davies[1]

[1]*Department of Geological Sciences and Natural Hazards Research Centre, University of Canterbury, Christchurch, New Zealand*
[2]*School of Biological, Earth, and Environmental Sciences, University of New South Wales, Sydney, NSW, Australia*
[3]*Geophysics Section, Meteorology Division, Ministry of Natural Resources and Environment, Government of Samoa, Apia, Samoa*
[4]*Australian Nuclear Science and Technology Organisation, Kirrawee, NSW, Australia*

ABSTRACT

The September 29, 2009 Samoa Tsunami provided the opportunity to sample the sediments deposited in the Samoan Islands landscape by the tsunami. Analysing the characteristics of the sediment deposits using an established suite of diagnostic criteria, and assessing how they differ from cyclone deposits enables the identification and dating of similar events in the geologic record. This helps to better understand the long-term frequency and likely magnitude of these events. Here we report on a pilot palaeotsunami field-sampling investigation carried out in 2010 at selected sites on Upolu and Savaii Islands in the Independent State of Samoa, and on Ta'u Island in American Samoa. We present empirical stratigraphic data for the investigated sites, and we demonstrate the existence of high energy marine inundation deposits at some of these sites which were laid down by past tsunamis and/or cyclones. We review and discuss the analytical outcomes, as well as summarise the overarching directions of this research. We propose that there is a need for this study to continue and for such studies to be carried out in other islands in the Pacific. By doing this, we can build on the sparse palaeotsunami database in the region, thereby helping to improve our understanding of the long-term frequency, impact distribution, and likely magnitude of these events. Further, we can start assessing their likely sources and the long-term risk these hazards pose to coastal cities and communities in the Pacific.

Vol. 32, No. 3, page 156 (2013)

1. INTRODUCTION

Following the September 29th 2009 tsunami in the Samoan Islands, public and national calls were made to improve our understanding of the medium- to long-term risks of tsunamis in the archipelago in order to mitigate their impacts. The historical database of tsunamis in Samoa, which extends back to 1837, indicates that these islands have been impacted from all the major source regions within the Pacific Rim of Fire (PARARAS-CARAYANNIS AND DONG, 1980: WILLIAMS AND LEAVASA, 2006). Given that there is virtually no specific reference to tsunamis in Samoa's prehistory (i.e. the approximate 3000 years prior to the arrival of the first official missionaries in 1830), it is difficult to ascertain the long-term frequency and subsequent risk of these hazards to the people of Samoa (WILLIAMS 2009; WILLIAMS ET AL., 2012).

This study aims to improve our long-term understanding of the frequency and magnitude distributions of tsunamis within the Samoan Islands through an interdisciplinary palaeotsunami investigation. Future modelling of potential sources attributed to the identified palaeotsunamis will improve our understanding of the frequency and potential magnitude distributions associated with individual source regions. This information can then be used to re-evaluate the medium- to long-term risk of tsunamis in Samoa.

This work builds on the recommendation made in the United Nations Educational, Scientific and Cultural Organization – Intergovernmental Oceanographic Commission International Tsunami Survey Team (UNESCO-IOC ITST) Interim Field Report of October 2009 for a national palaeotsunami study (DOMINEY-HOWES AND THAMAN, 2009). Preliminary discussions with the Assistant Chief Executive Officer - Meteorology Division of the Ministry of Natural Resources and Environment in February 2010 resulted in the implementation of this collaborative field investigation.

A summary of the provisional observations, local interviews, current analytical outcomes and deductions to date as well as directions for future work is presented.

2. FIELD OBJECTIVES AND METHODS

The overarching concept behind this study is that tsunamis, like cyclones, leave distinct sedimentary evidence in the coastal landscapes they impact (GOFF ET AL, 2001; GOFF ET AL, 2009). Many of these deposits are preserved in wetland environments, although they are not limited to these environment types.

Tsunami and cyclone deposits are generally known as catastrophic saltwater inundation (CSI) events, and distinguishing the two in the field remains a challenge. Recent characteristic and analytical advancements within the global tsunami community have proven successful in distinguishing these events based upon detailed laboratory analysis (e.g. CHAGUÉ-GOFF ET AL., 2011).

This field study involved geological investigations at targeted sites in Upolu, Savaii and Ta'u Islands in order to identify CSIs. These sites are listed in Table 1 and shown in Figure 1. Trenches

were dug at the sites shown in order to record the subsurface sediment stratigraphy and to identify CSI deposits. Sampling of sediment within the trenches was conducted for detailed laboratory analysis of their physical and geochemical characteristics. Core samples were also obtained from the sites shown, which were subsequently logged at the University of Canterbury in New Zealand.

Table 1: Summary of investigated sites.

Site	Coordinate Location	Distance inland from high tide mark (m)	Approximate elevation (m)	Stratigraphic depths (m)
Fagalii	$13^0$50.628' S; $171^0$44.131' W	150	< 10	3
Falealupo	$13^0$29.663' S; $172^0$46.523' W	165	< 10	0.5
Fale o le Fee	$13^0$55.134' S; $171^0$44.285' W	7.5	475	0.6
Lano	$13^0$37.176' S; $172^0$11.938' W	150	< 10	1.5
Ma'asina	$13^0$56.607' S; $171^0$33.585' W	40	< 10	0.7
Manono	$13^0$52.120' S; $172^0$04.263' W	75	< 5	2.5
Mulivai	$14^0$00.505' S; $171^0$47.651' W	25	< 5	1.02
Satitoa	$14^0$01.363' S; $171^0$25.754' W	280	<15	0.84
Satupaitea	$13^0$45.576' S; $172^0$19.209' W	75	< 10	1
Tau	$14^0$13.542' S; $169^0$30.921' W	140	< 5	0.67
Vaovai	$14^0$02.140' S; $171^0$40.832' W	20	< 5	0.72
Vaiula	$14^0$02.361' S; $171^0$39.631' W	100	< 10	0.7

Personal interviews were also conducted at Salimu (Fagaloa) and Vaovai on Upolu, and Lano and Falealupo-tai on Savaii.

Fault scarp sampling of the SE Upolu, Fagaloa and SW Savaii faults was conducted with the long-term objective of cosmogenically dating past landslide activity. These data would help establish

an understanding of the timing of catastrophic coastal landslides (and subsequent tsunamis) which resulted in the exposed escarpments. The assumption for such events occurring in these islands is based on the Ta'u catastrophic landslide scenario presented in Williams et al (2012). Reconnaissance of the Ologogo fault in NW Savaii, the largest fault in Samoa, was also conducted, although sampling was not undertaken due to the lack of accessible scarp outcrops.

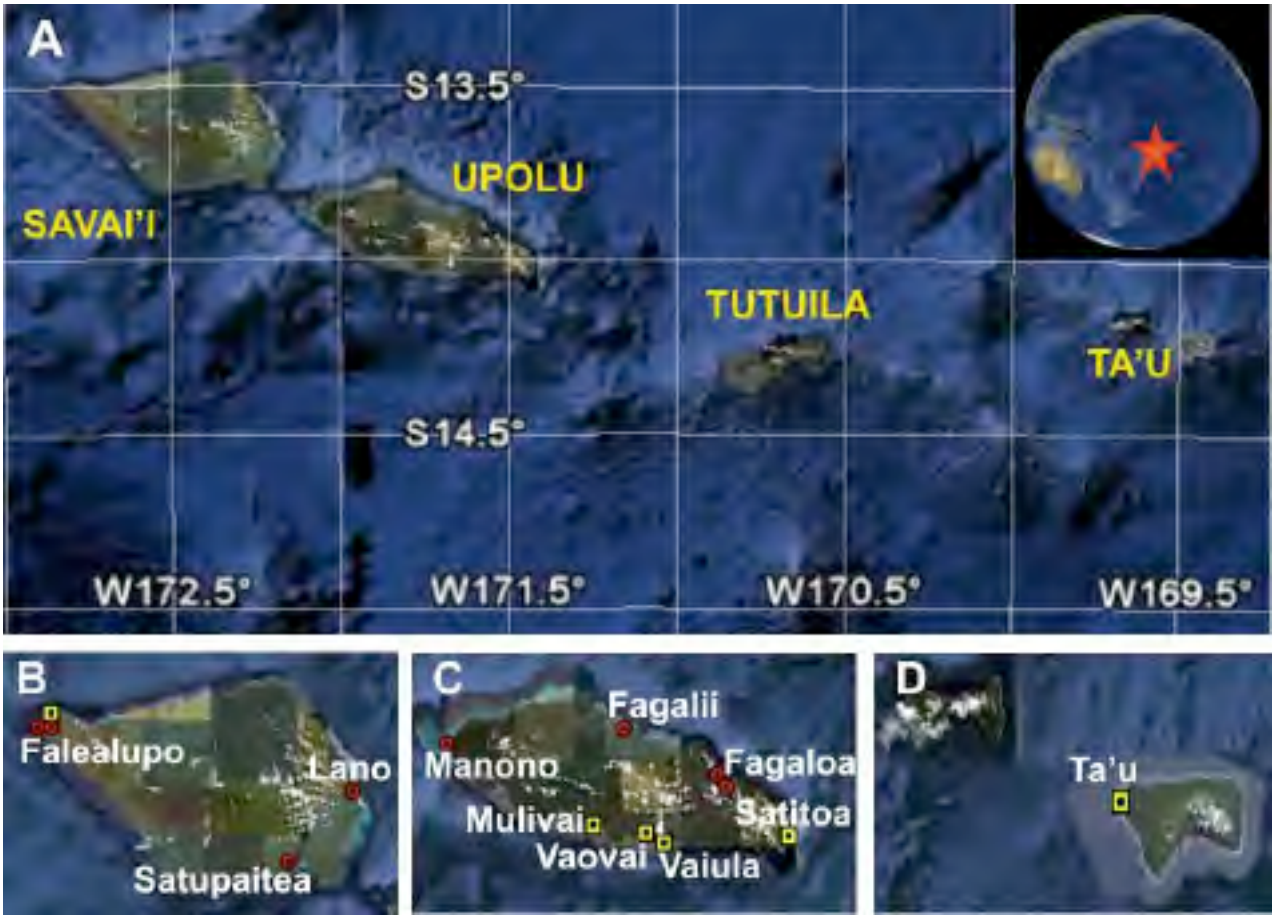

Figure 1: A) Location map of the Samoan Islands; Investigated palaeotsunami sites on B) Savai'i Island; C) Upolu Island; D) Ta'u Island. Yellow squares represent trench-sites and red circles represent core-sites (from Williams et al., 2011a). Note that Ma'asina is located at Fagaloa on NE Upolu.

2.1 Study Sites

Satellite images and field reconnaissance observations were used to select the study sites. Coastal areas with wetland or swamp depositional environments were chosen, followed by field reconnaissance to explore them in terms of their geomorphology and likelihood of preserving CSIs. Most of the areas visited had either been impacted by the 2009 tsunami, or had been impacted by an earlier event.

2.1.1 Trench and core sites

Trench studies were conducted at Mulivai near Coconuts Beach Resort, Vaiula and Vaovai, Satitoa, Falealupo, and Ta'u (Figure 1). A pit trench was also dug at Fale o le Fee to investigate possible calcareous deposits within the area. The Dwarfs Cave (Paia lava tube cave) in Savaii was also visited to investigate whether preserved sand deposits could be found.

Hand-drilled core samples were obtained from Maasina, Fagalii, and Manono-uta on Upolu. On Savaii, they were obtained from Satupaitea, Falealupo-tai, and Lano (Figure 1).

An erosional scour along the coastline at Mulivai (Safata), near the old Hideaway Resort, was also logged, although sampling at this site was not carried out. The stratigraphic log for this site is not presented in this report.

2.1.2 Fault scarps

One rock sample was obtained from the Fagaloa fault scarp on NE Upolu. Another rock sample was obtained from the SE Upolu fault scarp, as well as two rock samples from the SW fault scarp on Savaii. Attempts were made to obtain rock samples from the Ologogo fault on NW Savaii, although this was not completed due to the lack of sufficient scarp outcrops for sampling.

The faults mentioned are assumed to have undergone catastrophic ocean-island flank collapses (landsliding) in the past, with the potential to generate local tsunamis (e.g. WILLIAMS ET AL, 2012). It is planned to date these samples cosmogenically in order to constrain the likely ages of the respective collapses.

Figure 2: Stratigraphy of Mulivai trench showing six layered deposits. Layer 1 represents the 2009 tsunami deposit. Two more layers below Layer 6 are shown in Figure 3 below - not visible in this photograph due to obscuring from groundwater at Layer 6.

3. RESULTS AND OUTCOMES

Below are preliminary results associated with the investigated sites, based on field work observations. Hence, they should be treated as such. Detailed results will be reported in the future following laboratory analysis of the collected samples.

3.1 Trench logs

The subsurface stratigraphy associated with each trench was logged empirically. These serve as a benchmark for comparison with the (pending) detailed laboratory analysis of samples associated with each trench.

3.1.1 Mulivai trench (near Coconuts Beach Resort)

The trench at Mulivai was located at $14^0$00.505' S; $171^0$47.651' W, approximately 25 m inland from the high-tide water mark. A depth of 1.02m was logged (Figures 2 and 3), with bulk samples obtained from individual beds. Approximately 3 to 4 CSIs were identified empirically; the 2009 tsunami deposit at the surface, possibly the 1990 Cyclone Ofa (READY AND WOODCOCK, 1992) and the1991 Cyclone Val (ELMQVIST ET AL., 1994), and a CSI beneath the fibrous peat layer at > 1m depth.

^{14}C dating of the organic peat (sample number Wk30084) at ~1m depth (Layer 7 in Figure 3), yielded an upper-radiocarbon age limit of 528 ± 91 BP for the identified CSI at the base of the log (WILLIAMS ET AL., 2011A).

3.1.2 Vaiula trench

The trench at Vaiula was located at $14^0$02.361' S; $171^0$39.631' W, approximately 100 m inland from the high-tide water mark. A depth of 0.7 m was logged (Figures 3 and 4), with bulk sampling obtained from individual beds.

The 2009 tsunami is represented by a thin silty-sand deposit on the surface overlying a soil. A sequence of 6 layers was noted below this soil layer, and it is difficult to ascertain at this point whether this represents a series of different CSI events, or a combination of 1 or 2, with the layers representing different wave energies associated with a single event.

3.1.3 Vaovai trench

The trench at Vaovai was located at $14^0$02.140' S; $171^0$40.832' W, approximately 20 m inland from the present-day high-tide water mark. A depth of 0.72 m was logged, with detailed 1 cm sampling down to the base of the trench.

Approximately 3 to 4 CSIs were identified empirically; the 2009 tsunami deposit at the surface. It is possible that the CSI identified in layer 5 of the stratigraphic log (Figure 3) may be associated with the 1990 and 1991 cyclones.

A local *matai* (chief), Leleimalefao Ionatana, was interviewed and reported that his grandfather had told him a story of a strong earthquake and subsequent tsunami he had experienced while a child. The wave had swept through their village at night, although minimal damaged was experienced. Leleimalefao was born in 1957, meaning it is highly likely the story his grandfather

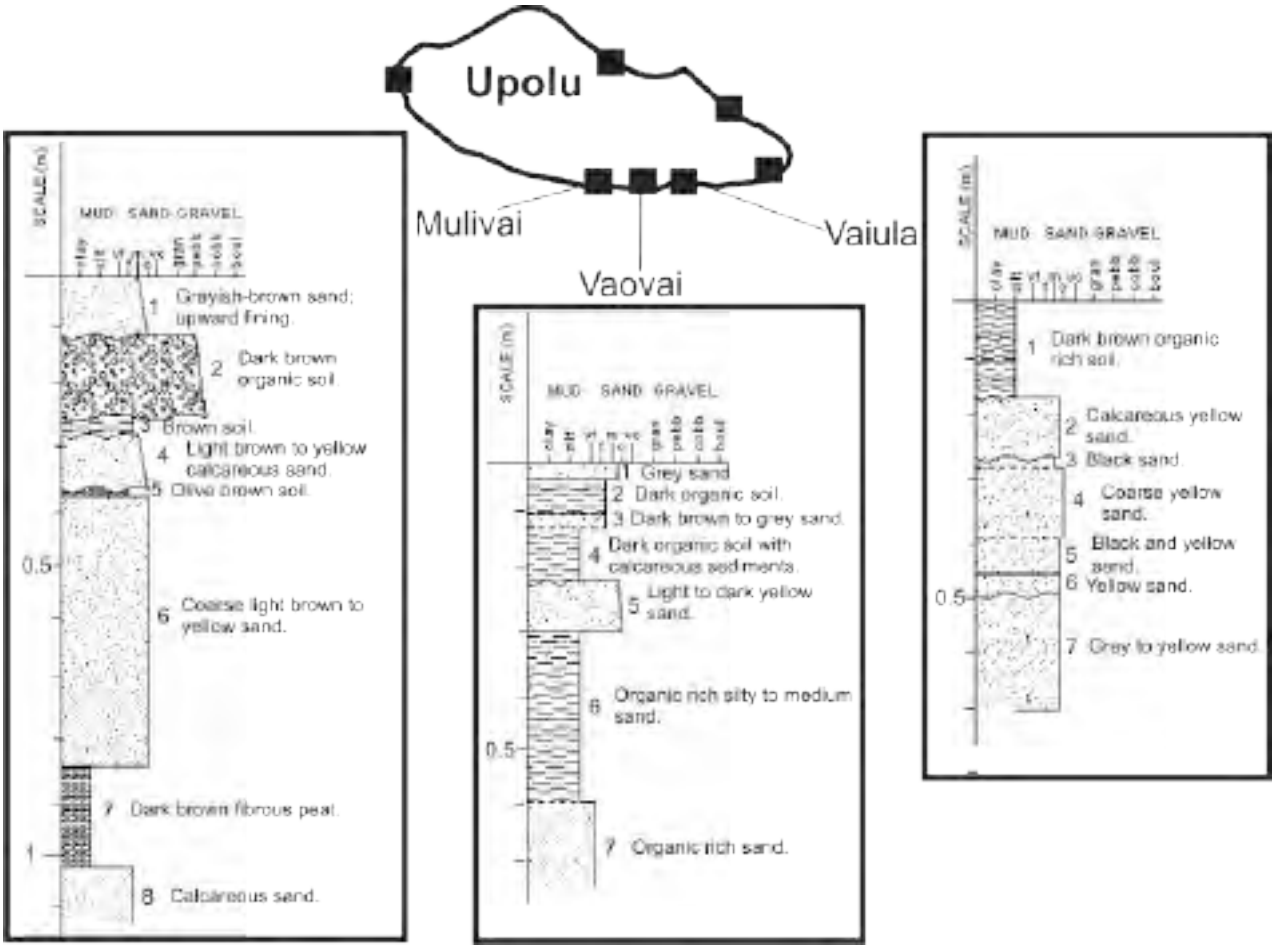

Figure 3: Empirical stratigraphic logs from Mulivai, Vaovai, and Vaiula trench sites on the south of Upolu Island. Stratigraphic depths shown are in metres. Sand particle sizes shown are; vc – very coarse; c – coarse; m – medium; f – fine; vf – very fine.

told him refers to the 1917 tsunami; assuming two generations (50 years) in the past. The 1917 tsunami originated from an M_{PAS} 8.7 earthquake at the northern Tongan Subduction bend (OKAL ET AL., 2011), about 200 km south of Falealupo and 120 km west of the 29/09 earthquake epicentre and 2009 Tsunami source. The earthquake occurred at 6:50 pm on June 25th 1917. However, there is no report in the tsunami catalogue (PARARAS-CARRAYANIS-AND DONG, 1980) of an inundation time. The fact that a strong earthquake was felt prior to the tsunami means it was local, suggesting it was most likely to be the 1917 event. Also, the fact that the wave was experienced at night further strengthens this argument since the 1917 earthquake occurred at 6:50 pm (night time) on a dry-season day. The tsunami would have inundated the Samoan islands several minutes after the earthquake; similar to the 2009 Tsunami impact time (DOMINEY-HOWES AND THAMAN, 2009; OKAL ET AL., 2011).

^{14}C-dating of an unidentified gastropod (sample number Wk30089) obtained from layer 7 in Figure 3 yielded a radiocarbon age of 576 ± 33 BP (Williams et al., 2011a). The dated gastropod is assumed to represent the age of the deposit.

Figure 4: Photograph of Vaiula L-shaped trench taken from (a) south and (b) east end of trench. (c) Northeast corner of trench which was logged (see Figure 5) and sampled.

3.1.4 Satitoa trench

The trench at Satitoa was located at 14^{0}01.363' S; 171^{0}25.754' W, approximately 280 m inland from the present-day high-tide water mark. A depth of 0.84 m was logged (Figure 5), with detailed 1 cm sampling down to 20 cm depth, followed by 2 cm sampling down to the base of the trench.

Approximately 5 to 7 CSIs were identified empirically with the 2009 tsunami deposit at the surface. There was equivocal evidence of deposits that may have been associated with the 1990 and 1991 Cyclones Ofa and Val suggesting that either these events did not impact far inland, that they did not leave any deposits, or the deposits were not preserved.

Interestingly, three pebbly layers were found within a silty-clay soil layer intermixed with calcareous sands, and two distinct calcareous sand deposits towards the base of the trench. It is likely that these are tsunami deposits; and the upper-age of the event directly below the organic layer at ~0.7 m depth can be constrained by ^{14}C-dating of the overlying organics.

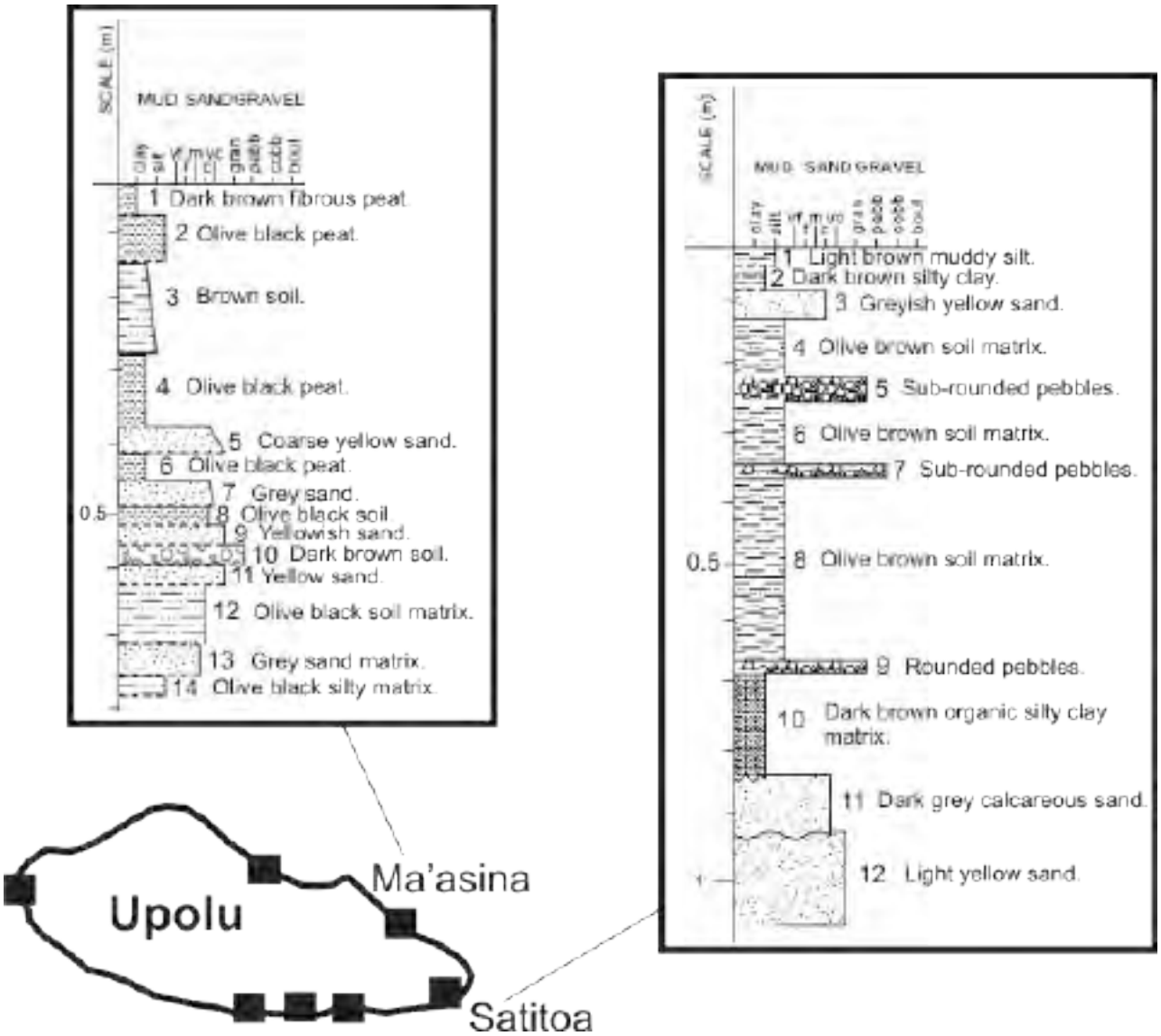

Figure 5: Empirical stratigraphic logs at Satitoa trench site on SE Upolu Island, and Ma'asina core site on NE Upolu. Stratigraphic depths shown are in metres.

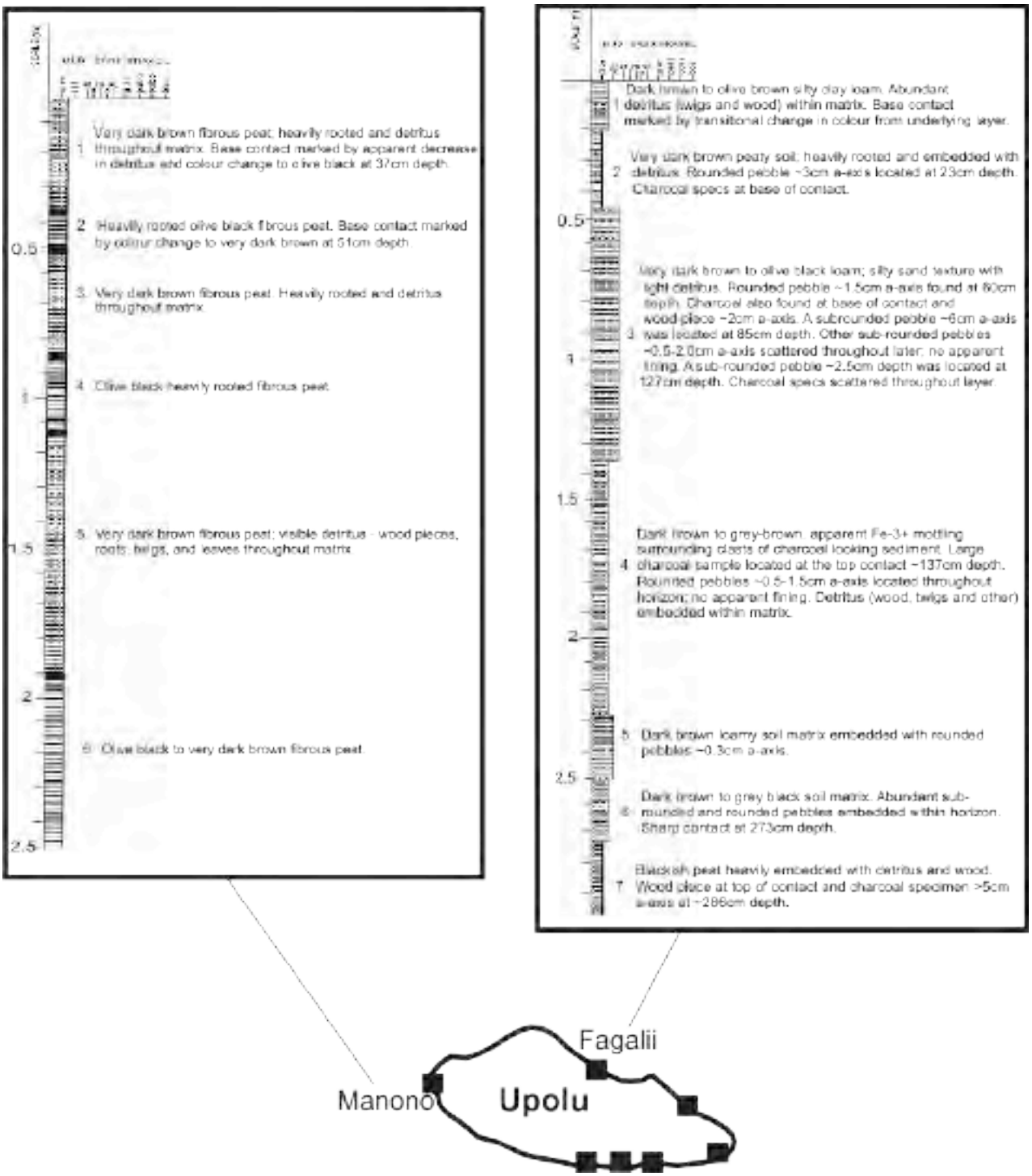

Figure 6: Empirical stratigraphic logs at Fagali'i and Manono core sites on north and west Upolu Island, respectively. Stratigraphic depths shown are in metres.

3.1.5 Falealupo trench

The trench at Falealupo was located at $13^0$29.663' S; $172^0$46.523' W, approximately 165 m inland from the present-day high-tide water mark. A 3.5 m high and 5 m wide storm berm (resembling a sand-dune) was present at the coastline. A depth of 0.5 m was logged at the trench site (Figure 7), with sampling in 1 cm intervals down to 20 cm depth, followed by 2 cm sampling down to the base of the trench.

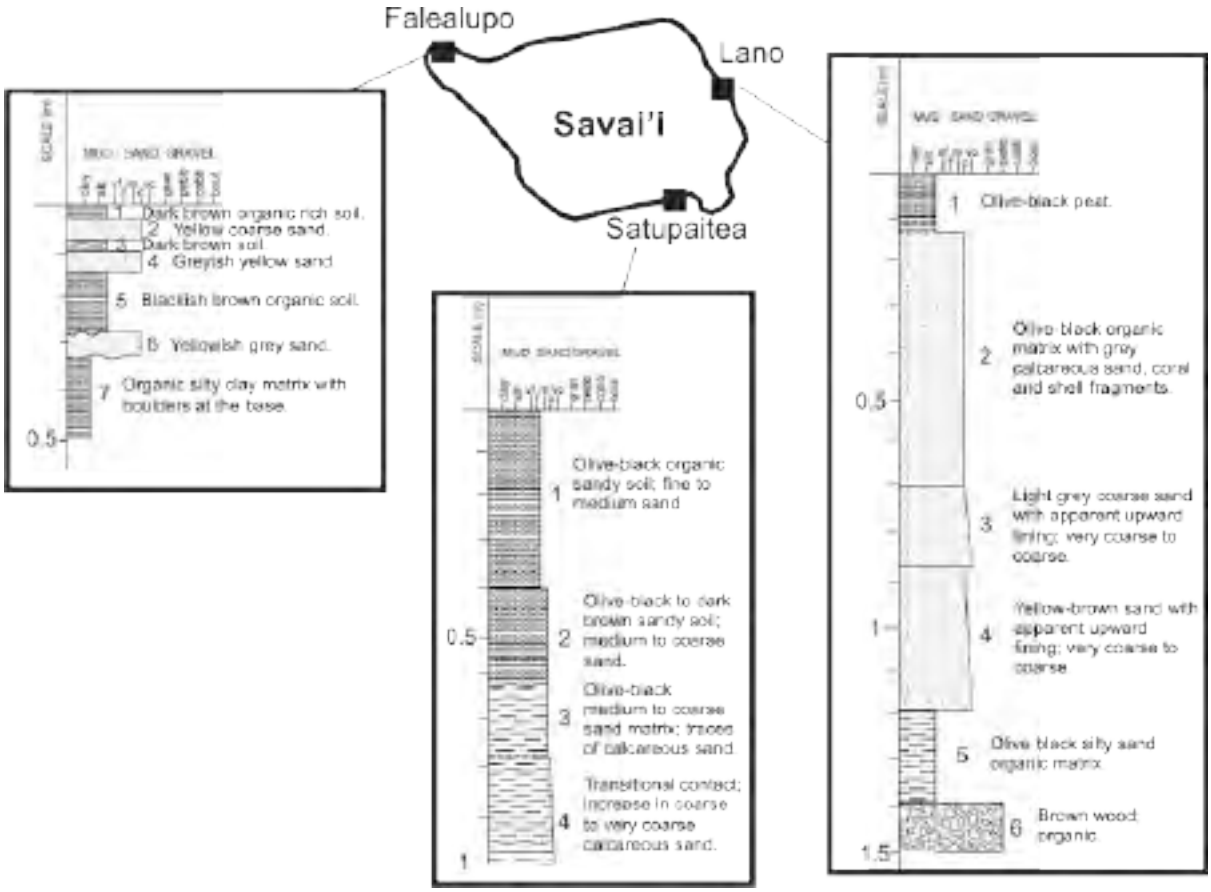

Figure 7: Empirical stratigraphic logs at Falealupo trench site on west Savai'i Island, and Lano and Satupaitea core sites on NE and SE Savai'i, respectively. Stratigraphic depths shown are in metres.

This site presents an interesting case as the primary goal was to investigate the 1990 and 1991 cyclones Ofa and Val deposits, which would serve as a baseline for distinguishing cyclone from tsunami deposits within this area. These events are most likely represented by the fine sand deposit directly beneath the surface soil layer.

The third sequence shown in Figure 8 likely represents the pre-1990 soil, while the coarse sand layer beneath that may have been deposited by an historical tsunami, possibly the 1917 tsunami. A local Falealupo resident, Mrs. Siuli Togia, reported that her father, born in 1886, told her a story of a large wave which swept through their village when he was a child. Apparently, he was returning to

the coast from their inland plantation when he saw a large wave sweep through their property, taking with it his parents. Fortunately he was able to swim out and rescue them using a log as a raft to haul them back to shore. It is very likely that this narrative is an account of the 1917 tsunami which impacted the Samoan islands.

The yellowish coarse sand deposit sandwiched between the two organic layers possibly represents an earlier tsunami. The 1990 Ofa and 1991 Val Cyclones are assumed to have laid down very-fine to fine sand deposits (layer 2 and 4, respectively, in Figure 7).

In this instance, a coarser sand deposit most likely indicates higher wave energy penetrating into the coastal environment. Also, boulders up to 30 cm a-axis were noted within the organic silty layers which sandwich the lower calcareous sand deposit, indicating that they were deposited by high wave energy events.

3.1.6 Ta'u trench

The 0.67 m trench at Ta'u was located at 14^{0}13.542' S; 169^{0}30.921' W, approximately 140 m inland of the present high tide water mark. Only two distinct sequences were observed in the stratigraphy (Figure 8). A sharp contact at approximately 51 cm depth separates the overlying organic soil horizon from the underlying very coarse, greying yellow calcareous sand deposit. This deposit also comprised coral cobbles (branching and brain corals), gastropod and other unidentified shells, as well as rounded basalt cobbles towards the base of the deposit matrix (WILLIAMS ET AL., 2011A).

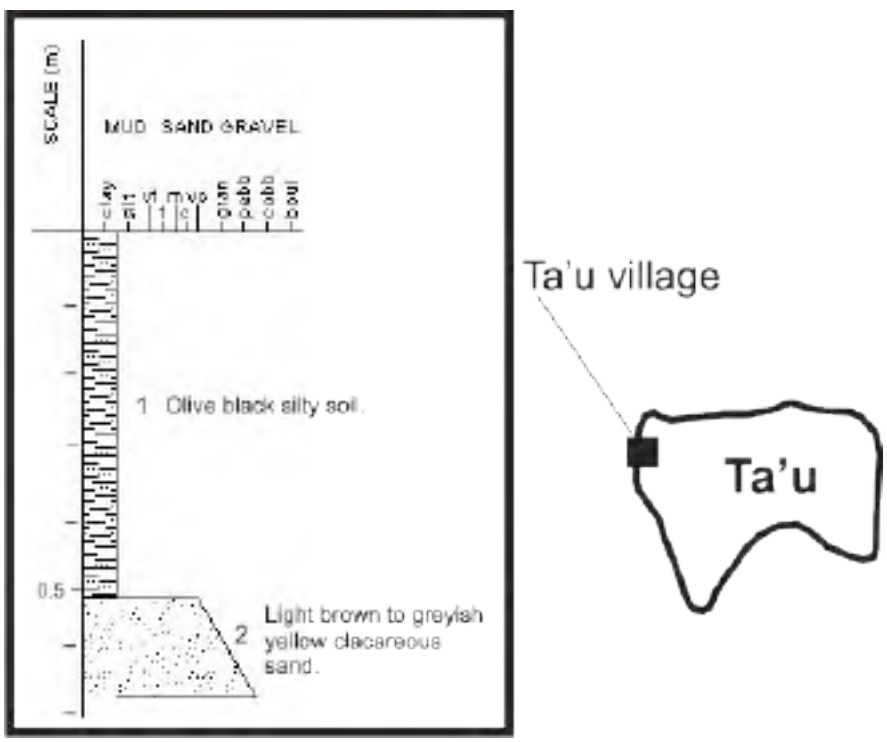

Figure 8: Empirical stratigraphic log at Ta'u trench site on NW Ta'u Island. Stratigraphic depth shown is in metres.

Recent Category 5 cyclones (eg. Cyclones Ofa in 1990 and Val in 1991 and Cyclone Heta in 2004 (MARRA ET AL., 2008) which have impacted this island had insufficient wave energy to inundate 140 m inland, and hence there is no evidence of deposits associated with recent cyclone activity at the site. Sequence 2 likely represents a high wave energy deposition source sufficient to transport the denser coral and basalt cobbles observed within the matrix. It is empirically assumed that this deposit is likely associated with a tsunami origin (WILLIAMS ET AL., 2011A), although further research is required to ascertain this.

3.1.7 Fale o le Fe'e reconnaissance pit-trench

Reconnaissance to Fale o le Fe'e was conducted in order to investigate the local belief that calcareous coastal deposits are present at the site. The site is ~7.5 km inland (south) of Apia and 475 m in elevation. The site is culturally significant in that it is the residence of the ancient war God of A'ana, the God Fe'e. It was visited to investigate whether coastal deposits are found this far inland, and what processes might have been involved in their deposition.

Reverend J.B Stair visited the site in 1845 and concluded that the (believed) limestone pillars and house remnants were basalts mined from a nearby outcrop (STAIR, 1894). He also concluded that (believed) corals on the nearby stream bed were actually stalagmites and calcareous spar which formed on the surface of outcrops, in association with the nearby stream.

Field observations made during this reconnaissance confirmed the former. Dense olivine basalt outcrops associated with the Salani volcanics (KEAR AND WOOD, 1959), appear to have been where the house pillars and associated building (rock) material were mined. The basalts appear to have a calcitic skin on their surface giving it a light grey colour, which likely formed as a result of secondary mineralisation of Mg/Fe olivines as they interact with CO_2 in air and water. The basalts also fracture prismatically and appear to resemble limestone at first glance. However, upon examining a few samples, visible olivine crystals ~1-3 mm along their a-axis can be seen embedded within a mafic matrix.

The (assumed) coral deposits further upstream of the site were not observed. A small calcitic pillar, including small stalactites and stalagmites were observed (during this study) in the Dwarf's lava-tube cave at Paia on Savaii; also located on olivine basalts. It is highly likely that Stair's conclusions of the calcitic like material he observed at Fale o le Fe'e formed in a similar way to that observed in the Dwarf's cave, and that they are not coastal calcareous deposits.

Calcite ($CaCO_3$) minerals formed at the coast are mainly derived from the fossils of calcareous marine organisms (Morse et al., 2007), whereas calcite formed within basalts is due to secondary mineralisation (a weathering process) involving CO_2-water-rock interactions (MATTER AND TAKAHASHI, 2007).

A pit-trench was also dug in order to rule out the possibility of a distinct sand deposit at depth (Figure 8). Interestingly, a well-preserved charcoal layer was observed at ~0.35 m depth, and is assumed to be anthropogenic. C^{14} dating of a sample (sample number Wk30088) of this charcoal presented in Williams (2011a) showed this deposit to have a radiocarbon age of 398 ± 73 BP; provisionally suggesting that likely worshipers of Fe'e occupied or used the site around this time.

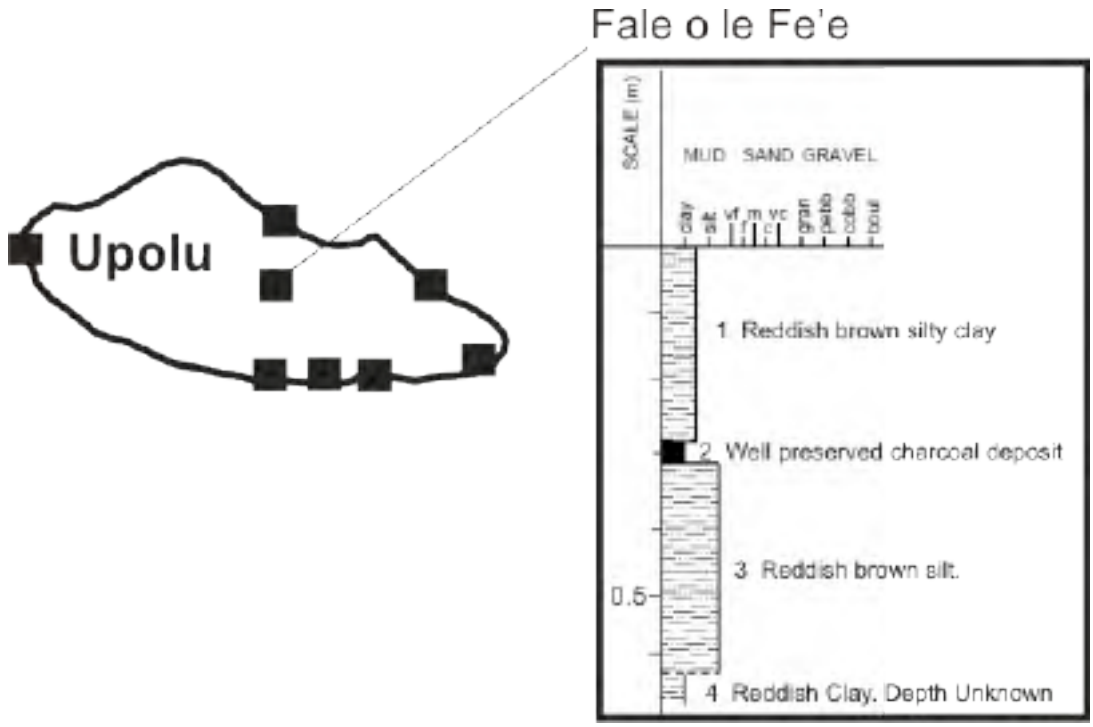

Figure 9: Empirical stratigraphic log at Fale o le Fe'e trench site on Upolu Island. Stratigraphic depth shown is in metres.

3.2 Core samples:

Core samples were obtained from the locations shown in Figure 1. The cores were not logged in the field due to time constraints. Logging and detailed laboratory analysis of the samples will be conducted in due course.

3.1.8 Ma'asina core sample

A 0.7 m core was obtained from Ma'asina village (Fagaloa Bay) in a small coastal marsh ~40 m inland of the high-tide mark A sand deposit was observed at approximately 0.4 – 0.8 m depth (Figure 8).

The historical database indicates that Fagaloa Bay has been impacted by tsunamis causing destructive damages in 1952, 1957, and 1960. The 1952 (1.8 m wave) and 1960 (2.4 m wave) tsunamis originated from major earthquakes in the Chile/Peru region. The 1957 (1.5 m wave) tsunami originated from an 8.5 magnitude earthquake in the Aleutian Islands (PARARAS-CARAYANNIS AND DONG, 1980).

3.1.9 Fagalii core sample

A 3 m core was obtained from a swamp at Fagalii village located at $13^0$50.628' S; $171^0$44.131' W, within the 8 km radius of Apia Township. The site was located ~150 m inland of the high-tide water mark, and directly behind the current Minister of Communication and Information Technology's residence.

No apparent CSI deposits were observed (Figure 6), although detailed laboratory analysis will clarify this. Interestingly, a charcoal deposit was observed at ~2.9 m depth which is likely to be anthropogenic. If the sample is found to be anthropogenic and older than 2800 BP, this finding could represent evidence for initial human settlement in Upolu older than the currently accepted ~2800 BP (DICKINSON AND GREEN, 2008). ^{14}C-dating of this sample (sample number Wk30087) yielded a radiocarbon age of 3,112 ± 50 BP (WILLIAMS ET AL., 2011A), but further study is required to ascertain its origin.

Historically, the most destructive tsunami to have impacted the Apia region was on 14 August 1868, which originated from a major earthquake in the Peru/Chile region (PARARAS-CARAYANNIS AND DONG, 1980). It was reported that the tsunami destroyed buildings in Apia, although there were no detailed accounts on the geographic extent and magnitude of damage, nor on loss of life.

3.1.10 Manono-uta core sample

A 2.5 m core was obtained from the Manono-uta marsh located at $13^0$52.120' S; $172^0$04.263' W, ~75 m inland of the high-tide water mark. No apparent CSI deposits were observed (Figure 6), although detailed laboratory analysis will clarify this. The site was chosen to identify CSIs which may have impacted east Upolu.

3.1.11 Lano core sample

A 1.5 m core was obtained from a swamp at Lano village, located at $13^0$37.176' S; $172^0$11.938' W; ~150 m inland of the high-tide mark. A distinct CSI deposit was observed at ~1 m depth (layer 4 in Figure 7). ^{14}C-dating of plant fragments (sample number Wk30083) obtained from layer 5 at 1.4 m depth yielded a radiocarbon age of ~798 ± 28 BP (WILLIAMS ET AL., 2011A). Detailed laboratory analysis of organics above and below the deposit will help to establish its age. This site was chosen to identify events along NE Savaii.

3.1.12 Falealupo core samples

Two core samples were obtained from two separate swamps at Falealupo. Falealupo Core-1 (FC-01) was located at $13^0$30.064' S; $172^0$47.161' W ~220 m inland of the high-tide water mark. Falealupo Core-2 (FC-02) was located at $13^0$29.670' S; $172^0$46.521' W ~160 m Inland of the high tide water mark. Both cores reached 1 m in depth, and FC-02 appeared to have 2 or 3 CSIs within them. These cores were subsequently not selected for analysis as the samples obtained from Falealupo trench (see Section 3.1.5) were sufficient for the purposes of this study.

3.1.13 Satupaitea core sample

A 1 m core sample was obtained from a swamp located at $13^0$45.576' S; $172^0$19.209' W, ~75 m inland of the high-tide water mark. The Satupaitea coastal area comprised mainly black sandy

sediments derived from inland basalts that have been transported to the coast by a network of streams and rivers, and some re-deposited by waves. Two distinct calcareous deposits were observed at 0.8 m and 0.95 m depths (Figure 7), indicating two separate CSI events. This area was chosen to identify events which may have impacted SE Savaii.

3.2 Personal Interviews

Four interviews were carried out at Salimu (Fagaloa Bay) and Vaovai on Upolu, as well as Lano and Falealupo on Savaii. One individual from each village was interviewed. Questions asked centred on any local stories related to tsunamis or unusual wave activity which were either experienced by the individuals or were told by older generations.

3.2.1 Salimu-Fagaloa interview

A 67 year old local *matai* from Salimu (Fagaloa), Limu Filifilia, stated that he had known of two unusual waves to have impacted his village while he was a teenager. The first one had slightly inundated Salimu, but had transported the local medical barge across the other side of the harbour and deposited it on the reef adjacent to Ma'asina (Fagaloa). Several years later, another wave struck which brought the barge back to its present day location (Figure 10).

Figure 10: Fagaloa harbour showing the present-day barge location relative to Salimu and Ma'asina villages. Photograph is taken facing north, and the straight-line distance from Salimu to Ma'asina is ~1.3km (standing are J. Ah Kau – left; and F. Sale – right).

The events he described are most likely the 1957 and 1960 tsunamis which impacted Fagaloa harbour. The 1957 tsunami originated from an 8.5 earthquake in the Aleutian Islands which ruptured at 3:22 am (local Samoan time) on March 9th. It had a 9 hour travel time, meaning it would have impacted Fagaloa bay at approximately 12:22 pm. 1.5 m and 1.05 m waves were reported at Taelefaga and Maasina villages, respectively (PARARAS-CARAYANNIS AND DONG, 1980).

The 1960 tsunami originated from an Mw 9.5 earthquake in the south Chile region which ruptured at 8:11am (local Samoan time) on May 22nd (PARARAS-CARAYANNIS AND DONG, 1980). The tsunami had a travel time 12.4 hours, meaning it would have impacted Fagaloa at approximately 9:00pm. 2.4 m waves reportedly inundated villages at Fagaloa, causing damage and flooding to local huts.

3.2.2 Vaovai interview

Refer to Section 3.1.3 for an account of the story told by Leleimalefao Ionatana (local matai of Vaovai village).

3.2.3 Lano interview

The late *sa'o* (head *matai*) of Lano village, afioga Vui Vaea (82 years of age in 2010), told of calcareous boulders which were deposited about 70 m inland from the core site. A local Lano story passed down to him while he was a child stated that the boulders were deposited by a large wave ages before. He viewed these coralline boulders when he was young and stated that they had average a-axes greater than 20 cm. There is no mention as to the timing of the event, and he did not indicate that it occurred during his parents or grandparents' generation. These boulders have since been removed due to recent development in the area, but it is likely they were deposited by a palaeotsunami. Further detailed geological studies in the area would be useful to clarify the nature and extent of this event.

3.2.4 Falealupo interview

Refer to Section 3.1.5 for an account of the story told by Mrs. Siuli Togia (local Falealupo-tai resident).

4. REVIEW OF PRESENT ANALYTICAL OUTCOMES

The samples collected were processed using a set of multi-proxy diagnostic criteria in relevant laboratories at the Universities of Canterbury and Waikato in New Zealand, and at the Australian Nuclear Science and Technology Organisation in Australia. The diagnostic proxy criteria used included sedimentological (stratigraphic logging, loss on ignition and grain size distributions), geochemical (elemental profiles), and geochronological (^{14}C and ^{210}Pb dating) techniques.

While the data are currently being analysed and will be communicated in due course, preliminary geochemical and geochronological aspects of the project were presented in Williams et al. (2011a and 2011b). Using elemental data collected with a portable X-Ray fluorescence spectrometer; it was found that the Ca/Fe and Ca/Ti ratio-relationships for the 2009 Samoa Tsunami deposits at investigated impact sites could be used to identify similar high energy deposits in their respective geologic records. However it was acknowledged that elemental proxies alone were insufficient in distinguishing between a tsunami and a cyclone deposit (WILLIAMS ET AL., 2011A, 2011B).

In some cases (eg. Satitoa and Ta'u), high energy deposits identified were provisionally assumed to be of a tsunami origin due to their relative locations inland from mean sea level. Moreover, we observed no evidence of any deposits at these sites which might have formed from recent cyclones over the past several decades, such as from Cyclones Ofa in 1990 and Val in 1991 (Ready and Woodcock, 1992; Elmqvist et al., 1994), and Cyclone Heta in 2004 (Marra et al., 2008).

In the case of Satitoa, a ^{14}C radiocarbon age obtained from the soil horizon (~0.81 m stratigraphic depth), overlying the assumed tsunami deposit provisionally suggests that the deposit may have been laid down by the 1917 Samoa Tsunami.

At Mulivai (near Coconuts Beach Resort) and Vaovai sites, high energy deposits with radiocarbon ages of ~437 – 619 BP (see Sections 3.1.1 and 3.1.3) were identified at both sites, respectively. Although it was assumed the respective deposits were formed by the same event, it was uncertain whether the deposits were of a tsunami or cyclone origin.

5. SUMMARY AND DIRECTIONS FOR FUTURE WORK

While the outcomes to date provide a provisional basis for starting to understand the long-term impacts of tsunamis at the investigated sites, much work remains to be carried out in order to allow us to draw conclusive evidence to distinguish between deposits of tsunami or cyclone origin. Only coupled with a suite of multi-proxy criteria (e.g. Goff et al., 2001; 2004; 2011; 2012; Morton et al., 2007; Chagué-Goff et al., 2011; Richmond et al., 2011), and assessed in the broader regional geochronological context can we develop more robust conclusions.

Further palaeotsunami studies on other islands and nations in the Pacific are required, as they can serve as point-sources of potential palaeotsunami information. This would contribute to the existing, but sparse, palaeotsunami database for the region, and would contribute to our geochronological and spatial understanding of long-term tsunami impacts. By doing this, we can start to better understand the long-term risk of coastal communities to tsunami hazards in the Pacific.

6. ACKNOWLEDGEMENTS

We thank Taulealeausumai Laavasa Malua, Mulipola Ausetalia Titimaea, the late Vui Vaea, Sulamanaia Montini Ott, Limu Filifilia, Leleimalefao Ionatana, Siuli Togia, Kwok Fai Cheung, Gegar Prasetya, Thomas Wilson, Kerry Swanson, Cathy Higgins, Bruce Kaiser, Geraldine Jacobsen, Atun Zawadzki, Henk Heijnis, Alan Hogg, Fiona Petchey, Yoshiki Yamazaki, Volker Roeber, Joshua Blackstock, Jarg Pettinga, Seong-Pil Kim, Jens Kruger, Litea Biukoto, Keleni Raqisia, Joan Williams, Jim Williams, Sialei (Sape) Vui, Pauli Ivan Williams, Leilua Mase Akapo, Moki Leoso, Chris Grimshaw, Peter McGuigan, Carolyn Boultan, and John Wardman for their help regarding various aspects of the project.

We acknowledge and thank the Macmillan Brown Centre for Pacific Studies – University of Canterbury, NZ-Fulbright Programme (IIE Grantee #15101271), the Department of Geological Sciences and Mason Trust – University of Canterbury, the Australian Institute for Nuclear Science and Engineering (Grant #ALNGRA12119P), the Building Research Capability in the Social Sciences Programme – Massey University, and Samoa Builders' Supplies & ACE Hardware Ltd for funding various aspects of this research to date.

7. REFERENCES

CHAGUÉ-GOFF, C., SCHNEIDER, J.-L., GOFF, J.R., DOMINEY-HOWES, D. AND STROTZ, L. 2011. Expanding the proxy toolkit to help identify past events: Lessons from the 2004 Indian Ocean Tsunami and the 2009 South Pacific Tsunami. *Earth-Science Reviews*, 107, 107-122.

DICKINSON, W.R., GREEN, R.C. (1998). Geoarchaeological Context of Holocene Subsidence at the Ferry Berth Lapita Site, Mulifanua, Upolu, Samoa. *Geoarchaeology: An International Journal*, 13 (3): 239–263.

DOMINEY-HOWES, D., THAMAN, R., (2009). UNESCO-IOC International Tsunami Survey Team Samoa: Interim Report of Field Survey 14th – 21st October 2009. Australian Tsunami Research Centre Miscellaneous Report No.2, October 2009.

ELMQVIST, T., RAINEY, W.E., PIERSON, E.D., COX, P.A. (1994). Effects of tropical cyclones Ofa and Val on the structure of a Samoan lowland rain forest. *Biotropica,* 26 (4): 384-391.

GOFF, J., CHAGUÉ-GOFF, C., NICHOL, S. (2001). Palaeotsunami deposits: a New Zealand perspective. *Sedimentary Geology*, 143: 1-6.

GOFF, J., MCFADGEN, B. AND CHAGUÉ-GOFF, C., 2004. Sedimentary differences between the 2002 Easter storm and the 15th-century Okoropunga tsunami, southeastern North Island, New Zealand. *Marine Geology*, 204: 235-260.

Goff, J., Nichol, S., Kennedy, D. (2009). Development of a palaeotsunami database for New Zealand. *Natural Hazards*. DOI: 10.1007/s11069-009-9461-5.

GOFF, J., CHAGUÉ-GOFF, C., DOMINEY-HOWES, D., MCADOO, B., CRONIN, S., BONTÉ-GRAPETIN, M., NICHOL, S., HORROCKS, M., CISTERNAS, M., LAMARCHE, G., PELLETIER, B., JAFFE, B., DUDLEY, W. (2011). Palaeotsunamis in the Pacific Islands. *Earth-Science Reviews*, 107 (2011): 141–146.

GOFF, J., CHAGUÉ-GOFF, C., NICHOL, S.L., JAFFE, B. AND DOMINEY-HOWES, D. (2012). Progress in palaeotsunami research. *Sedimentary Geology,* 243-244, 70-88.

KEAR, D., WOOD, B.L., (1959). The Geology and Hydrology of Western Samoa. New Zealand Geological Survey Bulletin (No.63).

MARRA, J.J., KARI, U.S., SABBATELLI, T.A. (2008). Anatomies of historical storm events in the Pacific. *Proceedings of the Solutions to Coastal Disasters Congress,* 2008, 312: 222-228.

MATTER, J.M., TAKAHASHI, T., 2007. Experimental evaluation of in-situ CO_2-water-rock reactions during CO_2 injection in basaltic rocks: Implications for geological CO_2 sequestration. *Geochemistry Geophysics Geosystems,* 8 (2): 19 pp.

MORSE, J.W., ARVIDSON, R.S., LÜTTGE, A., (2007). Calcium Carbonate Formation and Dissolution. *Chemical Reviews,* 107: 342 – 381.

MORTON, R.A., GELFENBAUM, G. AND JAFFE, B.E., 2007. Physical criteria for distinguishing sandy tsunami and storm deposits using modern examples. *Sedimentary Geology*, 200(3-4): 184-207.

OKAL, E., BORRERO, J. AND CHAGUÉ-GOFF, C., 2011. Tsunamigenic predecessors to the 2009 Samoa earthquake. *Earth-Science Reviews*, 107: 127-140.

PARARAS-CARAYANNIS, G., DONG, B., (1980). Catalog of Tsunamis in the Samoan Islands. International Tsunami Information Center, Honolulu, 75 pp.

READY, S., WOODCOCK, F. (1992). The South Pacific and southeast Indian Ocean tropical cyclone season 1989-1990. *Australian Meteorological Magazine,* 40 (2): 111-121

RICHMOND, B.M., WATT, S., BUCKLEY, M., JAFFE, B.E., GELFENBAUM, G., MORTON, R.A. (2011). Recent storm and tsunami coarse-clast deposit characteristics, southeast Hawai'i. *Marine Geology*, 283 (1-4): 79-89.

STAIR, J.B., (1894). "O le Fale o le Fe'e": or, ruins of an old Samoan temple. *The Journal of the Polynesian Society*, 3 (4): 239-244

WILLIAMS, S.P., (2009). Ocean-island flank collapse on the south of Ta'u, Manu'a Group, Samoa Islands: Implications for risk management. MSc Thesis. Department of Geological Sciences, University of Canterbury, NZ. UC Library Repository (http://hdl.handle.net/10092/3784).

WILLIAMS, S.P., LEAVASA, A.F.M., (2006). Exploring the status of tsunami early warning systems in Samoa. In: Taulealo, T., (ed). *Proceedings of the Samoa National Environment Forum 2005*. pp. 52-58

WILLIAMS, S., GOFF, J., PRASETYA, G., CHEUNG, K.F., CHAGUÉ-GOFF, C., DAVIES, T., WILSON, T. (2011A). Characterising diagnostic proxies for identifying palaeotsunamis in a tropical climatic regime, Samoan Islands. *OCEANS'11 - MTS/IEEE Kona Conference Proceedings, 19 – 22 September 2011, Hawai'i, USA*. Program Book, art. no. 6107137. ISSN 0-933957-39-8.

WILLIAMS, S.P., GOFF, J.R., SALE, F., AH KAU, J., PRASETYA, G., DAVIES, T.R.H., CHEUNG, K.F., WILSON, T. (2011B). Sands of Time: Evidence for palaeotsunamis and/or palaeostorms in Samoa, and what this means for tsunami risk reduction. In: Malua, T.L. (ed), *Proceedings of the Samoa National Environment Forum 2010*. pp. 15-25.

WILLIAMS, S., DAVIES, T. AND COLE, J. (2012). Catastrophic flank collapse on Ta'u island and subsequent tsunami: Has this occurred during the last 170 years. *Science of Tsunami Hazards* 31(3): 178-198.

ISSN 8755-6839

SCIENCE OF **TSUNAMI HAZARDS**

Journal of Tsunami Society International

Volume 32 **Number 3** **2013**

CHAOS THEORY AND THE ROLE OF EXPERT ANALYSIS AS A PERIODIC ATTRACTOR DURING THE 2004 INDIAN OCEAN TSUNAMI

Matthew O'Lemmon

O'Lemmon & Associates
San Bernardino, California, USA

ABSTRACT

The 2004 Indian Ocean Tsunami was epic in scale and scope and will go down as one of the largest natural disasters in human history. This paper presents an analysis of media coverage of the disaster and surveys of 206 local and international tourists in Khao Lak, Thailand, through the framework of chaos theory. Specifically, this paper examines the role of expert analysis as a periodic attractor during and after the tsunami. It will demonstrate how expert analysis brought disparate images and eyewitness testimony into greater focus, creating order in an otherwise chaotic environment.

Keywords: *2004 Indian Ocean Tsunami, chaos theory, periodic attractors, and expert analysis, Khao Lak, Thailand.*

Vol. 32, No. 3, page 176 (2013)

1. INTRODUCTION

This paper presents an examination of the 2004 Indian Ocean Tsunami and the influence of media analysis on the perceptions of 206 local and international tourists surveyed in Khao Lak, Thailand, through the use of chaos theory seven years after the disaster leveled the seaside resort. Specifically, this paper focuses on the role of expert/technical analysis as a periodic attractor and the effect knowledge creation has had on making the event understandable, thus, reducing anxieties related to it. When applied to the 2004 tsunami, chaos theory provides a paradigm for understanding the disparate images immediately following the disaster as coverage turned from disaster display to disaster analysis.

A crisis is an event with low predictability but high impact demanding explanation, analysis, and accurate information usually from experts and other professionals (WEICK K. 1995; SEEGER M. AND SELLNOW T. 1998). The 2004 tsunami was an unprecedented crisis for several reasons, two of which were its scale and the video/photographic evidence captured by individuals caught in the midst of the disaster. The tsunami was generated by an earthquake measuring more than 9.0 on the Richter scale off of the western coast of Northern Sumatra and devastated the shores of India, Indonesia, the Maldives, Myanmar, Sri Lanka, and Thailand. It was an epic disaster killing and displacing close to 300,000 people from Asia to Africa. Six coastal provinces along the Andaman Coast of Thailand were devastated; the affected areas included 25 districts, 95 *tambons*, and 407 villages with 47 villages completely destroyed (UNRC 2005). Hundreds of local fishing communities were leveled while more than 100,000 people lost a home or family member.

The destruction of Khao Lak was almost total. Most of the town's coastline including resorts, vegetation, and beaches were destroyed. SEI International (2009) cites the damage as resulting primarily from the shallowness of the offshore ocean shelves, low onshore elevations, and the large number of wooden and non-reinforced concrete structures along the coast. Over 4,000 of the more than 5,300 people who died in Thailand perished in Khao Lak, while unofficial estimates put the number at more than 10,000. In addition to the loss of life, approximately 90% of all housing in the region was either partially or totally razed.

Media coverage of the tsunami was longer than any other previous natural disaster and continued through January 2005 (WYNTER A. 2005). CNN had more than 80 personnel providing 24-hour coverage, as did other global and regional networks. The ongoing catastrophe dominated the front page of periodicals such as the New York Times, Time, Newsweek, The Economist and many others for weeks following the event (BROWN P. AND MINTY J. 2006).

With the rise of 24-hour news channels and dissemination of videos and photographs via the Internet, exposure to disasters such as the 2004 tsunami are now commonplace. This trend will likely increase with technological advances, the spread of internet connectivity, and the use of social media applications. However, disseminating images of disasters in a constant loop has a significant impact on those immediately affected as well as the broader public. Post-traumatic stress disorder (PTSD) and post-traumatic stress symptoms (PTSS) are now recognized as common products of repeated exposure.

Previous research has also demonstrated the effect of witnessing death and graphic images on television and the development of PTSS in children (NADER K. ET AL. 1993). Exposure to scenes of

terrorism, likewise, have been shown to increase levels of anxiety in test subjects in Israel (Slone M. 2000) and middle school students in the US state of Oklahoma following the bombing of the Murrah Federal Building in Oklahoma City (PFEFFERBAUM B. ET AL. 2001). In the wake of the 9/11 attack on the World Trade Center in New York City, a study of schoolchildren exposed to negative and positive (i.e. heroic) images from the attack found increased PTSD symptoms with the highest levels among those exposed to images on the Internet (SAYLOR C. F. 2003).

Following the 2004 tsunami surveys of residents in Hong Kong who viewed media coverage of the disaster repeatedly found similar increases in anxiety related disorders (LAU J. ET AL. 2006). However, media coverage was not restricted to images of the tsunami. In a separate study of survivors in India, researchers found that scientific and technical analysis provided by experts via television news reports eased tensions among those at risk (SRI JOTHI P. AND NEELAMALAR M. 2011). While PTSD for the general public witnessing such events electronically can occur, its severity is lower than that experienced by victims and significantly diminishes over time (NERIA Y. AND SULLIVAN G. 2011).

The widespread media coverage of the tsunami demonstrated the unpredictability of natural disasters and the devastating consequences, which can accompany them. The fact that the tsunami was caught on film by tourists while on holiday added another layer to that unpredictability, turning on its head an otherwise structured setting into one of chaos. Yet, it was through these firsthand images that order within the chaos began to emerge. As initial reports surfaced, the unpredictability of the disaster was assessed by scientists who provided key information regarding earthquake-generated tsunamis. Thus, information was not value free but fell within parameters defined by expert analysis.

While initial images of the disaster were ad hoc, varied, and presented in real time as information came in from throughout South and Southeast Asia, these impromptu field reports gave way to knowledgeable experts who presented the tsunami as a natural event with understandable causes. Unlike terrorist activities, which can originate from diverse sources and have multiple catalysts, expert analysis of the disaster presented objective reasons establishing a degree of order within a chaotic system.

The paper begins with a section on the limitations and origins of the study before detailing the methodology and demographic indicators of those surveyed. It will then provide a discussion divided into four parts. The first part presents an overview of Khao Lak and the 2004 tsunami. As will be seen, while an obvious recession in tourism occurred immediately after 2004, Khao Lak's status as an 'undiscovered' part of Thailand has been a draw for many tourists and over the years the town has built up a loyal following which helped sustain the area immediately after the disaster.

The second part examines current perceptions of Khao Lak, knowledge of the tsunami, and how this knowledge has influenced anxieties related to natural disasters along the Andaman Coast. This is followed by an examination of media coverage of the 2004 tsunami via chaos theory and specifically the role of expert analysis as a periodic attractor. The final section details external events since the disaster, which have contributed to the easing of tensions in the years that have followed.

1.1 Scope and Limitations

Research for this study was originally part of a larger project examining tourism redevelopment in Khao Lak seven years after the tsunami. As the original project did not focus specifically on expert

analysis as a mitigating factor in reducing anxieties related to the tsunami, certain questions were not included in the surveys as they were not under examination. For example, while questions were asked regarding knowledge of the disaster, its effect on travel plans, and the sources used in researching Khao Lak, questions pertaining to the direct effect of television and newspaper coverage at the time of the tsunami were not. Although it is acknowledged that due to this limitation the conclusions drawn are not definitive, the paper's main objective is to present a theory of how expert analysis of natural disasters through the dissemination of technical and scientific information reduces anxieties over time.

There were two further limitations in the original study. The first was that surveys were conducted during mid-October, 2011, which is the low season in Khao Lak. Although 206 surveys were completed, the number is likely less than that had they been conducted during the high season, roughly November – April. The second limitation is the inherent issue of conducting surveys of travelers on vacation and their motivation to participate in a study of a sensitive and potentially offensive subject matter. Although a small number of individuals chose not to take part in the study, in general people were willing to participate in the surveys and interviews.

2. METHODOLOGY

A comparative study of tourists and the experiences of Khao Lak's community are presented alongside an examination of the area's recovery. Research was conducted in October 2011 and consisted of surveys and interviews of 206 foreign and Thai tourists and 22 local Thai residents and business owners. The surveys were designed to gain insight into tourists' knowledge of Khao Lak, knowledge of the 2004 tsunami, and the perceived threat of natural disasters along the Andaman Coast. Interviews were conducted of local Thai business owners and residents in Nang Thong Beach and Biang Niang Beach. These individuals represented owners of restaurants and clothes shops, beach vendors, taxi drivers, dentists, internet café owners, pharmacists, optometrists, and travel agents. As the majority of those interviewed lived through the tsunami and Khao Lak's reconstruction, their views are a necessary part of any study of perceptions of the region.

Section 4.3 examines the role of media exposure and an increase in knowledge of the tsunami along with a decline in anxiety and association of Khao Lak with the event through the paradigm of chaos theory, and specifically expert analysis as a periodic attractor. First proposed by Lorenz (1963) who described how minor fluctuations in weather systems can lead to unpredictable and wide-ranging outcomes, chaos theory has been applied extensively from medicine to the social sciences. Chaos does not necessarily imply a lack of order as order and predictability may become evident as crises unfold.

The application of chaos theory in this paper follows the work of Sellnow et al. (2002) on communication within natural disasters but differs through the focus specifically on the role of expert and technical analysis as periodic attractors. Attractors are organizing principles created within complex systems and have limited values that define their boundaries. Thus, periodic attractors represent systems that settle into a cycle with defined roles, periodically achieving stability (THIÉTART R. AND FORGUES B 1995). While no one can predict the exact state of a system at any one time, it is known that they will be somewhere within the cycle.

2.1 Survey Population and Statistical Methodology

Surveys were conducted along Khao Lak Beach, Nang Thong Beach, and Biang Niang Beach. Respondents were divided into three principle categories: European/Western (80%), Thai (16%), and Other Asian/Indian (4%).

FIGURE 1

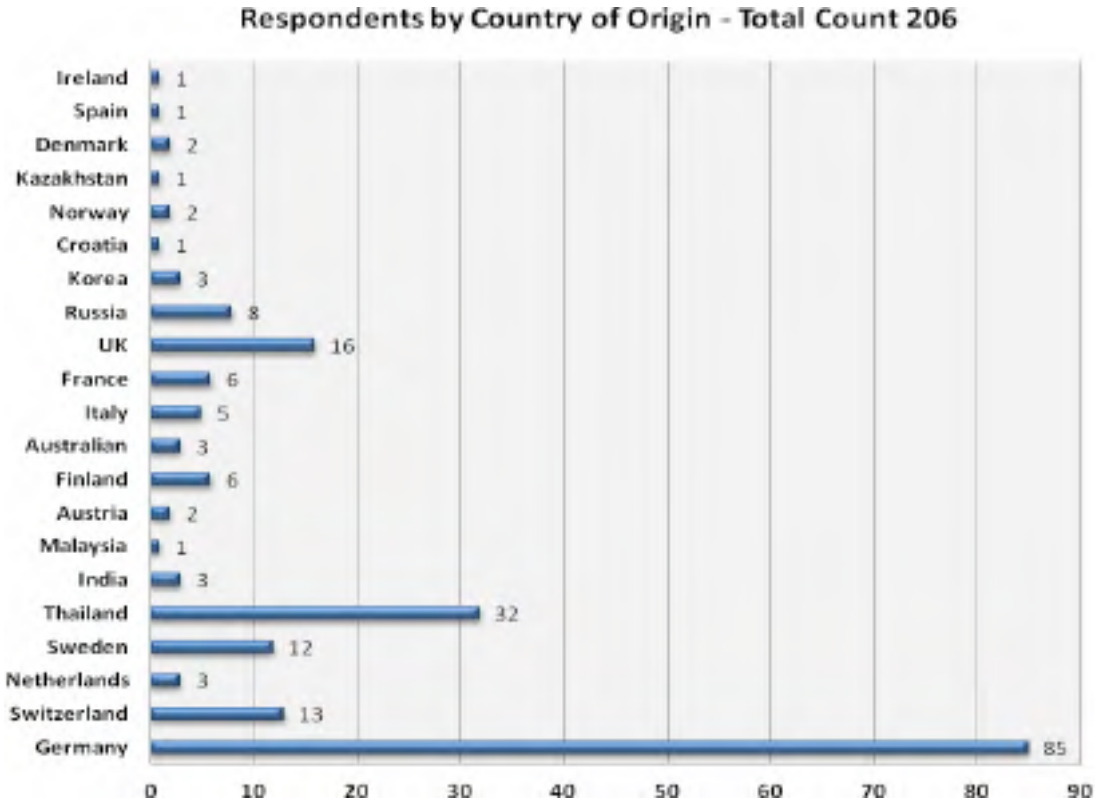

Each category was further subdivided according to age, gender, and the number of previous visits individuals had made to Khao Lak. The sample was balanced with 49.7% male and 50.2% female respondents from 22 countries with the majority coming from Europe, specifically Germany. Nearly 75% of all foreign and 73% of all Thai respondents were visiting Khao Lak for the first time.
Univariate statistical analysis was conducted on factors related to knowledge of the 2004 tsunami and perceptions of danger regarding natural disasters along the Andaman Coast; multivariate analysis was conducted on factors related to knowledge of the 2004 tsunami and its influence on travel plans to Khao Lak.

FIGURE 2

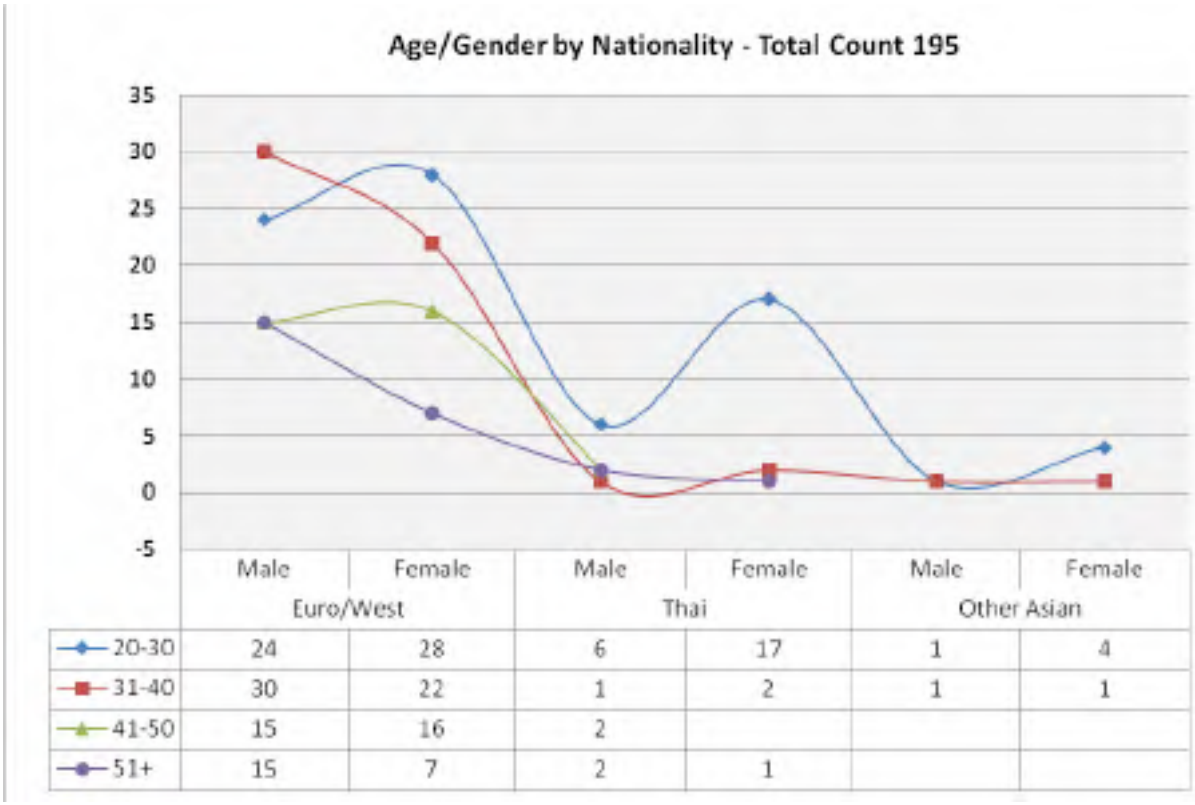

	Euro/West		Thai		Other Asian	
	Male	Female	Male	Female	Male	Female
20-30	24	28	6	17	1	4
31-40	30	22	1	2	1	1
41-50	15	16	2			
51+	15	7	2	1		

3. RESULTS

Summary of findings:

- Knowledge of the 2004 tsunami among foreigners and Thais was high.
- The tsunami's influence on travel plans for foreigners and Thais was low.
- Most foreigners and Thais did not think the Andaman Coast was dangerous in terms of natural disasters.
- The more individuals knew of the tsunami, the less it influenced their travel plans.

Although the tsunami's legacy has left a lasting impression on the region, this study demonstrates that it has not left the perception that the Andaman Coast is dangerous in terms of natural disasters. As noted above, German tourists represented the largest nationality, similar to pre-2004, followed by Thai tourists comprising 16% of respondents; this was higher than the 10% estimate given by Thai merchants interviewed in Khao Lak.

While respondents described their knowledge of the tsunami as high, the lasting effect of the tsunami on their travel plans was described as low. Further, there was not a direct relationship between the tsunami's legacy, perceived dangers along the Andaman Coast, and Khao Lak in general.

Although respondents were well aware of the disaster, it was a generalized knowledge and not connected with one specific location.

The most important finding, though, was that the more respondents knew of the tsunami, the less of an effect it had on their choosing Khao Lak as a holiday destination. The Internet and travel guides were cited as the main sources of information regarding Khao Lak. However, given the extent of the tragedy and the dominance it held over media of all types during and up to several months after the event, an inference is made that expert analyses via television, print, the Internet, or a combination of all three were influential in creating greater awareness and reducing anxieties related to earthquake generated tsunamis. These findings reflect the role of expert analysis as a periodic attractor, establishing a degree of order during the disaster, thus, making an otherwise rare and enigmatic event understandable and reducing subsequent anxieties related to it.

External events also overshadowed the tsunami's legacy and helped reduce negative imagery associated with Khao Lak. These include the 2006 military coup ousting Prime Minister Thaksin Shinawatra from power; the 'red-shirt' protests of 2009 and 2010; a military conflict with Cambodia over the historic Preah Vihear Temple in northeastern Cambodia; the election of Prime Minister Yingluck Shinawatra, Thailand's first female prime minister and sister of Thaksin Shinawatra, in 2011; and other natural disasters such as the severe floods in late 2011 in central Thailand which severely affected the capital, Bangkok, as well as the country's manufacturing and tourist sectors. Combined with other studies of the mass media's impact during natural disasters (SELLNOW T. ET AL. 2002), evidence from Cognitive-Based Therapies in stress reduction (NIMH 2009), as well as those affected by the 2004 tsunami (SRI JOTHI P. AND NEELAMALAR M. 2011), this study presents indirect evidence of the mass media's role in reducing anxieties surrounding crises while providing a model for how this mitigation occurs.

4. DISCUSSION

4.1 Khao Lak and the 2004 Tsunami

Khao Lak is located in Takua Pa district in the southwestern Thai province of Phang Nga. The area is well-known for its proximity to national forests and the Similan Islands and frequented by scuba divers and naturalists. Situated an hour's drive north of Phuket, Khao Lak comprises the communities of La On, Bang Niang, Khuk Khak, Pakweep and Bang Sak. While 'Khao Lak' refers to the beach itself, the area now connotes the entire area extending north of Coral Peninsula to Bang Sak Beach. The town is seen as out-of-the-way by many tourists, which has led to the development of a distinct identity: quiet, family-friendly, and lacking the high-rise hotels and condominiums of other popular destinations.

Prior to tourism locals were employed in fishing, tin mining, and agricultural industries such as rubber and coconut plantations. The area rarely saw foreign tourists and it was not until 1987 that the first resort was established along with dive trips to the Similan Islands. By the 1990s the tourism industry began to expand rapidly and in a little more than a decade the town went from a sleepy fishing village to a fast growing tourist destination. Following this transition, Khao Lak came to rely almost entirely on tourism.

Although growing in popularity, by the end of the 1990s Khao Lak was still a low-key getaway for European tourists and an alternative to urbanized destinations. Local ordinances were established limiting building heights and noise levels to help maintain its quiet image. Facing west with heavy downpours during its low season from June to November further ensured that development did not increase unchecked.

Following the tsunami the region experienced a sharp drop in tourism; yet, despite the upheaval Phang Nga and Khao Lak made a considerable comeback. By 2005 schools were reopened and close to 75% of all students returned to classes (UNRC 2005). Tourism also began to recover the same year with the German market returning the quickest followed by the Scandinavian and UK markets growing by 6% and 8% respectively (TOT 2005). This was due in part to the work of some savvy business owners who turned the event to their advantage by highlighting their situation to international markets. East Asian tourists were the slowest to return, a decrease attributed in part to a lack of knowledge and media coverage, which gave the impression that the entire country was devastated (ibid). The numerous international volunteers that arrived in Khao Lak to help in cleanup efforts likewise aided businesses and even helped create new tourist markets (SEI 2009).

By 2007 tourism levels returned to those of 2003. The majority of hotels in the region had reopened and local fishing villages were re-established. Government programs, such as low interest loans for hotel owners in Phuket and Khao Lak as well as social services for affected villages, were part of broader efforts by local and international partners to spur redevelopment. Due to the efforts by the Thai government, local and international NGOs, along with those of local business owners, land prices in Khao Lak increased by as much as 40% in 2006 (CHIEN D. AND FITZGERALD C. 2006).

One of the most significant differences between Thailand and its regional neighbors regarding the tsunami relates to the level of destruction the country experienced. As destructive as the tsunami was, it was far less than that experienced by Indonesia with an estimated 220,000 dead, Sri Lanka with 35,322 dead, and India with 12,405 dead. And although Indonesia was the first hit and suffered the most damage, it was also the last to receive relief while Sri Lanka lost hundreds of square kilometers of agricultural land to the inundation. A lack or destruction of infrastructure in all three countries further hampered relief efforts and likely led to higher death tolls in the days and weeks that followed.

In addition to the hundreds of thousands that perished, the tsunami caused hundreds of millions of US dollars worth of damage. However, despite affecting six provinces, disaster areas in Thailand differed from those in the above countries through the use of airports in Phuket and Krabi soon after the event. Thus, flights from Bangkok were able to ferry aid into disaster zones while ferrying victims out. The use of these facilities likely staved off a much higher death toll and shortened Khao Lak's recovery time in comparison to other devastated areas in the region.

4.2 Influence of 2004 Tsunami on Travel to Khao Lak

The fact that Khao Lak is primed to become one of Thailand's newest resort destinations is indicative of the fact that perceptions of the region have changed. The long term impact expert and technical analysis has had on current perceptions of Khao Lak cannot be stated with certainty by this study given the limitations outlined in Section 2. As noted, though, the event was covered by media of all types as no other natural disaster was covered before. Further, more than 70% of survey respondents cited the Internet and travel guides as their primary sources of information regarding

travel to Khao Lak. When taken together, it is apparent that visitors to Khao Lak are well aware of the events of 2004 and use multiple sources to make informed decisions prior to travelling.

This broad exposure has led to an increase in knowledge of the 2004 tsunami while limiting Khao Lak's connection to it. Approximately 80% of respondents described their knowledge of the tsunami as 'medium' to 'high' on a 4-point scale, including 81% of all Europeans/Westerners and 84% of all Thais.

FIGURE 3

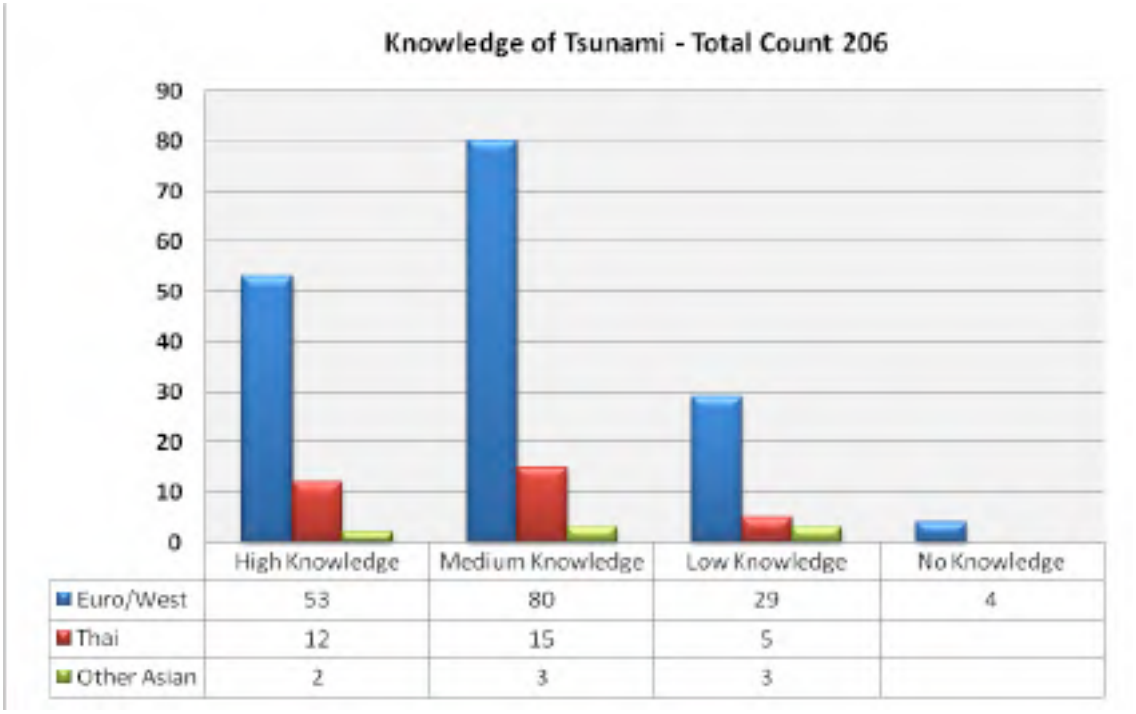

	High Knowledge	Medium Knowledge	Low Knowledge	No Knowledge
Euro/West	53	80	29	4
Thai	12	15	5	
Other Asian	2	3	3	

Further, 30% of Europeans/Westerners and 31% of Thais surveyed noted that their knowledge of Khao Lak fell within a similar 'medium' to 'high' range. However, of the total amount of respondents surveyed (206) only 29% reported that their knowledge of both Khao Lak and the tsunami fell within a 'medium' to 'high' range. What was more telling was that the vast majority of all respondents, 80%, noted that the tsunami had 'low' to 'no' influence on their travel plans.

One of the most significant findings, though, was that the more individuals knew about the tsunami, the less it affected their travel plans. More than 63% of those who described their knowledge of the disaster as 'medium' to 'high' also described it as having 'low' to 'no' affect on their travel plans. This data offers support for the conclusion that widespread media reporting of the disaster created a greater awareness of the event through analysis of earthquake-generated tsunamis. This awareness likely reduced the disaster's influence on travel plans to Khao Lak through educating individuals (both local and foreign) as to how tsunamis such as the one in 2004 are generated. At the same time, this has reduced Khao Lak's connection to the disaster and the specificity of areas destroyed.

This lack of specificity can also be attributed to the scale of the disaster and the fact that numerous

countries were struck by the tsunami, as well as the comparative level of destruction Khao Lak experienced and its relatively quick recovery compared to other countries. When coupled with the extensive media coverage which focused on the causes of the tsunami and the regional nature of the disaster (particularly in the case of Western media), this has likely reduced Khao Lak's connection to the disaster as reported by foreign tourists while remaining stronger among Thais. Of those Thais surveyed, close to 22% who described their knowledge of the tsunami as 'medium' to 'high', described its influence on their travel plans as 'low'. However, more than 40% of Thai respondents who described their knowledge of the event in similar terms cited its effects on travel plans as 'medium' to 'high'.

FIGURE 4

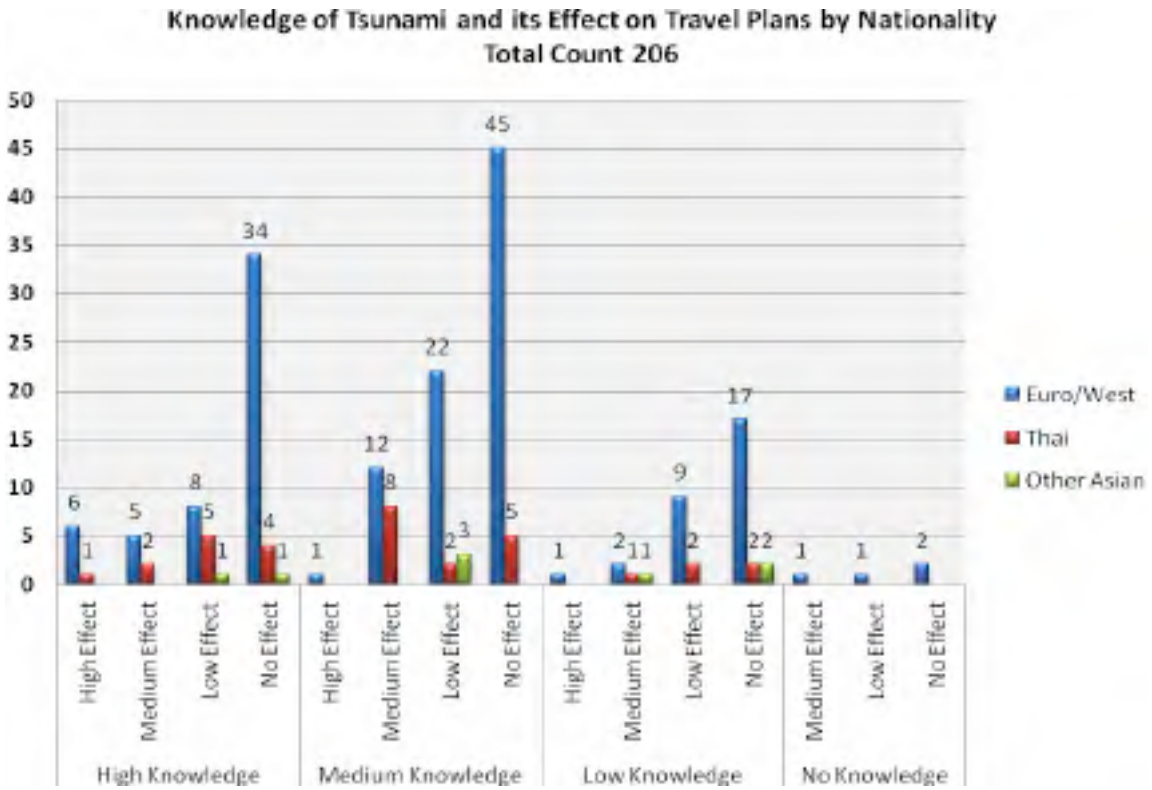

Respondents, likewise, did not attribute any specific or indistinct sense of danger with the broader Andaman Coast. When asked their position on the statement "Visiting the Andaman Coast of Thailand is potentially dangerous because of natural disasters," 50% of respondents cited their position as 'neutral'. As the graph below shows, there is an overall rise in those responding 'strongly disagree' to 'neutral' and a sharp decline in those responding that they 'agree' to 'strongly agree' that the Andaman Coast is dangerous. More than 91% of respondents stated that the Andaman Coast was either not dangerous or were neutral on the question.

FIGURE 5

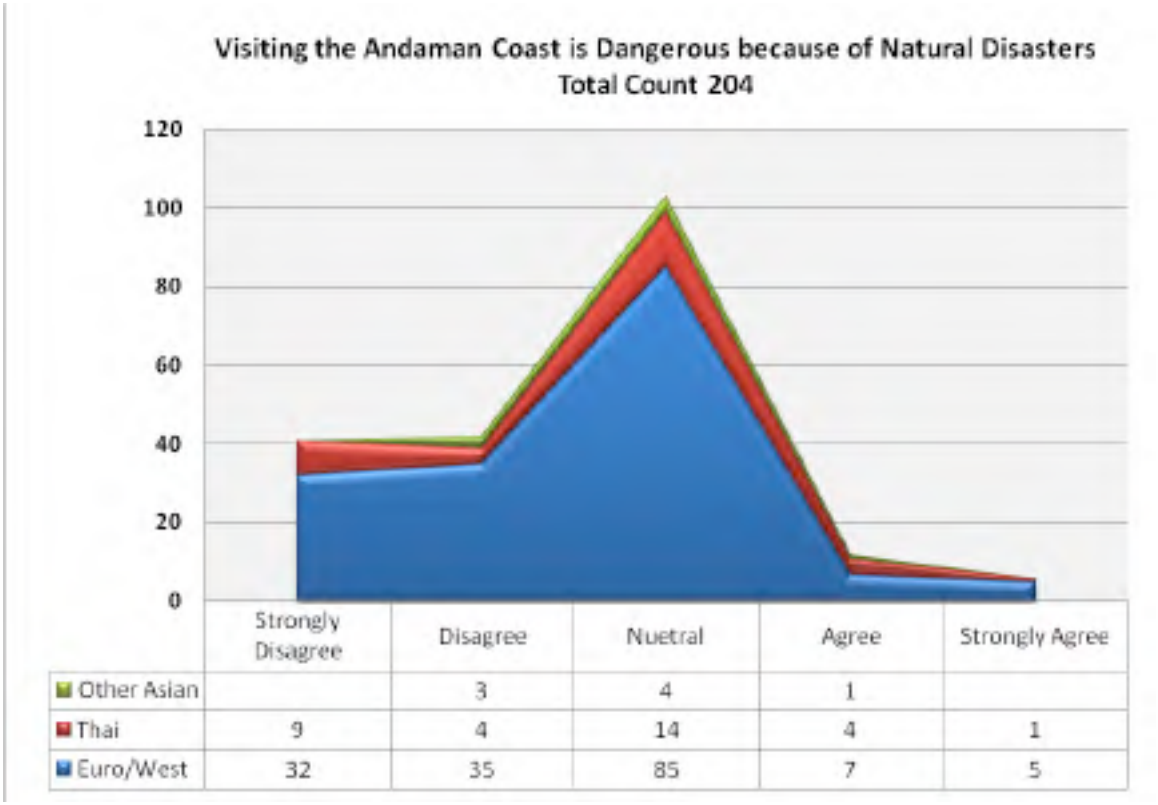

Interestingly, when asked "On a scale of 1–5 (1 equaling 'no threat'; 3 equaling 'neutral'; and 5 equaling 'high threat') how would you rate the threat of natural disasters along the entire coast of Thailand?" 23% of foreign tourists recorded a value of 3.5–5. Yet, approximately 74% of these respondents recorded a value of 1–3, meaning that the majority of foreign tourists described the Andaman Coast as less dangerous than the entire coast of Thailand. As noted above, these responses were given at the same time that central Thailand and Bangkok were experiencing their worst flooding in half a century.

Thai tourists responded similarly to the above question with 44% describing the potential for natural disasters along the Andaman Coast as 'neutral'. On a scale of 1–5, however, with 1 equaling 'no threat', 3 equaling 'neutral', and 5 equaling 'high threat', 90% of Thai tourists described the potential for natural disasters along the entire Thai coast as between 1–3 (33%, 27%, and 30% respectively), with approximately 60% describing the potential for natural disasters as 'low' to 'no threat'.

4.3 Expert Analysis as a Periodic Attractor

As a cosmology episode, or a total upheaval in everyday life, the tsunami brought untold changes to the lives of those in Khao Lak. Understanding the catalyst(s) for the event was dependent on two key pieces of data: pictures/videos and eyewitness testimony. Videos provided researchers with data

from which they were able to calculate the acceleration of wavefronts as the tsunami reached shorelines. This acceleration has helped explain the 'mesmerization' of victims during tsunamis (SYNOLAKIS C. AND BERNARD E. 2006); appearing slow on the horizon, observers are led to a false sense of security regarding a tsunami's speed. Once close to shore, though, the sudden acceleration of giant waves proves inescapable.

Eyewitness reports were able to provide information regarding wave height and direction. As a qualitative measurement, eyewitness testimony depends on an individual's position in relation to incoming waves. Yet, several independent studies found that individuals who lived through the disaster gave accurate estimates of wave heights (THANAWOOD C. ET AL. 2006; SKELTON A. 2008; KARLSSON J. M. ET AL. 2009). The continuity between testimonies and the similarity in their estimates allowed for greater clarity regarding wave complexity, how far inland the inundation travelled, and the time interval between waves.

The engrossing media coverage, which quickly began to create the story of the tsunami and Khao Lak initially, relied on these key sources of data. Such data are crucial to any initial study of a crisis and speak to their evidentiary value in determining post-disaster quantitative measurements. What testimony provided which images alone could not was the context of 'sets'; that is, the description of forces similar in size and shape coming at timed intervals. This information laid the groundwork for greater order through analysis.

Chaos theory holds that normally functioning states experience initial disturbances known as 'bifurcations' or the point where a system's normal functions are interrupted. We can identify two principle bifurcation points, which occurred at Khao Lak on December 24th, 2004. The first bifurcation point came around 10am when dramatic changes to the predictable tides occurred, drawing water far out to sea. The second bifurcation point came roughly 26–29 minutes later with the arrival of the first tsunami wave and inundation from 0.5km-1.5km inland (KARLSSON J. ET AL. 2009). The first point is critical given Khao Lak's shallow seabed, which made the retreat of seawater unnoticeable to some observers, and possibly lessened concerns, which would have likely been greater, had the water's retreat been more dramatic. By the time of the second bifurcation point it is obvious from videos taken at Khao Lak that many locals and visitors did not appreciate the severity of the situation – that 'mesmerization' noted above – with many standing on or near the beach observing the incoming waves.

Sellnow (2002) notes that following bifurcation self-organization and the building of new structures and understanding often develop. Self-organization is the process whereby order re-emerges from inner principles rather than external factors. It is within the initial videos and testimony coming out of Khao Lak that order began to re-emerge as it was reformed into scientific and technical information by experts. Thus, while the potential for order came out of Khao Lak, that order was shaped through expert analysis as a periodic attractor.

Attractors arise within crises providing some degree of order amidst ongoing chaos (SELLNOW T., 2002). Periodic attractors constrain behavior to predictable patterns as they move from one extreme, through a midpoint, to another. Within social behavior this is reflected in individuals mustering determination and choosing one course of action before losing momentum and altering course.

Initial reports and videos of the tsunami presented scenes of total chaos, yet, these required scrutiny as to the cause of the disaster and what could be expected in the immediate future. As it was unlikely that new data would be emerge beyond known or expected geophysical, seismic, and oceanic

knowledge, incoming information was repeatedly measured against existing knowledge. This knowledge represented the parameters or those defined roles and values (THIÉTART R. AND FORGUES B., 1995) found within chaotic systems noted above. This created a clearer picture of events and the catalyst for the tsunami and, thus, a higher degree of order through awareness.

The extent to which this order reverberates over time is dependent on the degree to which that order is expressed and retained as a knowledge creating event. However, with widespread media coverage of natural disasters as they occur, the end of a crisis is difficult to determine. Repeated exposure, particularly through digital media, allows people to relive events, keeping their memory alive and a continuing part of local cultural identity. As of the writing of this paper in 2013, a simple search of cnn.com, bbc.com, and youtube.com with the phrase "2004 tsunami" yielded 82, 459, and 17,200 results, respectively.

Researchers in Norway found that threat intensity levels in survivors did not diminish over time but increased from 6 to 24 months following the event. A lack of improvement in post-traumatic stress disorder symptoms was associated with this increase but not with other factors including the degree of exposure to stress, personality, or social support (TROND H. ET AL., 2009). The United Nations Country Team, Thailand, in 2006, similarly, reported that thousands of adults and school children in Phang Nga Province continued to undergo psychiatric therapy up to a year and a half following the tsunami with 40 hospitalized for aggression or insomnia (UNTC, THAILAND 2006).

As the cultural imprint of a crisis retains a stronger presence within an affected community than outside of it, lessons learned from the event take the form of retrospective sense making. Although the likelihood of experiencing a similar event is rather low, the initial fear of a reoccurrence represents what Sunstein (1999) calls the "probability of neglect". Sunstein (ibid) argues that when "emotions are intensely engaged, people's attention is focused on the bad outcome itself, and they are inattentive to the fact that it is unlikely to occur." Yet, as Weick (1995) notes, the issue is not that people need more information but more values, priorities, and clarity and less equivocality.

During crises, raw data, such as photos and videos come in quickly and often unedited as events unfold. However, at a certain point data will need clarification – a greater degree of order through analysis. Likewise, eyewitness reports alone provide only a partial picture, as they are dependent on an individual's position relative to a crisis' epicenter, although as noted eyewitness reports in Khao Lak have proven to be a reliable source of quantitative data regarding wave height.

The equation and diagram below are examples of how this clarity is realized over time. Let P (pictures), V (videos), and R (eyewitness reports) represent chaotic data symbolized by sine waves (data that comes in periodically as it is generated within a dynamical system) and E represent expert analysis.

$$E \ni (P \cap V) \cap R \Rightarrow P \square V \square R = \Delta(1/x + 1)\sin(x)$$

FIGURE 6

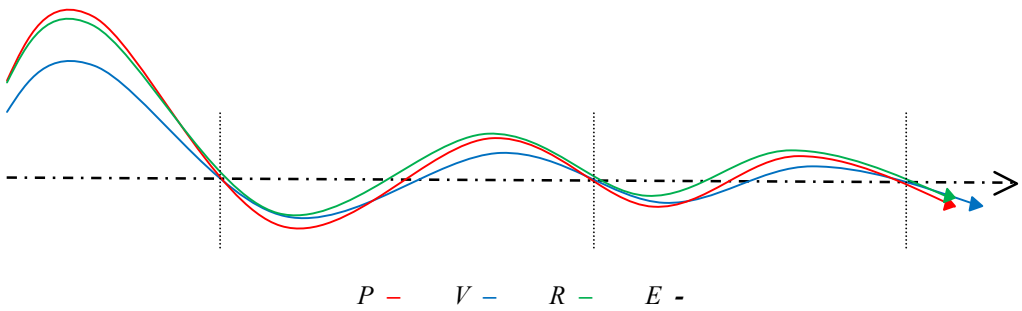

Over time the chaotic nature of data from the system will be clarified by expert analysis acting as an attractor bringing about a degree of order within the system. As time progresses and greater amounts of data are generated, more order is created given that testimony and imagery will provide a fuller account of the dynamical system but not necessarily provide information that is beyond the scope of that already received. The tsunami waves did not go on in perpetuity but had limited duration. New imagery and testimony would, therefore, be of the same waves albeit perhaps from different perspectives. In the above diagram *P*, *V*, and *R* would eventually taper off, growing incrementally closer to *E* given that with more data from the system expert analysis provides more order over time, not less.

Stewart and Ueda (2013) state that "The most severe catastrophic bifurcation is the total loss of stability of an attractor, so that when it is stepped from μ_I to μ_{I+1}, the system experiences a transient jump followed by settling to another attractor, whose location in phase space is remote from the attractor sustained at $\mu = \mu_I$." The above diagram depicts one attractor in one setting (Khao Lak) but in reality multiple attractors – i.e. multiple experts – would be providing analyses in multiple settings. An example of attractors losing stability in this scenario would be information coming in from another area hit by the tsunami – Sri Lanka, Indonesia, and so on. Yet, as analysis from within or in reference to this new data is applied to the broader system, order can remerge.

The large amount of information collected from pictures, videos, and eyewitness testimony provided experts with firsthand data through which they were able to relate critical news, in some cases as events unfolded. This has produced vital information for research institutes, universities, and communities at risk for tsunamis, while providing survivors of the event with explanations as to the processes of what happened and why. This is a far different situation from before the tsunami where the lack of response by those caught up in the event along with the absence of safety measures demonstrated that the lessons from previous tsunamis had not been widely disseminated (WEICK K., 1995).

Two related studies provide insight into expert analysis acting as a periodic attractor. In a survey of 604 Hong Kong residents who saw tsunami footage >10 times per day, 52.6% - 67.4% of respondents reported experiencing severe to very severe levels of stress; 30% - 39.5% of males and females respectively experienced mild PTSD symptoms while 5.9% - 8.7% experienced moderate to

severe PTSD symptoms (LAU J. ET AL. 2006). However, a survey of 209 women in the Indian state of Tamil Nadu found that media presentations of scientific and technical information regarding tsunamis helped educate women of tsunami risk factors and the need for compliance with tsunami warnings (SRI JOTHI P. AND NEELAMALAR M. 2011).

The Hong Kong survey would appear to contradict the thesis under consideration in this study while the one from Tamil Nadu supports it. The differences are likely the result of three principle factors: 1) those who lived through the disaster as opposed to those who witnessed it via media outlets; 2) the level of analysis presented to each group; 3) socioeconomic and cultural differences related to perceptions of the supernatural.

The first factor is likely the most significant as those who lived through the tsunami were still coping with its effects such as the loss of loved ones, housing, and agricultural land. Explanations of the causes and assurances that a similar event would not occur without comparable catalysts did much to alleviate concerns for individuals in such an agitated state. This relates to the second factor. The Hong Kong study is silent on the quality of exposure respondents experienced; that is, whether the vivid images were coupled with concomitant analysis. It states that "Media coverage, in terms of frequency of coverage, visual images, and distressful contents was a strong predictor of stressful responses related to the tsunami," (LAU J. ET AL., 2006) but does not elaborate on whether additional analysis played a role in respondents' stress levels.

In terms of socioeconomic and cultural differences, 40.1% of the Hong Kong respondents reported some post-secondary education while perceptions that disasters were the result of God's punishment were noted by researchers to be associated with mental health outcomes. The Tamil Nadu study, on the other hand, was conducted among individuals for whom "socio-economic conditions were generally low along with a very low literacy rate," while most were semi-literate (SRI JOTHI P. AND NEELAMALAR M., 2011). Although Sri Jothi and Neelamalar do not comment on beliefs related to supernatural causes of natural disasters, they did note that media attention increased awareness of tsunami risk factors and warnings as well as subsequent social problems such as teen marriages, prostitution, and alcohol abuse along with sanitation and hygiene issues. These proved particularly important given that many of the women in the study had lost their husbands and/or sons making them the head of their households and primary breadwinners.

Whereas the respondents in the Indian study had to contend with real-world rehabilitation and social concerns amid tragic loss, those from Hong Kong contended with repeated imagery. Although the Hong Kong respondents experienced stress through viewing these images, it was likely far less than the Indian respondents who lived through the tsunami. Without sufficient data as to the amount of analysis Hong Kong respondents experienced we are left with the conclusion that the frequency of viewing distressful content and images increased fears for those reporting PTSD symptoms, while the conclusive data from the Indian respondents demonstrate that extended analysis and technical information were crucial in reducing fears.

4.4 Internal and External Events

Political and economic events alongside other natural disasters grabbed headlines and focused attention away from Khao Lak at the same time it was making a recovery while its loyal following

among many foreign tourists helped speed its reconstruction. As noted in Section 3 these events include the 2006 coup in Thailand, the global economic slowdown in 2008, the 2009/2010 'red shirt' demonstrations, the election of Thailand's first female prime minister, the military conflict with Cambodia, and the extensive flooding of the capital and central Thailand in 2011.

It is reasonable to assume that attention regarding the tsunami diminished at least after 2006, the same year that Prime Minister Thaksin Shinawatra was overthrown in a military coup. The global economic recession in 2008 was also a determining factor, which affected reconstruction efforts and was cited by tourists and business owners alike as influencing travel to Khao Lak. Likewise, the election of Thailand's first female prime minister (and sister of the man who was overthrown in a military coup, no less), historical border issues with Cambodia, and flooding which hurt two key sectors of Thailand's economy – tourism and manufacturing – affected much larger segments of the population than the tsunami alone. Taken alongside Khao Lak's recovery, the broader effects of these more recent disasters and political/social disruptions may be more pronounced than the legacy of the 2004 tsunami in the future.

There have been other factors that have likely helped reduce anxieties over time, particularly in the areas directly affected by the disaster. Since the tsunami programs such as the FAST (Families and Survivors of Tsunamis) Project in Indonesia, Sri Lanka, and Thailand along with TARNS (Tsunami Alert Rapid Notification System) for Thailand, part of the Indian Ocean Tsunami Warning System, have been employed in an effort to increase awareness throughout the region. These and other programs have produced a greater understanding of the nature of tsunamis, the catalysts for them, and what to do in the event of a tsunami warning and have likely contributed to the overall abatement in fear in the months and years following the disaster. When taken as a whole, the role of expert analysis of earthquake generated tsunamis played a significant role in reducing anxieties related to their causes, while the impact of events within and without Thailand shifted media coverage away from the disaster and reconstruction efforts in the years that followed.

5. CONCLUSION

The 2004 Indian Ocean Tsunami was one of the greatest natural disasters in human history taking the lives of hundreds of thousands of people worldwide. Of these, more than 5,300 died in Thailand with the majority dying in or around Khao Lak. Overall damage from the disaster cost Thailand more than 510 million US dollars. Today, hotels have returned and the tsunami for many is a thing of the past. While it will always be part of Khao Lak it has not been the end of the town by any means.

When viewed through the perspective of chaos theory, the tsunami presented a scenario that quickly brought disorder and confusion to the lives of participants. Video and eyewitness evidence demonstrate that individuals became quickly overwhelmed as a cosmology episode unfolded, dashing any sense of normalcy that existed prior to the initial earthquake.

Yet, videos and eyewitness testimony also revealed that order could be found even in the midst of chaos. As information came in from disaster zones it was reconciled against the technical analysis provided by experts. As a periodic attractor, expert analysis acted as a fulcrum around which information from the field was constantly referred. Thus, videos and eyewitness accounts did not splinter off or stand apart but were constantly checked against objective scientific scrutiny providing clarity in the midst of chaos and a greater degree of order.

This analysis has been instrumental in alleviating anxieties of those who lived through the disaster, and from interviews of tourists and local Thais it has been integral in creating a greater degree of awareness and understanding of earthquake-generated tsunamis. Within this study respondents were not only very knowledgeable about the event but that knowledge did not have an adverse effect on their decision to visit Khao Lak. Indeed, the more individuals knew of the disaster the less it affected their travel plans. This supports the inference that the more a seemingly unknowable event is made understandable, the less anxiety individuals experience in reference to it.

Given that the majority of foreign and Thai tourists surveyed were first time visitors who travelled to the area specifically for its remote and quiet atmosphere, it is apparent from this study that fears of recurrent disasters are not as controlling as they once were. Instead, more everyday issues such as cost and travel time appear to be the principal issues tourists consider before visiting the area. Yet, the vast amount of data created in the wake of the disaster has lived on via the Internet meaning that the tsunami and lessons learned from it are available to a wider audience. Among the respondents surveyed in this study this has not increased Khao Lak's connection to the event but instead reflects a broader knowledge of the tsunami coupled with lower levels of anxiety in reference to it.

The seven years between the disaster and this study in all likelihood played a significant role in reducing anxiety levels. However, when viewed in its entirety what is seen is a crisis event turning into a learning event. The low anxiety levels coupled with the high levels of knowledge of the tsunami and the lack of negative effects the tsunami's legacy has had on travel plans as reported by the majority of respondents point to the impact of expert and technical analysis with defined values, i.e. periodic attractors. Random newsfeeds gave way to informed and measured reports by experts explaining what for most is a mysterious and once in a lifetime event. Thus, it appears to be the case regarding the 2004 tsunami that the more an otherwise enigmatic threat is made understandable, the less it is seen as a threat or at least as something that should be viewed as a credible threat.

REFERENCES

BROWN, P. AND J. MINTY. 2006. Media Coverage & Charitable Giving After the 2004 Tsunami. December, Working Paper No. 855. William Davidson Institute. University of Michigan, Ann Arbor.

CHIEN, D. AND C. FITZGERALD. 2006. Towards Sustainable Redevelopment: A Review of the Tourism Sector in Khao-Lak, Thailand since the December 2004 Tsunami. Kenan Institute Asia. Bangkok.

KARLSSON, J. M. ET AL. 2009. Reconstructions of the Coastal Impact of the 2004 Indian Ocean Tsunami in the Khao Lak Area, Thailand. In, Journal of Geophysical Research, vol. 114, c10023, 14 PP., 2009

LAU, J. T. F. ET AL. 2006. Impacts of Media Coverage on the Community Stress Level in Hong Kong after the Tsunami on 26 December 2004. In, Journal of Epidemiology and Community Health, vol. 60, no. 8, pp. 675-682, pp. 678. London: BMJ Publishing Group.

LORENZ, E.N., 1963. Deterministic Nonperiodic Flow. In, Journal of the Atmospheric Sciences, vol. 30, pp. 130-141. Boston: American Meteorological Society.

NADER, K. ET AL. 1993. A Preliminary Study of PTSD and Grief Among the Children of Kuwait Following the Gulf Crisis. In, British Journal of Clinical Psychology, vol. 32, pp. 407-416. Chichester: John Wiley & Sons, Ltd.

NERIA, Y. AND G. M. SULLIVAN. 2011. Understanding the Mental Health Effects of Indirect Exposure to Mass Trauma through the Media. In, JAMA, Sept. 28, vol. 306, no. 12., pp. 1374-1375. Chicago: American Medical Association.

OFFICE OF THE UN RESIDENT COORDINATOR. 2005. Tsunami Thailand One Year Later: National Response and Contribution of International Partners. United Nations Country Team in Thailand, Bangkok.

PFEFFERBAUM, B., NIXON, S., TIVIS, R., DOUGHTY, D., PYNOOS, R., GURWITCH, R., ET AL. (2001). Television Exposure in Children after a Terrorist Incident. In, Psychiatry: Interpersonal and Biological Processes, vol. 64, no. 3, pp. 202-211. New York: Guilford Press.

R. A. THIÉTART AND B. FORGUES. 1995. Chaos Theory and Organization. In, Organization Science, Vol. 6, No. 1, Focused Issue: European Perspective on Organization Theory (Jan.- Feb., 1995), pp. 19-31. Hanover: INFORMS.

SAYLOR, C. F. 2003. Media Exposure to September 11: Elementary School Students' Experiences and Posttraumatic Symptoms. In, American Behavioral Scientist, Aug., vol. 46, no. 12, pp. 1622-1642. Thousand Oaks: Sage Publishing.

SEEGER, M. W., SELLNOW, T. L., & ULMER, R. R. (1998). Communication, Organization and Crisis. In, M.E. Roloff, ed., Communication Yearbook 21. Thousand Oaks, CA: Sage.

SEI INTERNATIONAL. 2009. Destination Vulnerability Assessment for Khao Lak, Thailand. Environment Institute Project, Project Report – 2009. SEI, Stockholm.

SEI INTERNATIONAL. 2009. Sustainable Recovery and Resilience Building Strategies in the Tourism Industry of Khao Lak, Patong Beach and Phi Phi Don. SEI, Stockholm.

SELLNOW, T. L. ET AL. 2002. Chaos Theory, Informational Needs, and Natural Disasters. In, Journal of Applied Communication Research, vol. 30, no. 4.

SKELTON, A. 2008. Eye-witness reports of the Indian Ocean Tsunami of December 26, 2004, from the Khao Lak Area, Thailand. Presented at the International Geological Congress, Oslo, Aug. 6-14, 2008.

SLONE, M. 2000. Responses to Media Coverage of Terrorism. In, Journal of Conflict Resolution, Aug., vol. 44, no. 4, pp. 508-522. Thousand Oaks: Sage Publishing.

SRI JOTHI, P. AND M. NEELAMALAR. 2011. The Role of the Media in Science and Technology Education, Development, and Rehabilitation of Women Affected by the 2004 Tsunami in the State of Tamil Nadu. In, Science of Tsunami Hazards, vol. 30, no. 2. Tsunami Society International, Honolulu.

STEWART, H. B. AND Y. UEDA. 1991. Catastrophes with Indeterminate Outcome, in, Proceedings: Mathematical and Physical Sciences, vol. 432, no. 1884, pp.113-123. The Royal Society, London.

SUNSTEIN, C. R. 2003. Terrorism and Probability Neglect, in, Journal of Risk and Uncertainty, March-May, vol. 26, no. 2/3, pgs. 122. Springer, London.

SYNOLAKIS, C. E. AND E. N. BERNARD. 2006. Tsunami Science before and beyond Boxing Day 2004. In, Philosophical Transactions: Mathematical, Physical and Engineering Sciences, Aug., vol. 364, no. 1845, pp. 2241, pp. 2231-2265. London: The Royal Society.

THANAWOOD, C. ET AL. 2006. Effects of the December 2004 Tsunami and Disaster Management in Southern Thailand. In, Science of Tsunami Hazards, vol. 24, no. 3, pp. 206-217. Honolulu: Tsunami Society International.

TOURISM AUTHORITY OF THAILAND. 2005. Tourism Situation Concerning Inbound Foreign Visitors in 2005.

TROND H., AURAN PIATIGORSKY AND LARS WEISÆTH. 2009. Longitudinal Changes in Recalled Perceived Life Threat after a Natural Disaster, in, British Journal of Psychiatry, 194:510-514. RC Psych, London.

UNITED NATIONS COUNTRY TEAM, THAILAND. 2006. Building Back Better in Thailand: Tsunami Affected Areas. April-July. Bangkok.

WEICK, K. E. 1995. Sensemaking in Organizations. Thousand Oaks: Sage Publications.

WYNTER, A. 2005. Humanitarian Media Coverage in the Digital Age, in, Red Cross Red Crescent World Disasters Report 2005, pgs. 126-149. Kumarian Press Inc., Broomfield.

ISSN 8755-6839

SCIENCE OF **TSUNAMI HAZARDS**

Journal of Tsunami Society International

Volume 32 **Number 3** **2013**

'HANGING TEN': MEASURING BIG WAVE INTENSITIES

Nancy Livingston Potter

Department of Mathematics & Computer Science
Western New Mexico University, Silver City, New Mexico, USA

ABSTRACT

The entire world is still feeling the effects of the devastating 2011 Honshu earthquake and tsunami. The Cascadia subduction zone, spanning over 800 miles from Vancouver Island to northern California, is soon expected to complete its 500-year quake cycle with a magnitude 8+ tsunamigenic earthquake. Much attention is being given to planning for this potential disaster and its collateral impacts from landslides, fires, hazardous material spills and infrastructure damages. The devastating impact of future tsunami events in this region and elsewhere, may result in millions of deaths and billions of dollars in damages. Over the years numerous attempts have been made to quantify tsunami severity but none of the devised scales have been completely satisfactory. The present study reviews and discusses the scales of magnitude and intensity that have been developed to describe the severity of tsunami events both qualitatively and quantitatively. Furthermore, it defines a new quantitative scaling measure of tsunami severity which is an improvement over widely reported current scales, by comparing the 'Top Ten Lists' of devastating tsunami as calculated by each of the scales.

Keywords: *tsunami severity, wave intensities, tsunami magnitude, top ten tsunamis.*

1. INTRODUCTION

In surfing, 'hanging ten' is the term used to describe a surfer's position on the surfboard, in such a way that the back of it is covered by the wave and the rider is free to walk to the front and hang all ten toes over the nose of the board (see the photograph in APPENDIX I). Of course, this cannot be done with tsunami waves which simply cannot be surfed. In this paper, we have borrowed the term "hanging ten" to identify the top ten most devastating tsunamis, based on our newly defined scale of intensity.

The most severe tsunamis are generated from major and great earthquakes near zones of subduction. At boundaries of subduction, the colliding tectonic plates remain locked for long periods of time until a threshold limit of elastic deformation is reached, at which time the stress is released by an earthquake and a tsunami is generated by the vertical and horizontal crustal movements of the ocean floor. The 11 March 2011 tsunami in Honshu, Japan was such a long-overdue extreme event, generated by a great earthquake with magnitude 9.0+ (NGDC, 2011). The tsunami was primarily responsible for most of the great destruction and the deaths of well over 15,000 people. Collateral tsunami damage included the spread of debris across the Pacific Ocean and the destruction of the Fukushima-Daichi nuclear plant, which released large quantities of radioactive Cesium-137 and other radionuclides – subsequently uptaken by migratory fish such as tuna. We have studied extensively this particular tsunami and its effect on the Japanese prefectures as they relate to the distribution of extreme tsunami wave heights (Potter, October, 2011 in review).

The 26 December 2004 mega-tsunami generated along the Island of Sumatra and in the Andaman Sea, was another event that devastated many countries bordering the Indian Ocean Basin and killed more than a quarter of a million people. It was triggered by an earthquake of magnitude 9.1 resulting when the India plate suddenly subducted beneath the Burma microplate. To the list of other historical mega-tsunamis we must also include the one generated by the magnitude 9.2, 1964 Good Friday earthquake in Alaska which affected many other areas in the Pacific and the Hawaiian Islands. Even Vancouver Island which was over 1,100 miles away from the source region, experienced millions of dollars in damages from this tsunami. In addition to the major tsunami generated in the Gulf of Alaska, many more local, extremely destructive tsunamis were generated by this event in Prince William Sound and in the Valdez basin.

Presently, there are many more regions in the Pacific and elsewhere in the world where future destructive tsunamis can be expected. One such region is the Cascadia subduction zone off the US. Northwest coast where the Juan de Fuca and the North American plates collide. This seismic zone spans over 800 miles from Vancouver Island to Northern California. The recurrence interval for great quakes along this zone has been estimated to vary between 300 – 600 years. Earthquakes with magnitude 8 or greater have been estimated to occur on the average of about 500 years – the last one in 1700 A.D. Needless to say that much attention is being given to planning for this expected tsunami event and its collateral consequences, such as landslides, fires, hazardous material spills and building damages. The Cascadia Region Earthquake Workgroup (CREW, 2005) has concentrated on preparing this region with the intention of reducing the potential risk.

Ongoing research suggests that a rupture along the Cascadia zone would cause the sea floor to be raised by 20 feet or more, setting off powerful waves in the near field region. The first tsunami waves could hit coastal communities within 30 minutes or less -- too rapidly for the current warning system to respond adequately and save lives. Thus it is important to discover as much as possible about this expected tsunami hazard and engage in proactive behavior in planning, preparedness and in ascertaining as much as possible about the source region and the expected severity. Such efforts can only serve to improve the regional warning system and tsunami preparedness.

2. TSUNAMI MEASURES THEN AND NOW

In attempting to quantify tsunami severity for the purpose of comparing events, numerous attempts have been made over the years but for many reasons none have been completely satisfactory. Calculating the total power and energy for most tsunamis is very difficult today due to lack of ability in technology and resources to both measure and collect the needed vast amounts of data. The challenge continues to be in discovering the balance between the appropriateness and the availability of the statistical data to use in determining what exactly should be quantified. A thorough review of quantification of tsunami up to 2001 can be found in the literature (IMAMURA, 2001).

In 1956, the Iida magnitude scale (Iida, 1956) was developed to measure tsunami magnitude. It is defined as $M = \log 2H$, where H is the maximum wave height. Then in the 1970's, the Soloviev – Iida Intensity Scale was introduced as a variation on the magnitude scale where $I = 12 + \log 2H$. Subsequently in 1979, the Abe Magnitude Scale (Abe, 1979) for earthquake-generated tsunami appeared as $Mt = \log A + a \log R + D$, where A is the maximum amplitude of tsunami waves, R is the distance (km) from the earthquake epicenter to the tide station and a and D are constants which attempt to coincide with the Richter scale magnitude.

In 1980, Murty & Loomis developed the ML magnitude scale (LOOMIS, 1980), where $ML = 2(\log E - 19)$ and E is the total potential energy at time of generation of the tsunami, which involves calculating the elevation or subsidence and the area of the ocean bottom affected at the time of generation. The range of scale values lies in the interval [-4, 10]. This ML magnitude scale was tested on a partial list of tsunamigenic earthquake events prior to 1974 (LOOMIS, 1980), where it was mentioned that the values should be treated as strictly tentative at best since data estimates were often conflicting. In addition to the extreme difficulties in calculating potential energy of an event, this measure also does not take into consideration tsunami propagation effects like ocean floor topography and bathymetry, which do have great influence over the event. This measure is therefore not widely used or reported. Also, none of these magnitudes or intensities measured degree of impact or event effects. Instead, they all calculated a magnitude based on the physical parameter of wave height of the natural event measured at a particular location.

In the 1990's, Shuto developed the Shuto Intensity Scale (SHUTO, 1991), which combined magnitude and intensity for the purpose of predicting expected tsunami impact as a function of wave height. Shuto defined six grade intensities in the range 0 – 5 based on divisions of $i = \log 2H$. Finally, in 2001, Papadopoulos & Imamura introduced their Qualitative Intensity Scale (IMAMURA, 2001) based on Twelve Divisions (I-XII) arranged in order according to effects on humans, effects on objects and nature and damage to buildings. This scale is independent of the physical parameters that control the type and extent of effects in that it does not explicitly involve their measurements.

Currently, the NGDC reports tsunami magnitude and intensity using the Iida magnitude and the Soloviev intensity scales. The Abe Magnitude Scale is also occasionally reported for some earthquake-generated tsunamis. Each of these scales relies on wave height of the event as the determining statistic. The current tsunami warning system using DART gages for detection is triggered by a threshold wave height value (MILBURN, PMEL NO. 2836). The power, the energy flux (Zygmunt, 2008), the magnitude, the intensity (McIntyre, 2005), the velocity or wave speed and the underwater friction coefficients (Xu, 2007) of a tsunami are all determined by or at least in part by the maximum wave height of the tsunami.

3. A MISSING DETERMINING PHYSICAL PARAMETER

Every one of the quantitative measures widely reported to date uses maximum wave height measured at a particular location as its determining physical parameter. None of these measures have been satisfactory because as it turns out wave height is not the only determining factor in a devastating tsunami event. By taking a look at two major events, we can see there is something missing in these measures.

The Mt. St. Helens' volcano-generated tsunami of 1980 at Spirit Lake holds the record for the second highest wave since 1900. Its Iida magnitude is at 7.97, Soloviev intensity at 8.47, Shuto index of I = 5 and P&I index of XII. The 2004 Indonesian earthquake-generated tsunami has a waveheight only 20% that of Spirit Lake Tsunami, but it is the deadliest tsunami in recorded history - having killed many more than a quarter of a million people. Its Iida magnitude is at 5.67, the Soloviev intensity at 6.17, the Shuto index of I = 5 and the assigned P&I index is XII. A summary of these event statistics can be found in APPENDIX II. These Iida and Soloviev numbers accurately detect the 200 meter difference in the wave heights of these events. The Shuto and P&I indices do not distinguish between these events. But the overall power of these events was vastly different.

In general, the exact computation of the power of an event is difficult due to lack of ability in technology to measure and economics to collect all the data needed. In considering what we mean by tsunami power, we need to determine the energy delivered by the individual waves to the shoreline, as well as how much shoreline experiences the wave in the event. We define the power of a tsunami event as:

$$P\ tsunamievent = allwavesPwavefront * Dshorelin$$,

where $Pwavefront$ is the power of a wave front per meter of shoreline and $Dshoreline$ is the distance in meters of shoreline affected by the wave. Now, $Pwavefront = Edensity \cdot C\ \ Js/m$ (watts per meter), where $Edensity = \rho water \cdot g \cdot H28\ kgs2$ (Joules per square meter) $= 1{,}225H2\ kgm2$, and C is the celerity *or* wave front velocity measured in m/s. It's easy to see that the vast amount of data needed to compute these quantities exactly and uniformly would be very difficult to obtain considering economic and technological restraints.

However, we can develop an approximation to the power formula that will be useful in distinguishing such events. See APPENDIX III for a discussion on such an approximation and its use in calculating approximations for power of the Spirit Lake and Indonesian tsunami events. The Mt.

St. Helens tsunami delivered 1100 giga-watts of power to the shores of Spirit Lake. That's more than 500 times the peak power generation of the Hoover Dam. It is worth noting that the entire length of shoreline affected in the Indonesian tsunami is vast because its effects were felt around the world. Sri Lanka alone was hit by a total power of half a terawatt (0.5×1012) by the Indonesian tsunami. Half a terawatt could power about 5 billion 100-watt light bulbs at the same time. Half a terawatt is 3% of the annual world power consumption.

The Iida and Soloviev numbers accurately detect the 200 meter difference in the wave heights of these two events but fail to account for the extreme severity of the Indonesian event in comparison to the Spirit Lake event. The difference between them was the run-up values. A run-up occurs when the crest of the wave hits the shore, sea level rises and the momentum of wave motion results in some higher value of flooding inland. Run-up information is not accounted for in these magnitude and intensity measurements – only the wave heights. There may be quite a difference in the degree of severity of a tsunami and the resulting run-up values, depending on coastal topography and on wave energy focusing due to offshore refraction.

The Mt. St. Helens volcano-generated tsunami of 1980 at Spirit Lake holds the record for the second tallest wave since 1900 but had only two run-ups, while the 2004 Indonesian earthquake-generated tsunami in the Pacific Ocean had a wave height only 20% of that of Spirit Lake tsunami but had 1058 run-ups – the second highest number of run-ups in tsunami history! In addition to tall waves, the number of run-ups in an event turns out to also be a crucial factor in determining severity and devastation.

In APPENDIX V, we form the top ten lists of devastating tsunami (since 1900) by deaths in Table (i.) and by damages in Table (iii.), and compare those to the top ten by wave height and again by run-ups. Most entries in the list 'By Deaths' don't have significant wave heights. Instead they have vast numbers of run-ups, which further demonstrates the importance of considering large run-up quantities in measuring devastation.

Table (ii) shows the 'Wave height' list misses 80% of the most deadly tsunamis and underestimates the devastation in 100% of those it does manage to find. Table (iv) shows the 'Wave height' list misses 60% of most devastating tsunamis by damages and underestimates the devastation of 75% of those it manages to include. The 'Run-Ups' list in Table (v) finds 10% more devastating tsunami by deaths than the 'Wave-heights'. The 'Run-Ups' list in Table (vi) captures 60% of the devastation by damages in the Top 10 'By Damages' list versus 'Wave height', which captures 40%. The 'Run-Ups' list tends to overestimate damages in 75% of those it captures which contrasts the 100% underestimation of 'Wave heights'.

This trend continues when even more events are considered. For example, by comparing the top 25 events by wave height and deaths or damages, we find the 'Wave height' list coincides with only 24% of the 'By Deaths' list and 44% of the 'By Damages' list. Note that after the top 25, observed wave heights all fall short of 20 meters, and, after the top 50, they fall short of 11 meters. By comparing the top 50 events in the wave height and deaths lists, we find 42% coincidence. There are 39 reported events on the entire 'By Damages' list, and a comparison of this list with the 'By Wave height' produces 38% coincidence.

It is interesting to note that, in the 'By Deaths' list, 80% of events were caused by earthquakes and 20% by landslides. In the 'By Damages' list, 90% of events were caused by earthquakes and 10% by landslides. In contrast, in the 'Run-Ups' list, 90% of events were caused by earthquakes, while 10% resulted from a volcano; and, in the 'Wave heights' list, 40% resulted from an earthquake, while 30% were from landslides and the rest from volcanoes. From our analysis, we can see it is essential to include both height and run-up statistics in building models to help analyze certainty and severity of tsunami events.

4. A NEW MEASURE OF TSUNAMI SEVERITY

We now define a quantitative measure of tsunami severity which includes the run-up number statistic and show it in Section 5 to be a major improvement over current measures by comparing the most devastating tsunami as calculated by each measure with respect to deaths and damages. We want to be able to compare tsunami universally by degree of severity. The most severe storms have the largest wave heights and most run-ups (power behind them).

A natural way to associate the power of an event with a severity index is to compute the index using the determining variables in the power estimation. The maximum wave height observed in a tsunami event determines the maximum power per meter wave front of the event. If there are N run-ups and H is the maximum observed wave height in the event, we associate the power per meter wave front of the event with that of the tallest wave. Then we can further associate the power of a tsunami event with the product of run-ups and the measure of the tallest wave:

$$P\ tsunamievent \quad N*H$$

A detailed description of this association can be found in Appendix IV. We define an index to capture tsunami devastation in magnitude and intensity.

Define the Log – Power (LP -) Index of a tsunami event as

$$\boldsymbol{LP} = \mathbf{log}\boldsymbol{N*H},$$

where N = number of event run-ups and H = maximum run-up height in the event. Values generally lie in the interval (-6, 6), and so it is straightforward to adjust the index (by a constant shift) to provide a correlation to the Shuto Intensity or P & I Qualitative index scales, which are partitioned according to maximum wave heights. The association described is very convenient for common use since the events are popularly and routinely reported by citing maximum wave height and run-ups experienced by the event (NGDC, 2011).

5. 'TOP TEN' LISTS OF DEVASTATING TSUNAMI

Table (vii) in APPENDIX V shows the Top 10 Most Severe Tsunami identified by the LP-Index. The first event on the LP-Index Top 10 List is the 2011 Honshu event, which is the costliest tsunami in recorded history and the second highest in death toll. The second event is the 2004

Indonesian tsunami, which is the deadliest tsunami in recorded history and the third highest in damages. The LP - Top 10 coincides with 50% of the 'Wave height' Top 10 list. Now 60% of those events on the LP - Top 10 but not on the 'Wave height' Top 10 list coincide with the 'By Damages' Top 10, while 20% coincide with the 'By Deaths' Top 10. So, entries appearing on the LP list that don't coincide with those on the 'By Wave height' list are more severe than those with higher wave heights due to few or no deaths or damages reported.

The LP – Top 10 also coincides with 70% of the 'Run-ups' Top 10 list and of course includes all entries simultaneously on both 'Run-Ups' and 'Wave height' Top 10 lists. Now 20% of those events on the LP – Top 10 but not on the 'Run – Ups' Top 10 list coincide with both 'By Deaths' and 'By Damages' Top 10 lists. So, 67% of entries appearing on the LP list that don't coincide with those on the 'By Run-Ups' list are more severe than those with more run-ups due to few or no deaths or damages reported. The only tsunami on the LP – Top 10 list that does not appear on one of the two 'By Run-Ups' or 'By Wave height' Top 10 lists is the 1933 Sanriku, Japan tsunami which had a 29 *m* wave height, 295 run-ups and 3,022 deaths. This event does appear sixth on the 'By Deaths' Top 10 list.

How accurately the LP-Index detects devastation by deaths and by damages can be found by comparing Tables (i), (iii.) and (vii). The Top 10 'By LP-Index' coincides with 70% of the Top 10 'By Damages' and 30% of the Top 10 'By Deaths'. This represents a 43% and a 34% improvement over current measures, respectively, because 40% of Top 10 by wave height made the Top 10 by damages, and 20% of the Top 10 by wave height made the Top 10 by deaths as shown in Section 4.

These LP – Index results are far more satisfactory than any of the magnitude or intensity scales widely reported today since those rely solely on the wave height statistic. This improvement trend continues when considering greater numbers of top events. For example, by comparing the top 25 events by LP-Index and deaths or damages, we find the LP-list coincides with 36% of the top 'By Deaths' and 56% of the top 'By Damages' lists. This represents a 34% and 22% improvement over the top 25 "By Wave height' list in comparison with the top 25 'By Deaths' and 'By Damages' lists, respectively. Again, note that after the top 25, observed wave heights all fall short of 20 meters, and, after the top 50, they fall short of 11 meters. By comparing the top 50 events by LP-Index and deaths, we find a 46% coincidence, an 18% improvement over considering wave heights alone. There are 39 reported events on the entire 'By Damages' list, and a comparison of this list with the 'By LP-Index' list produces 46% coincidence, a 12% improvement over considering wave heights alone.

Similar results are found for the Top 100 categories. A 58% coincidence in the Top 100 'By Deaths' and 'By LP-Index' coincide. It is not surprising to note that there is over 70% coincidence in the Top 100 'By Wave height' and the Top 100 'By LP-Index' lists. It is also important to note 30 of the last 100 wave heights on the Top 100 'By Wave height' list are fewer than 6 meters tall, 39 of 100 of these have recorded damages, and that 39 of these events also have fewer than 20 deaths. Comparing the Top 100 'By Wave height' to the Top 100 list 'By Deaths' yields 54% coincidence, respectively. So, for these events which include many non-devastating and many incompletely reported storms, the LP-Index represents a 7% overall improvement in the 'By Deaths' category on the top 100 events.

Therefore the LP-Index makes a significant improvement over current measures with vast improvement seen in comparing current measures of the most severe events with respect to damages and deaths. It is clear that including the run-ups statistic in the computation of tsunami intensity and

magnitude makes an important contribution and should therefore not be ignored. The LP-Index is very appropriate for common use because the events are popularly reported by citing maximum wave height and run-ups experienced in the event. Moreover, the LP-Index is independent of the cause of the tsunami event. The closer we can approximate the severity of tsunami events, the more capable we will be in comparing and contrasting their potential devastation. This will aid in planning for their arrival and predicting their severity, thereby enabling us to improve tsunami warning systems and protect our shores.

APPENDIX I. Hanging Ten

'Hanging ten' is when the surfer positions the surfboard in such a way that the back of it is covered by the wave, and the wave rider is free to walk to the front of the board and hang all ten toes over the nose of the board.

APPENDIX II. Measure Comparisons of Two Major Events

Measures	Spirit Lake Event	Indonesian Event
Maximum Waveheight (*m*)	250	50.9
Deaths	-	226898
Iida Magnitude	7.97	5.67
Soloviev Intensity	8.47	6.17
Shuto Index	5	5
P & I Index	XII	XII

Note: The Shuto and P & I Indices quoted here are the maximum value in each scale, representing the most completely devastating tsunami (Imamura, 2001).

APPENDIX III. Estimating Power

The power per meter wave front is the product of energy wave density and the celerity of the wave (wave speed). With seawater density measured as $\rho water=1000\ kg/m3$, h= depth below mean sea water level in meters, H=twice the wave height above mean sea water level (twice the amplitude), and the gravity constant $g=9.8m/s2$ (as in Figure 3), then the power per meter wave front is:

$Pwavefront=Edensity{\cdot}C\ \ Js/m$ (watts per meter), where $Edensity= \rho water{\cdot}g{\cdot}H28\ kgs2$ (Joules per square meter) $=1,225H2\ kgm2$, and C is the celerity *or* wave front velocity measured in m/s.

The maximum wave height observed in a tsunami event determines the maximum $Edensity$ of the event. The energy per meter of wavefront, $Ewavefront$, is the energy wave density per meter wavefront. To compute the total energy of a single tsunami wave affecting a region, multiply the energy per meter wavefront by the meters of shoreline affected. To compute the total energy of all tsunami waves in an event affecting a region, sum the energies per wave over all waves in the event. This describes the energy per meter wave front of the tsunami event at one region, but often many regions are affected by the same event. A sum over all regions is needed.

The 2004 Indonesia tsunami had over 950 regions reporting event observations around the globe, reaching areas ranging from France to New Zealand. The regions experiencing and recording a wave from a tsunami event coincide with the recorded run-ups of that event. The actual total energy of the tsunami is then a sum over all run-up regions of the total energy of the waves experienced by the region. In the case of the Mt. St. Helens and Indonesian tsunami, the respective energy densities of the wave with the maximum height are 76,562,500 $Jm2$ and 3,173,742 $Jm2$, indicating the difference in wave heights. Even if this density occurs when the celerity is small, approximately 1 m/s, then the actual power per meter wave front, according to the above formulae, of each wave is 76.6 megawatts and 3.2 megawatts, respectively.

The total energy per meter wave front, considering all run-ups, of each tsunami is 138,578,000 *J/m* for the St. Helens event and 14,846,600,000 *J/m* for the Indonesian event. These values are much more indicative of the contrast in total destruction caused by each tsunami than the previous measures of magnitude or intensity by maximum event wave height alone. If, again, a conservative estimate of celerity at 1 *m/s* is used, the actual power per meter wavefront of each wave is 138.6 megawatts at Mt. St. Helens and 14.8 gigawatts in the entire Indonesian tsunami, respectively.

In all, that's 14,800 gigawatts per km of shoreline for the Indonesian tsunami and 138.6 gigawatts per km of shoreline at Spirit Lake. Spirit Lake, prior to 1980, had a surface area of about 5.26 square kilometers, which represents approximately 8 km of shoreline. That means 1100 gigawatts of power were delivered by the Mt. St. Helens tsunami to the shores of Spirit Lake. The total length of shoreline affected in the Indonesian tsunami is vast because its effects were felt around the world. It has been estimated (McIntyre, 2005) that Sri Lanka alone was hit by a total power of half a terawatt (0.5×1012) by the Indonesian tsunami.

APPENDIX IV. Derivation of the LP-Index

We describe how the association of the LP-Index with the power of a tsunami event is eventually derived. Recall the power of a tsunami event is defined as:

$$P_{tsunamievent} = \sum_{allwaves} P_{wavefront} * D_{shoreline}$$

First, remove shoreline distance from the variable list (the run-up factor remains). Notice, per region, an average $D_{shoreline}$ could also be used to compute $P_{tsunamievent}$ (another constant). This provides an association of event power with event power per meter shoreline:

$$P_{tsunamie\square\square en\ t} \quad P_{tsunamievent} \quad per\ meter \quad shoreline$$

Next, approximate tsunami power using the upper bound of power per meter wave front for the highest wave in the event. The maximum wave height observed in a tsunami event determines the maximum power per meter wave front of the event:

$$P_{wavefront} P_{wavefront\ of\ high\ wave}$$

In this way with N = number of run-ups, we have removed the need for the sum and we have the association:

$$P_{tsunamievent\ p.ms.} \quad N * P_{wavefront\ of\ highest\ wave}$$

Because the maximum wave height, H, observed in a tsunami event determines the maximum power per meter wavefront of the event, we can further make the correspondences:

$$P_{wavefront\ of\ highest\ wave\ H}$$

And finally

$$P_{tsunamievent} \quad N * H \ .$$

APPENDIX V. 'Top Ten' Tables

Table (i). BY DEATHS

Year	Country	Region	Wave height (m)	Run-Ups	Deaths
2004	INDONESIA	OFF W. COAST OF SUMATRA	50.9	1058	226898
2011	JAPAN	HONSHU	38.9	5776	15854
1976	PHILIPPINES	MORO GULF	8.5	30	4376
1945	PAKISTAN	MAKRAN CST	15.24	7	4000
1952	RUSSIA	KAMCHATKA	18	290	4000
1933	JAPAN	SANRIKU	29	295	3022
1998	PAPUA NEW GUINEA	PAPUA NEW GUINEA	15.03	67	2205
1923	JAPAN	SAGAMI BAY	13	103	2144
1946	DOMINICAN REPUBLIC	NE COAST	5	8	1790
1946	JAPAN	S HONSHU	6.6	298	1362

Table (ii). BY WAVEHEIGHT SHOWING DEATHS

Year	Source Location	Wave height (m)	Deaths
1958	Lituya Bay, Alaska	525	5
1980	Spirit Lake, WA	250	NO REPORT
1936	Lituya Bay, Alaska	149.35	NO REPORT
1936	Norway	74	73
1964	Alaska	67.1	124
1993	Niigata, Honshu, Japan	54	208
2004	Indonesia	50.9	226898
2000	Paatuut, Greenland	50	NO REPORT
1905	Nessoden, Norway	40.5	61
2011	Honshu, Japan	38.9	15854

Table (iii). BY DAMAGES

Note: Damages reported by the NGDC represent the dollar value at the time of the event. For the purpose of comparison, damages reported in the event years were converted to damages representing the same buying power as in 2011 using the Consumer Price Index Inflation Calculator available at the Bureau of Labor Stats of US Department of Labor.

Year	Country	Region	Wave height(m)	Run-Ups	2011-ADJ. Damages(Mil)
2011	JAPAN	HONSHU	38.9	5776	$210000
2010	CHILE	S. COAST	29	597	$30946
2004	INDONESIA	W. COAST SUMATRA	50.9	1058	$11908
1993	JAPAN	SEA OF JAP.	54	176	$1879
1983	JAPAN	NOSHIRO, JAP	14.93	227	$1807
1964	USA	PRINCE WM SOUND, AK	67.1	394	$864
1964	JAPAN	NW. HONSHU	5.8	165	$581
1960	CHILE	CENTRAL CHILE	25	1049	$570
1976	PHILIPPINES	MORO GULF	8.5	30	$530
1946	USA	UNIMAK ISL, AK	35.05	511	$302.9

Table (iv). BY WAVE HEIGHT SHOWING DAMAGES

Year	Source Location	Wave height (m)	2011-Adjusted Damages in Millions
1958	Lituya Bay, Alaska	525	$0.8
1980	Spirit Lake, WA	250	NO REPORT
1936	Lituya Bay, Alaska	149.35	NO REPORT
1936	Norway	74	NO REPORT
1964	Alaska	67.1	$864
1993	Niigata, Honshu, Japan	54	$1879
2004	Indonesia	50.9	$11908
2000	Paatuut, Greenland	50	NO REPORT
1905	Nessoden, Norway	40.5	NO REPORT
2011	Honshu, Japan	38.9	$210000

Table (v). BY RUN-UPS SHOWING DEATHS

Year Of Tsunami	Source Location	Wave height (meters)	Run-Ups	Deaths
1960	Chile	25	1049	1203
2004	Indonesia	50.9	1058	226898
2010	Chile	29	597	156
2009	Samoa	22.35	579	192
1946	Unimak Island, Alaska	35.05	511	164
2011	Iwate, Honshu, Japan	38.9	5776	15854
1964	Prince William Sound, Alaska	67.1	394	124
1957	Adreanof Islands, Alaska	22.8	323	NO REPORT
1968	Honshu, Japan	6	306	NO REPORT
1946	South Coast, Honshu, Japan	6.6	2981362	

Table (vi). BY RUN-UPS SHOWING DAMAGES

Year Of Tsunami	Source Location	Wave height (meters)	Run-Ups	2011-AdjustedDamages in Millions
1960	Chile	25	1049	$570
2004	Indonesia	50.9	1058	$11908
2010	Chile	29	597	$30946
2009	Samoa	22.35	579	$288
1946	Unimak Island, Alaska	35.05	511	$303
2011	Iwate, Honshu, Japan	38.9	5776	$210000
1964	Prince William Sound, Alaska	67.1	394	$864
1957	Adreanof Islands, Alaska	22.8	323	$40
1968	Honshu, Japan	6	306	NO REPORT
1946	South Coast, Honshu, Japan	6.6	2981362	NO REPORT

Table (vii). BY LOG POWER INDEX SHOWING WAVEHEIGHT, RUN-UPS, DEATHS AND DAMAGES

YEAR	COUNTRY	REGION	WAVE HEIGHT	RUN-UPS	Log-Power Index	Damages Adjusted to 2011 (Millions)	Deaths
2011	JAPAN	HONSHU ISLAND	38.9	5776	5.351577	$210000	15854
2004	INDONESIA	OFF W. COAST OF SUMATRA	50.9	1058	4.731203	$11908	226898
1964	USA	PRINCE WILLIAM SOUND, AK	67.1	394	4.422219	$864	124
1960	CHILE	CENTRAL CHILE	25	1049	4.418715	$570	1203
1946	USA	UNIMAK ISLAND, AK	35.05	511	4.253109	$303	464
2010	CHILE	OFF SOUTHERN COAST	29	597	4.238372	$30946	156
2009	SAMOA	SAMOA ISLANDS	22.35	579	4.111956	$288	192
1993	JAPAN	SEA OF JAPAN	54	176	3.977906	$1879	208
1933	JAPAN	SANRIKU	29	295	3.93222	NO REPORT	3022
1958	USA	SE. ALASKA, AK	525	15	3.896251	$0.8	5

REFERENCES

ABE, K. (1979). Size of great earthquakes of 1837-1974 inferred from tsunami data. *J. Geophys. Res., 84* , 1561-1568.

CREW, C. R. (2005). *Cascadia Subduction Zone Earthquakes: A magnitude 9.0 earthquake scenario.* Oregon department of Geology and Mineral Industries.

IIDA, K. (1956). Earthquakes accompanied by tsunamis occurring under the sea off the islands of Japan. *J. Earth Sciences Nagoya Univ. 4* , 1-43.

IMAMURA, G. P. (2001). A Proposal For A New Tsunami Intensity Scale. *ITS Session 5, Number 5-1*, (pp. 569-577). Athens.

KOWALIC, Z. (2008). Energy flux as a tool in locating tsunami secondary sources. Science of Tsunami Hazards, Vol. 27, No. 3 , 1-29.

LOOMIS, T. M. (1980). A New Objective Tsunami Magnitude Scale. *Marine Geodesy 4:3* , 267 - 282.

MCINTYRE, M. (2005). Speed and power of a long tsunami wave, from Bernoulli's Theorem. *Plus Magazine...Living Mathematics*.

MILBURN, H. B. (PMEL NO. 2836). *Technology Developments in Real-Time Tsunami Measuring, Monitoring and Forecasting.* NOAA, Pacific Marine Environmental Laboratory.

NGDC. (2011). *National Geophysical Data Center Tsunami Event Database.* www.ngdc.noaa.gov/nndc/

POTTER, N. L. (OCTOBER, 2011 IN REVIEW). Modeling Tsunami Probability Using Generalized Extreme Value and Pareto Distributions with Case Studies in the Japanese Prefectures. *Journal of Applied Statistics*

SHUTO, N. (1991). Tsunami intensity and disasters. In e. b. Tinti, Tsunamis in the World (pp. 197-216). Dordrecht: Kluwer Academic Publishers.

XU, Z. (2007). The All-Source Green's Function and Its Applications to Tsunami Problems. Science of Tsunami Hazards, Vol. 26, No.1 , 59-69.

ISSN 8755-6839

SCIENCE OF **TSUNAMI HAZARDS**

Journal of Tsunami Society International

Volume 32 **Number 3** **2013**

TSUNAMI SOCIETY INTERNATIONAL, 1741 Ala Moana Blvd. #70, Honolulu, HI 96815, USA.

WWW.TSUNAMISOCIETY.ORG